Summer 8-15-2021

Peripheral Nerve Macrophages and Their Implications in Neuroimmunity

Peter Leon Wang
Washington University in St. Louis

WASHINGTON UNIVERSITY IN ST. LOUIS

Division of Biology and Biomedical Sciences
Immunology

Dissertation Examination Committee:
Gwendalyn J. Randolph – Chair
Jeffrey Milbrandt – Co-chair
Maxim Artyomov
Marco Colonna
Hongzhen Hu
Brian Kim
Haina Shin

Peripheral Nerve Macrophages and Their Implications in Neuroimmunity

By

Peter Leon Wang

A dissertation presented to
The Graduate School
of Washington University in
partial fulfillment of the
requirements for the degree
of Doctor of Philosophy

August 2021
St. Louis, Missouri

Table of Contents

List of Figures

List of Tables

Acknowledgments

I extend my sincere gratitude to Gwen Randolph and Jeff Milbrandt for their outstanding mentorship throughout the course of my doctoral work. Even before my own research began, Gwen gave me a chance to come to St. Louis and work on a subject I had no experience in. This opportunity was one of the most important events of my life. As my research direction became more clear, Jeff likewise provided me with the chance to address my interests and bring them to reality. This dissertation would not exist without the tools, expertise, and personal guidance they generously made available to me. I cannot thank them enough for giving me the opportunity to develop not only as a scientist, but as a person. I also thank my committee members, Brian Kim, Hongzhen Hu, Haina Shin, Max Artyomov, and Marco Colonna for their ideas and contributions that made this dissertation possible. I thank Michael Holtzman for providing me with funding through the Pulmonary Training Grant (T32 HL007317-41).

The current and past members of the Randolph and Milbrandt labs have also been a vital part of my research journey and will remain treasured friends. I especially thank Aldrin Yim for his invaluable contributions to data analysis and for allowing me to constantly bug him with questions and requests. I also thank Kiwook Kim, Stoyan Ivanov, and Jesse Williams for imparting foundational knowledge and techniques. I thank Bernd Zinselmeyer for training me in microscopy as well as Amy Strickland and Amber Hackett for providing experimental guidance and support. Lastly, I am grateful for the comradery, discussions, and shared times with Shashi Bala, Andrew Elvington, Paul Huang, Osamu Baba, Emma Erlich, Rafa Czepielewski, Nan Zhang, Mary Wohltmann, Brian Saunders, and Michael Wilkinson.

Finally, I would like to thank my family: my father Wenchao for coaching me through a PhD, my mother Wei for constant prayers, support and love, my sister Anna for being my

inspiration and my partner Candace for encouraging me through the tough times while accomplishing her own incredible feats.

Peter Leon Wang

Washington University in St. Louis

August 2021

This work is dedicated to my dear parents.

ABSTRACT OF THE DISSERTATION

Peripheral Nerve Macrophages and Their Implications in Neuroimmunity

by

Peter Leon Wang

Doctor of Philosophy in Biology and Biomedical Sciences

Immunology

Washington University in St. Louis, 2021

Professor Gwendalyn J. Randolph, Co-Chair

Professor Jeffrey Milbrandt, Co-Chair

Macrophages are innate immune cells that protect against pathogens and maintain tissue integrity. In vertebrates, macrophages reside in every tissue where they perform specific functions from early development through adulthood. While macrophages provide important functions across all tissues, a major focus in recent years has been the role of resident brain macrophages, known as microglia, in neurodegeneration. As microglia have been shown to affect brain development, homeostasis, and disease, they demonstrate how immune cells critically mediate neurological health and point to the broader significance of neuroimmune interactions, or the coordinated actions of the nervous and immune systems for maintaining tissue health. However, the nervous system also includes peripheral nerves, which not only enable the brain to communicate with the external environment, but are indispensable for maintaining bodily functions. While the peripheral nervous system (PNS) also contains resident macrophages, they are much less characterized than brain microglia. For my dissertation, I set out to investigate PNS macrophages and compare them with their counterparts in the central

nervous system (CNS). My work began with the identification and transcriptional characterization of PNS macrophage across peripheral nerves. I found that self-maintaining PNS macrophages were transcriptionally related to CNS microglia and expressed many transcripts previously thought to be exclusive to microglia. PNS macrophages also expressed unique transcripts reflecting tissue-specific roles and, remarkably, genes previously identified to be upregulated by activated microglia during aging, neurodegeneration, or loss of Sall1. I next examined the developmental features of PNS macrophages and found that they rely on IL-34 for maintenance and arise from both embryonic and hematopoietic precursors. The majority of transcriptional signatures in PNS macrophages did not differ by ontogeny, suggesting that nerve environment specifies PNS macrophage identity at steady state. Finally, my work reveals the responsiveness of PNS macrophages to changes in nerve environment. PNS macrophages shifted their gene expression to become more microglia-like in a dysmyelination model. After injury, PNS macrophages strikingly expressed a set lipid-handling genes that resembled "foamy" macrophages. Targeting of lipid metabolism by high fat diet improved nerve regeneration in a manner suggesting partial dependence on PNS macrophages. Collectively, these findings uncover shared and unique features between neural resident macrophages, emphasize the role of nerve environment for shaping PNS macrophage identity, and point to the therapeutic potential for PNS macrophages in nervous system disorders.

1. Introduction

1.1 Macrophages in host defense and tissue homeostasis

The discovery of macrophages stems back to studies in the late nineteenth century by Ilya Metchnikoff [1]. In his seminal observation, he saw that motile cells in starfish larvae, which he believed were important for the animals' immune defenses, congregated around rose thorns that were inserted into their bodies. These cells, which he also found in vertebrates, were called "phagocytes" because of their ability to take up particulate matter. Experiments from Metchnikoff and others revealed that phagocytosis is an important process that protects the body from foreign invaders [2]. This finding serves as a foundational principle for the field of immunology.

In mammals, macrophages are organized in defined patterns across all tissues and their components, with each cell occupying its own microanatomical domain [3]. This integration of macrophages into tissues positions them as a first line of defense against invading pathogens. Evidence for this concept in humans became apparent during the first half of the twentieth century as research in pathology and immunology turned to the role of macrophages in pulmonary tuberculosis [2]. While it was known at the time that *Mycobacterium tuberculosis* (*M. tuberculosis*) could survive and replicate in macrophages, it was unclear how macrophages influenced infection. A culmination of work from notable scientists, including Florence Sabin and Max Lurie, suggested that macrophages and monocytes, phagocytic leukocytes in blood that can differentiate into tissue macrophages, were central players in the control of *M. tuberculosis* [2]. This concept was further expanded by George Mackaness, who observed in the 1960s that macrophage phagocytosis of bacteria could be increased by factors from sensitized T

lymphocytes, a process that he termed macrophage "activation" [4]. These early studies would lead to extensive research detailing the roles of macrophages in immunity.

Indeed, the current understanding of innate and adaptive immunity, which refer to the more primitive immune system found in metazoans and the acquired immune system found in vertebrates, respectively, can be significantly attributed to the study of macrophages. As professional phagocytes that broadly recognize and destroy infectious agents via pattern recognition receptors (PRRs) that bind to microbes, macrophages are recognized as key players in innate immunity [5]. However, macrophages also coordinate adaptive immune functions that arise when innate immune responses are insufficient to control infection. Adaptive immune responses are dependent on the activation of T cells by specialized antigen presenting cells (APCs), such as dendritic cells (DCs) and macrophages, which capture foreign material, known as antigen, and present them on MHC molecules to naïve T cells [6]. In response to antigen presentation and co-stimulation by MHC-II+ APCs, CD4+ T cells differentiate into helper T (T_h) cells, which clonally expand and secrete cytokines that target specific pathogens, in part by activating macrophage responses [7]. Follicular T_h cells in secondary lymphoid organs also facilitate the production of highly specific antibodies from B cells, which can bind to pathogens and further enhance their uptake by macrophages [8]. Thus, the capability to present antigens, enhance the antigen presentation process via inflammatory mediators, and respond to effector mechanisms by lymphocytes places macrophages in a key position to coordinate both innate and adaptive immunity.

The ability of macrophages to interpret microenvironmental changes and actuate tissue responses is not just important for orchestrating effective immune responses; it is also critical for proper tissue development and homeostasis. For instance, in mice with genetic deletion of colony

stimulating factor 1 (CSF1), a survival factor for macrophages that signals through the colony stimulating factor 1 receptor (CSF1R), there is severe osteopetrosis due to the absence of bone macrophages or osteoclasts, which normally function to facilitate bone remodeling [9]. The absence of macrophages in these mice is also associated with abnormal vascular patterning and altered brain development [10]. Remodeling deficiencies in CSF1 null mice have also been observed in other tissues, including the mammary gland, kidney and pancreas [11]. These findings suggest a general requirement for macrophages in tissue development and remodeling.

In both development and homeostasis, macrophages phagocytose apoptotic cells that have undergone programmed cell death. This process, also known as efferocytosis, prunes down apoptotic cells and is necessary to dispose of short-lived or underdeveloped cells [12]. Evidence from mouse models and patients with systemic lupus erythematosus (SLE) indicate that failure to engulf and degrade dead cells and debris can cause widespread inflammation and autoimmune disease affecting the skin, kidney, lungs, blood vessels, and nervous system [13]. Of note, the phagocytosis of apoptotic cells in homeostatic conditions does not result in inflammatory cytokine production by macrophages. Rather, macrophage uptake of dying cells has been shown to suppress inflammation and auto-immunity in response to self-antigens that might arise during homeostasis [14].

Macrophages also play important roles in lipid metabolism and inflammatory disease. In obesity, adipose tissue macrophages are significantly expanded due to Ly6C+ monocyte recruitment and differentiation into macrophages [3]. The production of inflammatory cytokines, such as TNFα, IL-6, and IL-1β, by these cells contribute to low-grade inflammation and insulin resistance [3,15]. The inflammatory role of macrophages is also well known in atherosclerosis. In atherosclerotic plaques, oxidized LDL is taken up by macrophages via scavenger receptors,

which leads to high intracellular levels of cholesterol and the "foamy" appearance of such macrophages [16]. While recent work by our group has shown that the production of inflammatory cytokines comes from non-foamy macrophages in atherosclerotic plaques [17], the role of inflammation in disease progression remains undisputed [16]. Importantly, the regulation of inflammation in macrophages is closely linked to their own lipid metabolism [18]. Indeed, this feature has important implications across all studies of inflammatory disease.

1.2 Characterization of macrophages: historical and modern approaches

The enormous progress in macrophage research over the past century cannot be separated from the development of new scientific tools and technologies. Since the early investigations of macrophages using dyes to stain and distinguish them as mononuclear phagocytes, there have been numerous key techniques that have enabled breakthroughs in macrophage characterization.

As systematic assessments of tissues indicated that macrophages were present in different organs, including liver, brain, lungs, and bone, researchers began to investigate their origins. By the 1930s, evidence existed that blood monocytes could give rise to tissue macrophages, usually after pathological insult [2]. In 1965,Volkman and Gowans confirmed using radioactive tracing and parabiosis, a technique which surgically joins the circulatory systems of two living organisms, that macrophage precursors could arise from bone marrow during inflammation [19]. This led to the popular belief that macrophages arose from blood-circulating monocytes, which themselves came from progenitors in the adult bone marrow [20]. In 1969, Van Furth and colleagues proposed the "mononuclear phagocyte system" (MPS) to classify promonocytes and

their precursors in the bone marrow, monocytes in the peripheral blood, and macrophages in tissues [2]. While the MPS classification is still used today, we now know that tissue resident macrophages are mostly maintained independently of bone marrow and rely almost exclusively on self-renewal [20, 21]. Furthermore, it has been revealed that most tissue-resident macrophages arise from embryonic sources during development [22]. These studies provide a basis for understanding ontogeny within the MPS.

The more widespread use of immunohistochemistry (IHC), confocal imaging, and flow cytometry in the 1980s brought on further advancements in macrophage characterization, including the identification of macrophage "specific" markers such as F4/80, Mac1 (CD11b), and ED1 (CD68) that could be observed and quantified in cells of interest [23-25]. Around the same time, evidence emerged to indicate that certain cytokines derived from CD4+ helper T cells could promote differential activation states in macrophages. Specifically, it was shown that T_h1 cytokines, such as IFNγ, could polarize macrophages towards a pro-inflammatory or "classical" phenotype, while T_h2 cytokines, such as IL-4, polarized macrophages towards an anti-inflammatory or "alternative" phenotype [26-29]. These findings and techniques set the stage for modern macrophage phenotyping and demonstrated the programmable specialization of macrophage responses.

A more recent approach in the past two decades for characterizing macrophages is transcriptional profiling [30]. By providing a snapshot of the transcriptome, or sum of all RNA transcripts, in samples of interest, this approach has revolutionized the understanding of what constitutes a particular cell type through the quantitative assessment of genes that are expressed [30]. Thanks to key efforts contributed by the Immunologic Genome Project (ImmGen), a collaborative consortium of immunology and computational biology laboratories, a thorough

dissection of gene expression and its regulation in the immune system of the mouse has been made publicly available [31]. Importantly, transcriptional profiling of resident macrophages by ImmGen reveals that macrophages show great transcriptional diversity, reflecting many unique classes with distinct "identities" and specialized functions across tissues [31]. As even more recent technologies in single cell RNA sequencing (SC RNA-seq), epigenomic analysis, and various types of high-throughput screening are now available, there is new opportunity for uncovering insights into macrophage heterogeneity and function.

1.3 CNS microglia: key players in neuroimmunology

First identified through cell staining techniques at the beginning of the twentieth century, microglia were later revealed by Rio-Hortega in 1919 to be phagocytic cells in the brain [32]. While the name microglia comes from their belonging to a group of specialized neural support cells called "glia" (meaning glue), they are indeed macrophages with critical roles in immunity and tissue homeostasis [2].

Microglia were initially observed in connection to human pathology by neurologists examining neurotropic viral infections such as rabies [33], and later in neurodegenerative diseases, including Alzheimer's disease (AD) [34] and multiple sclerosis (MS) [35]. Since then, microglia have been characterized as the resident macrophages and primary innate immune effector cells in the CNS parenchyma [36]. Microglia are yolk sac-derived cells that arise during embryogenesis and play crucial roles in brain development by regulating neuron survival, neurite process outgrowth, synaptic pruning, hypothalamic-pituitary axis formation, and brain vascularization [36]. Their own development has been shown to be partially dependent on interleukin 34 (IL-34), an alternative ligand to CSF1 that also signals through CSF1R [37]. Under homeostatic conditions, microglia are

ramified cells that sample surrounding tissues for ionic balance, damaged cells, or infectious agents [38]. In pathologic conditions, however, microglia rapidly become ameboid and respond locally to injury signals [39]. Microglia function to control neuronal infection and have been shown to regulate inflammation in a variety of CNS injury and disease contexts [40, 41].

In recent years, there has been growing interest in the role of microglia in neurological disease. Initial observations confirmed the importance of microglia in humans when monogenic disease patients with mutations in CSF1R were found to have major morphological alterations in brain structure and severe neurological symptoms [42]. Further evidence for the role of microglia in pathogenesis were revealed by studies showing that sequence variations in TREM2 and TYROBP, which are highly enriched in microglia and also expressed on other myeloid cells, results in a recessive chronic neurodegenerative disease characterized by early-onset progressive dementia and bone cysts [43,44]. Another microgliopathy with neurological symptoms is observed in both mouse mutants as well as patients lacking the negative type I interferon receptor regulating protease USP18 in microglia [45,46]. Furthermore, a potential role for somatic mutations in fetal macrophage precursors, including those that give rise to microglia, was linked to CNS histiocytoses and late-onset neurodegeneration in mice [47].

Given the evident role of microglia in nervous system disorders, it is no surprise that they have been a focal point in the recent rise of interest in neuroimmunology, which focuses on the interplay between the nervous and immune systems in development, health, and disease. Indeed, the enormous growth in knowledge of microglia in the past decade, driven in large part by advancements in transcriptomics, has significantly shaped how we view the nervous and immune systems. One key finding was that microglia have distinct transcriptional signatures compared to other tissue-resident macrophages [48]. These signatures are strongly dependent on TGF-β1, a

molecule that regulates basal microglia phenotype through TGFBR1 and TGFBR2 [49]. In mice, loss of TGF-β signaling in microglia has been shown to cause microgliosis and fatal demyelinating disorder [50]. These studies imply that factors in the nerve environment are critical for maintaining microglial homeostasis. Single cell transcriptomic studies further showed that developmental microglia as well as activated microglia in neurodegenerative contexts downregulate homeostatic signatures and upregulate disease-associated genes [51,52]. These observations have sparked great interest in the regulation of homeostatic and activation-associated genes in microglia and their relevance for development, neuroinflammation, and disease susceptibility [52]. Targeting microglia to improve or prevent CNS diseases is a current topic of intense and exciting study.

1.4 PNS macrophages: a new frontier in neuroimmunology

In addition to the CNS, the nervous system also includes the peripheral nervous system (PNS), which represents the part of the nervous system that is outside of the brain and spinal cord. The PNS enables direct communication between the CNS and peripheral tissues and is therefore required for the body's ability to: 1) sense and respond to external stimuli through sensory and motor nerves; and 2) maintain homeostatic processes, including cardiovascular, immune, endocrine, digestive, and respiratory system regulation via autonomic nerves [53,54].

While the peripheral nervous system (PNS) also contains resident macrophages, they are much less characterized than brain microglia. Indeed, most existing research on PNS macrophages is based on histological studies following nerve injury. Early mouse studies of PNS macrophages dating back to observations by Olsson and Sjostrand in 1969 demonstrated that

after peripheral nerves are crushed, macrophages rapidly invade the site of trauma and the distal part of the nerve which undergoes Wallerian degeneration [55-57]. It was also noted at the time that activated macrophages in nerve injury appeared "foamy" likely as a result of phagocytosing myelin [58,59]. Besides clearing myelin, it was also suggested that peripheral nerve macrophages signal to Schwann cells and fibroblasts, and induced nerve growth [59]. Remarkably, many of these PNS macrophage functions have been shown decades later with modern techniques [60-62].

As it became clear that there existed both hematogenous macrophages that arise after injury and an endogenous macrophage compartment in normal nerves, attempts were made to determine their differential contributions after injury [63]. However, the limitation of precise lineage tracing tools has prevented accurate characterization of macrophage origins until recent years. Nevertheless, it was suggested in 1992 by Monaco and colleagues that resident endoneurial macrophages in the PNS were "microglial-like cells" that could act as the major antigen-presenting cells in the peripheral nerve given their constitutive MHC-II expression [59].

Despite the inherent similarity of PNS macrophages to CNS microglia by virtue of residing within the nervous system, little is known about their function or identity. Indeed, at the beginning of this dissertation work, there was no existing transcriptional profile of PNS macrophages. Key reasons for this may be the technical barrier of isolating PNS macrophages as well as prohibitive costs for transcriptomic sequencing. However, recent advancements in sequencing technologies have enabled much better sequencing of small samples at a much lower cost. It is at this point that my research begins. In the subsequent chapters, I describe my work to investigate PNS macrophages and compare them with their counterparts in the central nervous system (CNS).

1.5 References

1. Kaufmann, S.H. Immunology's coming of age. *Front. Immunol*. 10, 684 (2019).
2. Yona, S., and Gordon, S. From the reticuloendothelial to mononuclear phagocyte system - the unaccounted years. *Front. Immunol.* 6, 328 (2015).
3. Wynn, T.A., et al. Macrophage biology in development, homeostasis and disease. *Nature* 496, 445-55 (2013).
4. Van Epps H. L. Macrophage activation unveiled. *J. Exp. Med. 202*, 884 (2005).
5. Mosser, D. and Edwards, J. Exploring the full spectrum of macrophage activation. *Nat. Rev. Immunol.* 8, 958–969 (2008).
6. Lanzavecchia, A., and Sallusto, F. Regulation of T cell immunity by dendritic cells. *Cell* 106, 263-6 (2001).
7. Mosser, D., and Edwards, J. Exploring the full spectrum of macrophage activation. *Nat. Rev. Immunol.* 8, 958–969 (2008).
8. Crotty, S. T follicular helper cell differentiation, function, and roles in disease. *Immunity* 41, 529-42. (2014).
9. Marks S.C., and Lane, P.W. Osteopetrosis, a new recessive skeletal mutation on chromosome 12 of the mouse. *J. Hered*. 67, 11-18 (1976).
10. Fantin A., et al. Tissue macrophages act as cellular chaperones for vascular anastomosis downstream of VEGF-mediated endothelial tip cell induction. *Blood* 116, 829-40 (2010).
11. Wynn, T.A., et al. Macrophage biology in development, homeostasis and disease. *Nature* 496, 445-55 (2013).
12. Elliott, M.R., et al. Efferocytosis signaling in the regulation of macrophage inflammatory responses. *J. Immunol.* 198, 1387-94 (2017).
13. Nagata, S., et al. Autoimmunity and the clearance of dead cells. *Cell* 140, 619-30 (2010).
14. Savill, J., et al. A blast from the past: clearance of apoptotic cells regulates immune responses. *Nat. Rev. Immunol*. 2, 965-47 (2002).
15. Olefsky, J.M., and Glass, C.K. Macrophages, inflammation, and insulin resistance. *Annual review of physiology* vol. 72 (2010): 219-46.
16. Moore, K.J., et al. Macrophages in atherosclerosis: a dynamic balance. *Nat. Rev. Immunol*. 13, 709-21 (2013).

17. Kim, K., et al. Transcriptome analysis reveals nonfoamy rather than foamy plaque macrophages are proinflammatory in atherosclerotic murine models. *Circ. Res*. 123, 1127-42 (2018).
18. Yan J., and Horng, T. Lipid metabolism in regulation of macrophage functions. *Trends Cell. Biol*. 30, 979-89 (2020).
19. Volkman A., and Gowans, J.L. The origin of macrophages from the bone marrow in the rat. *Br. J. Exp. Pathol.* 46, 62–70 (1965).
20. Ginhoux F. and Guilliams M. Tissue-resident macrophage ontogeny and homeostasis. *Immunity* 44, 439-449 (2016).
21. Hashimoto, D., et al. Tissue-resident macrophages self-maintain locally throughout adult life with minimal contribution from circulating monocytes. *Immunity* 38, 792-804 (2013).
22. Gomez Perdiguero, E., et al. Tissue-resident macrophages originate from yolk-sac-derived erythro-myeloid progenitors. *Nature* 518, 547-551 (2015).
23. Springer, T., et al. Mac-1: a macrophage differentiation antigen identified by monoclonal antibody. *Eur. J. Immunol*. 9, 301-6 (1979).
24. Austyn, J.M., and Gordon, S. F4/80, a monoclonal antibody directed specifically against the mouse macrophage. *Eur. J. Immunol*. 11, 805-15 (1981).
25. Dijkstra, C.D., et al. The heterogeneity of mononuclear phagocytes in lymphoid organs: distinct macrophage subpopulations in the rat recognized by monoclonal antibodies ED1, ED2 and ED3. *Immunology* 54, 589-99 (1985).
26. Nathan, C.F., et al. Identification of interferon-gamma as the lymphokine that activates human macrophage oxidative metabolism and antimicrobial activity. *J. Exp. Med.* 158, 670–689 (1983).
27. Celada, A., et al. Evidence for a gamma-interferon receptor that regulates macrophage tumoricidal activity. *J. Exp. Med.* 160, 55–74 (1984).
28. Stein, M., et al. Interleukin 4 potently enhances murine macrophage mannose receptor activity: a marker of alternative immunologic macrophage activation. *J. Exp. Med.* 176, 287–292 (1992).
29. Mills, C.D., et al. M-1/M-2 macrophages and the Th1/Th2 paradigm. *J. Immunol.* 164, 6166-73 (2000).

30. Weber, A.P.M. Discovering new biology through Sequencing of RNA. *Plant Physiol*. 169, 1524-31 (2015).
31. The Immunological Genome Project., et al. ImmGen at 15. *Nat. Immunol.* 21, 700–703 (2020).
32. Nutma, E., et al. Neuroimmunology – the past, present and future. *Clin*. *Exp. Immunol.* 197, 278-293 (2019).
33. Babeş, V.M. Certains caractères des lesions histologiques de la rage [Certain characteristics of the histological lesions of rabies]. *Annales de l'Institut Pasteur*. 6, 209–23 (1892).
34. Alzheimer, A. Über einen eigenartigen schweren erkrankungsprozeβ der hirnrincle. *Neurol. Cent.* 25, 1134 (1906).
35. Dawson, J.W. The histology of disseminated sclerosis. *Edinb. Med. J*. 17, 229-241 (1916).
36. Li, Q. and Barres, B.A. Microglia and macrophages in brain homeostasis and disease. *Nat. Rev. Immunol.* 18, 225-242 (2018).
37. Wang, Y., et al. IL-34 is a tissue-restricted ligand of CSF1R required for the development of Langerhans cells and microglia. *Nat. Immunol.* 13, 753-760 (2012).
38. Birgit O. et al. Chapter 3 - The blood–brain barrier, *Handbook of Clinical Neurology*, 133, 39-59 (2016).
39. Zhou, X., et al. Microglia and macrophages promote corralling, wound compaction and recovery after spinal cord injury via Plexin-B2. *Nat. Neurosci.* 23, 337–350 (2020).
40. Chhatbar, C., and Prinz, M. The roles of microglia in viral encephalitis: from sensome to therapeutic targeting. *Cell. Mol. Immunol.* 18, 250–258 (2021).
41. Loane, D.J., and Byrnes, K.R. Role of microglia in neurotrauma. *Neurotherapeutics* 7, 366-77 (2010).
42. Rademakers R., et al. Mutations in the colony stimulating factor 1 receptor (CSF1R) gene cause hereditary diffuse leukoencephalopathy with spheroids. *Nat. Genet*. 44, 200–5 (2011).
43. Paloneva J., et al. Mutations in two genes encoding different subunits of a receptor signaling complex result in an identical disease phenotype. *Am. J. Hum. Genet.* 71, 656–62 (2002).
44. Kleinberger G., et al. TREM2 mutations implicated in neurodegeneration impair cell surface transport and phagocytosis. *Sci. Transl. Med*. 6, (2014).
45. Goldmann T., et al. USP18 lack in microglia causes destructive interferonopathy of the mouse brain. *EMBO J.* 34, 1612–29 (2015).

46. Meuwissen M.E., et al. Human USP18 deficiency underlies type 1 interferonopathy leading to severe pseudo-TORCH syndrome. *J. Exp. Med.* 213, 1163–74 (2016).
47. Mass E., et al. A somatic mutation in erythro-myeloid progenitors causes neurodegenerative disease. *Nature* 549, 389–93 (2017).
48. Gautier, E. L., et al. Gene-expression profiles and transcriptional regulatory pathways that underlie the identity and diversity of mouse tissue macrophages. *Nat. Immunol.* 13, 1118-1128 (2012).
49. Butovsky, O., et al. Identification of a unique TGF-beta-dependent molecular and functional signature in microglia. *Nat. Neurosci.* 17, 131-143 (2014).
50. Qin, Y., et al. A milieu molecule for TGF-β required for microglia function in the nervous system. *Cell* 174, 156-171 (2018).
51. Keren-Shaul, H., et al. A unique microglia type associated with restricting development of Alzheimer's Disease. *Cell* 169, 1276-1290 (2017).
52. Deczkowska, A., et al. Disease-associated microglia: a universal immune sensor of neurodegeneration. *Cell* 173, 1073-1081 (2018).
53. Ordovas-Montanes, J., et al. The regulation of immunological processes by peripheral neurons in homeostasis and disease. *Trends Immunol*. 36, 578-604 (2015).
54. McCorry L.K. Physiology of the autonomic nervous system. *Am. J. Pharm. Educ.* 71, (2007).
55. Olsson, Y., and Sjöstrand, J. Origin of macrophages in Wallerian degereration of peripheral nerves demonstrated autoradiographically. *Exp. Neurol*. 23, 102-12 (1969).
56. Perry, V.H. et al. The macrophage response to central and peripheral nerve injury. A possible role for macrophages in regeneration. *J. Exp. Med*. 165, 1218-23 (1987).
57. Stoll G., et al. Wallerian degeneration in the peripheral nervous system: participation of both Schwann cells and macrophages in myelin degradation. *J. Neurocytol*. 18, 671-83 (1989).
58. Griffin J.W., et al. Macrophage responses in inflammatory demyelinating neuropathies. *Ann. Neurol*. 27, (1990).
59. Monaco S. et al. MHC-positive, ramified macrophages in the normal and injured rat peripheral nervous system. *J. Neurocytol.* 21, 623-34 (1992).
60. Stratton, J. A., et al. Macrophages regulate Schwann cell maturation after nerve injury. *Cell Rep.* 24, 2561-2572 (2018).

61. Cattin, A. L., et al. Macrophage-induced blood vessels guide Schwann cell-mediated regeneration of peripheral nerves. *Cell* 162,1127-1139 (2015).
62. Hervera, A., et al. Reactive oxygen species regulate axonal regeneration through the release of exosomal NADPH oxidase 2 complexes into injured axons. *Nat. Cell Biol.* 20, 307–319 (2018).
63. Mueller, M., et al. Macrophage response to peripheral nerve injury: the quantitative contribution of resident and hematogenous macrophages. *Lab. Invest.* 83, 175-185 (2003).

2. Identification and transcriptional characterization of peripheral nerve resident macrophages

The work described in this chapter was published in the journal *Nature Communications* under the following citation:

Wang PL, Yim AKY, Kim KW, Avey D, Czepielewski RS, Colonna M, Milbrandt J, Randolph GJ. Peripheral nerve resident macrophages share tissue-specific programming and features of activated microglia. *Nat Commun*. 2020 May 21;11(1):2552.

AUTHOR CONTRIBUTIONS: P.L.W. purified macrophage populations, designed, and performed the experiments, analyzed data, and wrote the manuscript. A.Y. analyzed RNA-seq data and helped with experiments and writing of the manuscript. K.K. purified macrophage populations and discussed results. D.A. and R.C. helped with experiments and discussed results. M.C. provided conceptual feedback and the IL-34$^{-/-}$ strain. G.J.R. and J.M. designed and supervised the experiments, acquired funding, and edited the manuscript. The Immunological Genome Project set standards for data acquisition, conducted sequencing, QC, and generation of raw data for bulk RNA samples.

2.1 Introduction

The significant role of resident neural macrophages in neuroinflammation and disease progression is increasingly appreciated in mouse models and individuals with neurodegeneration [1-3]. Such advances, which largely rely on the interpretation of data from transcriptional analyses and human genome-wide association studies of Alzheimer's disease (AD) and other neurodegenerative conditions, have led to critical findings about cellular and molecular processes underlying such diseases [4-6]. Most of these studies, however, have focused on resident macrophages in the brain (microglia) and, to a lesser extent, the spinal cord. Meanwhile, the transcriptional identity and functions of resident macrophages in the peripheral nervous system (PNS) remain mostly unknown.

The PNS consists of a multitude of neuronal networks that relay motor and sensory information between the central nervous system (CNS) and the rest of the body [7]. Although it has the capacity to regenerate, the PNS is also prone to injury and degeneration[8]. Studies of PNS injury have shown that PNS macrophages play important roles for debris clearance, pain development, and regeneration [9-11]. While the contribution of recruited monocytes cannot be excluded, these studies demonstrate the importance of PNS macrophages in nerve injury. Understanding the roles of these cells in homeostasis and disease may be broadly beneficial for resolving neuroinflammation.

In addition to monocyte-derived macrophages in nerve injury, there are also resident macrophages in the PNS at steady state [12,13] . While their residence in neuronal tissues is inherently microglia-like, PNS macrophages exist within a unique peripheral nerve microenvironment. Here we show that self-maintaining PNS-resident macrophages are a distinct population with transcriptional signatures relating to specific functions in neuronal tissue. PNS

macrophages significantly express genes that resemble not only homeostatic microglia but also activated microglia from aging and neurodegenerative conditions. These findings highlight shared and unique transcriptional programs in neural resident macrophages.

2.2 Results

2.2.1 PNS macrophages are self-maintained resident cells

To examine resident macrophages in the PNS, we imaged a variety of nerve types at steady state using CX3CR1GFP/+ reporter mice. In these mice, green fluorescent protein (GFP) effectively labels microglia and has been shown to label nerve-associated macrophages in adipose, skin, lung, and enteric tissues [14-18]. CX3CR1GFP/+ cells in peripheral nerves were ramified with elongated cytoplasmic processes and appeared to be in direct contact with blood vessels, Schwann cells, and endoneurial fibroblasts (Fig. 1). CX3CR1GFP/+ cells were found in dorsal root ganglia (DRG), vagal nerves (VNs), cutaneous intercostal fascial nerves (FNs), and sciatic nerves (SNs) (Fig. 2a). CX3CR1GFP/+ cells were located in the endoneurium (Fig. 2b) and expressed CSF1R, also known as CD115 (Fig. 2c). As expected, these cells were susceptible to CSF1R signaling blockade, as administration of a monoclonal antibody to CSF1R effectively depleted them in nerves (Fig. 3). Using flow cytometry, we found that CX3CR1GFP/+ cells also expressed the common macrophage marker CD64 (FcγR1) [19] and intermediate levels of CD45 (Fig. 2d–f). Thus, CX3CR1GFP/+ cells in peripheral nerves are indeed macrophages with resemblance to CNS microglia based on both endoneurial localization and surface marker expression

To determine whether PNS macrophages depend on circulating precursors or are maintained via local signals, we performed parabiosis in CD45.1+ wild type and CD45.2+ Lyz2Cre × tdTomatofl/fl mice, and assessed the extent to which cells circulating from the parabiotic partner gave rise to PNS macrophages. Ten weeks after joining the parabionts, we found minimal exchange of PNS macrophages in all of the nerve types examined, whereas blood T cells and monocytes exchanged robustly (Fig. 2g and Fig. 4). Indeed, most of the tdTomato+ cells that could be seen in the wild-type parabiont were localized to the tissue surrounding the nerves (Fig. 2h). We also performed pulse-chase labeling of PNS macrophages using tamoxifen-inducible CSF1RMer-iCre-Mer × tdTomatofl/fl mice. In these mice, tdTomato expression persists in self-maintaining cells, but not in monocytes, which mostly turn over by 3–4 weeks after tamoxifen removal [20,21]. Heterozygous mice were fed tamoxifen diet for 4 weeks and then switched to normal diet (Fig. 2i). Just following tamoxifen removal, 96% of PNS macrophages (pooled from all PNS sites), 99% of CNS microglia, and 100% of blood monocytes were tdTomato+ (Fig. 2j–l and Fig. 5). Whereas only 20% of nonclassical and classical monocytes were still tdTomato+ by 3 weeks after tamoxifen removal, 98% of CNS microglia and 95% of pooled PNS macrophages remained labeled up to 8 weeks following tamoxifen removal (Fig. 1l and Supplementary Fig. 2). Taken together, these results indicate that PNS macrophages are mostly self-maintained in adult mice.

2.2.2 Transcriptional characterization of PNS macrophages

As we and others have previously demonstrated, unique gene expression profiles can be obtained in tissue-resident macrophage populations across tissue types [19,22]. To identify signature genes in peripheral nerve macrophages, we performed bulk RNA sequencing (RNA-seq) to

compare purified PNS resident macrophages sorted from DRG, VN, cutaneous intercostal FN, and SNs (Fig. 6) with CNS microglia from the brain and spinal cord, as well as previously characterized conventional macrophage populations from the spleen, peritoneal cavity, and lungs. Global transcriptomic analysis revealed similarities within resident neural macrophages from both PNS and CNS, with PNS macrophages clustering more closely to CNS microglia than to conventional macrophages (Fig. 7a). A substantial number of genes were uniquely enriched in PNS macrophages and CNS microglia compared with the other tissue-resident macrophages, including microglial signature genes *Tmem119*, *P2ry12*, *Siglech*, *Trem2*, and *Olfml3* (Fig. 7b, c). PNS macrophage-specific genes were also identified (Fig. 7b).

To determine potential functions of PNS macrophages associated with their shared and unique gene expression profiles, we performed Gene Ontology analysis on transcripts that were common between PNS macrophages and CNS microglia, and those that were specific to PNS macrophages. Consistent with the idea that PNS macrophages may share functions with CNS microglia, pathway analysis identified functions including synaptic plasticity, microglial motility, and positive regulation of neurogenesis (Fig. 7d). Pathways that were unique to PNS macrophages included angiogenesis, collagen fibril organization, regulation of BMP signaling, and peripheral nerve structural organization and axon guidance (Fig. 7e).

Next, we identified transcripts that were 4-fold or more enriched in CNS microglia and PNS macrophages relative to their expression in all other conventional macrophage populations (Fig. 7f). These upregulated genes included *Abhd6*, *Ophn1*, *P2rx7*, *Pld1*, *Sgce*, *Tgfbr1*, *Tfpi*, and *Tmem173*. We also identified several genes that were downregulated in CNS microglia and PNS macrophages (Fig. 8). Notably, the transcriptional regulator that defines microglial identity and function, *Sall1*, was not expressed by PNS macrophages (Fig. 7c). Modest detection

of *Sall1* in the DRG could not be corroborated by further analysis (Fig. 9). This may reflect unique adaptations in PNS and CNS macrophages. Indeed, we identified 72 genes, including *Sall1*, which were highly specific to CNS microglia (Fig. 10).

To examine unique gene expression in PNS macrophages, we identified transcripts that were at least fourfold higher or lower in PNS macrophages compared with other resident macrophages, including CNS microglia (Fig. 7g and Fig. 11). We found 48 genes specifically enriched in PNS macrophages, including *Aplnr*, *Cp*, *Il1rl1*, *Maoa*, *Pla2g2d*, and *St8sia4*, as well as interferon-induced genes *Ifi202b*, *Ifi211*, and *Oas2*. We also identified *Ms4a14*, *Ms4a4a*, *Ms4a4c*, *Ms4a6c*, and *Ms4a7*. These signatures reveal unique transcriptional programming in PNS macrophages and may provide clues about their involvement in neuronal health and disease.

We next investigated transcriptional differences within PNS macrophage populations (Fig. 12). Using a fourfold cutoff, we identified 24 genes enriched in SN macrophages, 23 genes enriched in cutaneous intercostal (fascial) nerve macrophages, and 12 genes enriched in VN macrophages. We observed similar numbers of downregulated genes in each population. We also compared nerve-resident macrophages to those residing within the dorsal root ganglion and found that they were significantly different, with many differentially expressed transcripts. Therefore, we re-analyzed this data using a more stringent 8-fold cutoff and identified 79 upregulated genes and 52 downregulated genes. These results suggest that although PNS macrophages are transcriptionally similar, significant differences exist between those adjacent to axons and those residing close to neuronal cell bodies.

2.2.3 PNS macrophages constitutively express transcripts associated with activated microglia

To investigate differentially expressed genes (DEGs) within resident neural macrophages, we refined our analysis to CNS microglia and PNS macrophages (Fig. 13a). We identified 396 genes enriched in PNS macrophages and 180 genes enriched in CNS microglia. As the upregulation of *MS4A* family and interferon-induced genes has been reported to characterize aged and neurodegenerative disease-associated microglia [6,23,24], we wondered whether PNS macrophages expressed other genes associated with microglial activation. By cross-referencing published data [6], we determined the number of connections between disease-associated genes that were upregulated in activated microglia from aging, phagocytic, and neurodegenerative conditions and neural macrophage-enriched genes from either PNS macrophages or CNS microglia (Fig. 13b). We found 148 disease-associated genes that were enriched in PNS macrophages compared to 17 that were enriched in CNS microglia (Fig. 13b). From the highest connectivity groups 6–4, we identified 25 genes that were significantly higher in PNS macrophages, including *Ch25h*, *Anxa2*, *Cd52*, *Ifitm3*, *Cybb*, *Fxyd5*, *Igf1*, and *Apoe*(Fig. 13c).

Microglia lacking certain genes for homeostatic regulation have also been found to shift their gene expression towards an activated phenotype [25,26]. *Sall1* has been identified as a transcriptional regulator of microglia identity and function, with Sall1$^{-/-}$ microglia resembling inflammatory phagocytes [25]. As PNS macrophages did not express *Sall1*at steady state, we examined whether genes that are reportedly dysregulated in Sall1$^{-/-}$ microglia showed the same pattern of expression in PNS macrophages. Indeed, we found a high correlation between genes enriched in PNS macrophages and Sall1$^{-/-}$ microglia, including *Apoe*, *H2-Aa*, *Ms4a7*, *Clec12a*, *Aoah*, and *Cybb* (Fig. 13d). These data suggest that, beyond the difference in *Sall1*-driven gene expression, PNS macrophages may share common genetic regulators with CNS microglia.

As microglia activation may occur under cell sorting conditions [27], we were concerned that the activation signature in PNS macrophages might be attributed to tissue preparation. Thus, we stained freshly fixed peripheral nerves for Clec7a and MHCII, which are induced in microglia across many activation states [6,26,28]. Resting PNS macrophages were clearly marked by Clec7a and MHCII (Fig. 13e), suggesting that the signature obtained in PNS macrophages is not a technical artifact that arose from activation induced by disaggregation of tissue. Since microglial activation signatures have been associated with phagocytosis of nerve material [6], we speculated that PNS macrophages may be more phagocytic compared to microglia. To test this, we assessed fluorescent bead uptake in microglia and sciatic nerve macrophages. Indeed, we saw that a higher proportion of sciatic nerve macrophages (23%) engulfed beads compared to brain microglia (0.2%) (Fig. 14). Taken together, these data show that PNS macrophages not only express a wide array of microglial activation genes at steady state, but also appear to be more phagocytic than CNS microglia.

2.2.4 Zonation of PNS macrophage-enriched transcripts in neural resident macrophages

Given the difference in gene expression between PNS macrophages and CNS microglia, we wanted to further discriminate the influence of microenvironment on neural macrophage identity. Thus, we examined spinal cord microglia, which reside in a distinct microenvironment from brain microglia. Interestingly, we found a set of genes that were high in PNS macrophages, intermediate to high in spinal cord microglia and low in brain microglia (PNS to CNS zonation) (Fig. 15a). These included PNS macrophage-specific genes (*Cp*, *Il1rl1*, *Maoa*, and *Cdr2*), microglial activation genes (*Clec7a*, *Spp1*, *Lpl*, *Axl*, *Ms4a4c*, and *Ms4a6c*), interferon-induced

genes (*Ifi204*, *Ifi207*, *Ifi209*, and *Oasl2*), mitochondrially encoded genes (*mt-Nd1*, *mt-Nd2*, *mt-Nd4*, *mt-Nd5*, and *mt-Nd6*), and several transcription factors (*Hivep2*, *Zfp704*, and *Rbpj*) (Fig. 15b, c). While we confirmed Clec7a expression in spinal cord microglia by immunostaining (Fig. 15c), Clec7a+ microglia appeared to be confined to areas of white matter, suggesting that activation-associated genes in spinal cord microglia may be specific to myelinated regions (Fig. 16). Importantly, microglia from spinal cord and brain did not significantly differ by expression of homeostatic genes *Sall1*, *Olfml3*, and *Tmem119* (Fig. 17). In fact, certain microglial genes, including *Tgfbr1* and *P2ry12*, were more highly expressed in spinal cord compared with brain microglia. These findings suggest that transcriptional programs underlying PNS macrophages and activated microglia may be present during normal physiological conditions and further support the role of nerve environment for specifying neural macrophage identity.

2.3 Discussion

Here we characterized the transcriptomes of PNS resident macrophages across various nerve types spanning both axons and cell bodies and innervating a wide range of somatic targets. We show that self-maintaining PNS macrophages lack expression of the master regulator Sall1 conferring CNS microglial identity, but nonetheless express a substantial number of genes that define homeostatic and activated microglia.

Our findings demonstrating that PNS macrophages share a significant overlap in gene expression with CNS microglia are in line with recent findings that show microglial genes being expressed in nerve-associated macrophages in gut, skin, and adipose tissues [14-17]. Given that our study focuses on PNS macrophages residing in the nerve proper whereas these studies examined macrophages positioned in close proximity to nerves, including nerve termini, it seems likely

that common tissue-derived factors may induce nerve-imprinted signatures in macrophages along the entire neuron. One such factor may be transforming growth factor-β (TGF-β). TGF-β signaling is vital for the expression of homeostatic genes in microglia [2,5]. The higher expression of *Tgfbr1* in PNS macrophages and CNS microglia at steady state supports the role of TGF-β signaling in neural resident macrophages.

Although common instructive signals may exist, *Sall1* expression was very low to absent in PNS macrophages. This likely represents a key difference in PNS and CNS nerve environments. The identification of additional genes that were purely expressed in CNS microglia may provide clues for the basis of this difference. Future studies should address genetic and environmental factors that regulate *Sall1*expression and examine whether it is expressed in a context-dependent manner in PNS macrophages.

The constitutive expression of a broad set of microglial activation genes in PNS macrophages and, to a lesser degree, in spinal cord microglia suggests that such programs may be intrinsic to their functioning in distinct neuronal environments. Indeed, it was found that sympathetic nerve-associated macrophages and macrophages at CNS interfaces also appear to be constitutively activated [14,29,30]. In addition, an overlap in many of the same activation genes are induced in phagocytic microglia localized to white matter tracts during brain development [31]. In addition to their role in phagocytic functions, activation-associated genes may also play a role in pathogen response. This is supported by the recent finding that nerve-associated macrophages residing in lungs readily respond to viral infection [18]. Further studies are needed to determine whether immune response to pathogens or phagocytic and tissue remodeling programs are more prevalent at steady state in PNS macrophages.

2.4 Materials and methods

Experimental animals

Mouse care and experiments were performed in accordance with protocols approved by the Institutional Animal Care and Use Committee at Washington University in St. Louis under the protocols 20170154 and 20170030. Mice were kept on a 12 h light–dark cycle and received food and water ad libitum. The following strains were used: C57/B6 CD45.1 (stock number 002014), CX3CR1$^{GFP/+}$(Cx3cr1tm1Litt/LittJ; stock number 008451), LysM$^{cre/+}$ (stock number 004781), and Rosa$^{Lsl\text{-}Tomato}$ (stock number 007905) mice were purchased from Jackson Laboratory (JAX) and bred at Washington University. CSF1R$^{Mer\text{-}iCre\text{-}Mer}$ mice [32] were obtained from JAX (stock number 019098) and backcrossed fully to C57BL/6 background using the speed congenics core facility at Washington University. MPZ-Cre mice, previously described [33], were crossed with CX3CR1$^{GFP/+}$ mice. Sall1-^{GFP}mice [25,34] were kindly provided by M. Rauchman.

Immunohistochemistry

For whole-mount imaging, samples were harvested and immediately stored in 4% paraformaldehyde (PFA) containing 40% sucrose overnight. Samples were then washed in phosphate-buffered saline (PBS), blocked, stained, and imaged. For frozen sections, samples were collected, stored in PFA/sucrose, and embedded into optimal cutting temperature compound. Fifteen-micrometer cuts were made for SNs. Sections were then blocked in 1% bovine serum albumin, stained, and imaged. Antibodies to the following proteins were used: anti-GFP, Clec7a (Clone R1-8g7), CSF1R (R&D Systems, accession number P09581), MHCII (IA/IE clone M5/114.15.2), and LYVE1 (ab14917).

Preparation of single-cell suspensions

For blood, mice were bled from the cheek immediately before killing and cells were prepared as previously described. For nerves and all other tissues, mice were killed and perfused with PBS. Nerves were collected and kept on ice until dissociation. For ImmGen samples, nerves from 4 to 20 mice were pooled for each replicate. Cells were then incubated with gentle shaking for 20 min in digestion media containing collagenase IV, hyaluronidase, and DNAse. Cells were then washed and filtered through 70 μm cell strainers. For brain and spinal cord, myelin was removed using a 40/80% Percoll gradient.

Flow cytometry

Single-cell suspensions were stained at 4 °C. Dead cells were excluded by propidium idodide (PI). Antibodies to the following proteins were used: B220 (clone RA3-6B2), CCR2 (clone SA203G11), CD3e (clone 145-2C11), CD4 (clone RM4-5), CD8 (clone 53-6.7), CD11b (clone M1/70), CD16 (clone 2.4G2), CD45 (clone 30-F11), CD64 (clone X54-5/7.1), CD115 (clone AFS98), GR1 (clone 1A8), and Ly6C (clone HK1.4). Cells were analyzed on a LSRII flow cytometer (Becton Dickinson) and analyzed with FlowJo software.

Cell sorting

For bulk RNA-seq, cells from 6-week-old male mice were double sorted on a FACSAria II (Becton Dickinson) for a final count of 1000 cells into lysis buffer according to the ImmGen Consortium standard operating protocol. Tissues were collected into culture medium on ice and subsequently digested with collagenase IV, hyaluronidase, and DNAse. Following digestion, samples were washed and kept on ice until sorting. The sort was repeated so that all

macrophages were sorted twice, with a minimum of 1000 cells recovered. During the second round, cells were sorted directly into 5 µl TCL buffer (Qiagen) containing 5% beta-mercaptoethanol. Samples were kept at −80 °C until further processing.

Parabiosis

Parabiotic pairs were generated as previously described [35]. C57/B6 (CD45.1) mice were paired with Lyz2Cre tdTomato (CD45.2) mice. Mice were injected with buprenorphine-SR subcutaneously prior to surgery. After 10 weeks, mice were killed and nerve tissue was examined by flow cytometry and imaging to detect hematopoietic contribution to PNS resident macrophages. T cells in blood was used as a positive control.

Antibody depletion

Adult mice were injected intraperitoneally (i.p.) with anti-CSF1R monoclonal antibody (mAb) at a concentration of 2mg per animal. 10 days later, mice were sacrificed for imaging and flow cytometric analysis.

Pulse chase

Male and female heterozygous $CSF1R^{Mer\text{-}iCre\text{-}Mer}$ tdTomato were fed tamoxifen diet for 4 weeks to label resident cells. Blood was collected at day 0, 3 weeks, 4 weeks, and 8 weeks after tamoxifen removal. Peripheral nerves from SNs, FNs, VNs, and DRG were pooled (PNS) and examined along with pooled brain and spinal cord (CNS) by flow cytometry at day 0 and 8 weeks following tamoxifen removal.

Bead uptake assay

Brains and sciatic nerve tissues were collected from CX3CR1GFP/+ mice and minced. Tissues were then digested with Collagenase IV for 30 minutes at 37 degrees Celsius, during which time the same amount of red fluorescent latex beads were added to brain and sciatic nerve homogenates. Samples were then prepared normally for flow cytometry as previously described .

RNA-seq and data analyses

Library preparation, RNA-seq, data generation and quality-control was conducted by the ImmGen Consortium according to the consortium's standard protocols (https://www.immgen.org/Protocols/ImmGenULI_RNAseq_methods.pdf). In short, the reads were aligned to the mouse genome GRCm38/mm10 primary assembly and gene annotation vM16 using STAR 2.5.4a. The raw counts were generated by using featureCounts (http://subread.sourceforge.net/). Normalization was performed using the DESeq2 package from Bioconductor. Differential gene expression analysis was performed using edgeR 3.20.9 in a pairwise manner among all conditions, and a total of 12,240 DEGs were defined with a *p*-value ≤ 0.001 and $\geq$4-fold difference. To construct the correlation plot, Euclidean distance among samples were calculated based on the differential expression matrix and clustering was performed using the ward.D2 algorithm in R. CNS/PNS shared, PNS-specific, and CNS-specific genes were determined by subclustering the DEGs based on the expression pattern with a refined *k*-mean clustering using R followed by manual curations. Expression data was visualized using Morpheus (https://software.broadinstitute.org/morpheus). For neuronal microenvironment analysis, only the transcriptome profile of macrophages and microglia from PNS and CNS were used and analyzed through the same pipeline as mentioned above.

Comparison of published microglia data

External datasets for circos plot were obtained from Krasemann et al. [6]. Genes that are enriched in SOD1G93A, aging brain, MFP2$^{-/-}$, brain irradiation, AD (5XFAD), and phagocytic microglia conditions were previously generated in Krasemann et al. [6]. By comparing the PNS- and CNS-enriched genes with the disease signatures, we were able to define the number of conditions shared by the genes and coined the term as "connectivity". Only genes with connectivity of two or above are shown in the circos plot. For the comparison with Sall1$^{-/-}$ data set [21], the $\log_2$ fold change of genes between CNS microglia and PNS macrophages were calculated and compared against the public data set. Correlation coefficient and *p*-value were calculated by lineregress in Scipy using Python3.

References

1. Keren-Shaul, H., et al. A unique microglia type associated with restricting development of Alzheimer's Disease. *Cell* 169, 1276-1290 (2017).
2. Li, Q. and B. A. Barres. Microglia and macrophages in brain homeostasis and disease. *Nat. Rev. Immunol.* 18, 225-242 (2018).
3. Frost, J. L. and D. P. Schafer. Microglia: architects of the developing nervous system. *Trends Cell Biol.* 26, 587-597 (2016).
4. Deczkowska, A., et al. Disease-associated microglia: a universal immune sensor of neurodegeneration. *Cell* 173, 1073-1081 (2018).
5. Butovsky, O., et al. Identification of a unique TGF-beta-dependent molecular and functional signature in microglia. *Nat. Neurosci.* 17, 131-143 (2014).
6. Krasemann, S., et al. The TREM2-APOE pathway drives the transcriptional phenotype of dysfunctional microglia in neurodegenerative diseases. *Immunity* 47, 566-581 (2017).

7. Kaucka, M. and I. Adameyko. Non-canonical functions of the peripheral nerve. *Exp. Cell Res.* 321, 17-24 (2014).
8. Chandran, V., et al. A systems-level analysis of the peripheral nerve intrinsic axonal growth program. *Neuron* 89, 956-970 (2016).
9. Klein, D. and R. Martini. Myelin and macrophages in the PNS: an intimate relationship in trauma and disease. *Brain Res.* 164, 130-138 (2016).
10. Shepherd, A. J., et al. Macrophage angiotensin II type 2 receptor triggers neuropathic pain. *Proc. Natl. Acad. Sci. USA* 115, E8057-E8066 (2018).
11. Cattin, A. L., et al. Macrophage-induced blood vessels guide Schwann cell-mediated regeneration of peripheral nerves. *Cell* 162,1127-1139 (2015).
12. Goodrum, J. F. and D. L. Novicki. Macrophage-like cells from explant cultures of rat sciatic nerve produce apolipoprotein E. *J. Neurosci. Res.* 20, 457-462 (1988).
13. Monaco, S., et al. MHC-positive, ramified macrophages in the normal and injured rat peripheral nervous system. *J. Neurocytol.* 21, 623-634 (1992).
14. Pirzgalska, R. M., et al. Sympathetic neuron-associated macrophages contribute to obesity by importing and metabolizing norepinephrine. *Nat. Med.* 23, 1309-1318 (2017).
15. De Schepper, S., et al. Self-maintaining gut macrophages are essential for intestinal homeostasis. *Cell* 175, 400-415 (2018).
16. Chakarov, S., et al. Two distinct interstitial macrophage populations coexist across tissues in specific subtissular niches. *Science* 363, (2019).
17. Kolter, J., et al. A subset of skin macrophages contributes to the surveillance and regeneration of local nerves. *Immunity* 50, 1482-1497 (2019).
18. Ural, B. B., et al. Identification of a nerve-associated, lung-resident interstitial macrophage subset with distinct localization and immunoregulatory properties. *Sci. Immunol.* 5, (2020).
19. Gautier, E. L., et al. Gene-expression profiles and transcriptional regulatory pathways that underlie the identity and diversity of mouse tissue macrophages. *Nat. Immunol.* 13, 1118-1128 (2012).
20. Dick, S. A., et al. Self-renewing resident cardiac macrophages limit adverse remodeling following myocardial infarction. *Nat. Immunol.* 20, 29-39 (2019).
21. Di Liberto, G., et al. Neurons under T cell attack coordinate phagocyte-mediated synaptic stripping. *Cell* 175, 458-471 (2018).

22. Lavin, Y., et al. Tissue-resident macrophage enhancer landscapes are shaped by the local microenvironment. *Cell* 159, 1312-1326 (2014).
23. Deming, Y., et al. The MS4A gene cluster is a key modulator of soluble TREM2 and Alzheimer's disease risk. *Sci. Transl. Med.* 11, (2019).
24. Friedman, B. A., et al. Diverse brain myeloid expression profiles reveal distinct microglial activation states and aspects of Alzheimer's disease not evident in mouse models. *Cell Rep.* 22, 832-847 (2018).
25. Buttgereit, A., et al. Sall1 is a transcriptional regulator defining microglia identity and function. Nat. Immunol. 17, 1397-1406 (2016).
26. Lund, H., et al. Fatal demyelinating disease is induced by monocyte-derived macrophages in the absence of TGF-beta signaling. *Nat. Immunol.* 19, 1-7 (2018).
27. Haimon, Z., et al. Re-evaluating microglia expression profiles using RiboTag and cell isolation strategies. *Nat. Immunol.* 19, 636-644 (2018).
28. Ziv, Y., et al. Immune cells contribute to the maintenance of neurogenesis and spatial learning abilities in adulthood. *Nat. Neurosci.* 9, 268-275 (2006).
29. Goldmann, T., et al. Origin, fate and dynamics of macrophages at central nervous system interfaces. *Nat. Immunol.* 17, 797-805 (2016).
30. Van Hove, H., et al. A single-cell atlas of mouse brain macrophages reveals unique transcriptional identities shaped by ontogeny and tissue environment. *Nat. Neurosci.* 22, 1021-1035 (2019).
31. Li, Q., et al. Developmental heterogeneity of microglia and brain myeloid cells revealed by deep single-cell RNA sequencing. *Neuron* 101, 207-223 (2019).
32. Qian, B. Z., et al. CCL2 recruits inflammatory monocytes to facilitate breast-tumour metastasis. *Nature* 475, 222-225 (2011).
33. Feltri, M. L., et al. P0-Cre transgenic mice for inactivation of adhesion molecules in Schwann cells. *Ann. NY Acad. Sci*. 883, 116-123 (1999).
34. Takasato, M., et al. Identification of kidney mesenchymal genes by a combination of microarray analysis and Sall1-GFP knockin mice. *Mech. Dev*. 121, 547-557 (2004).
35. Kim, K. W., et al. MHC II+ resident peritoneal and pleural macrophages rely on IRF4 for development from circulating monocytes. *J. Exp. Med.* 213, 1951-1959 (2016).

Figures

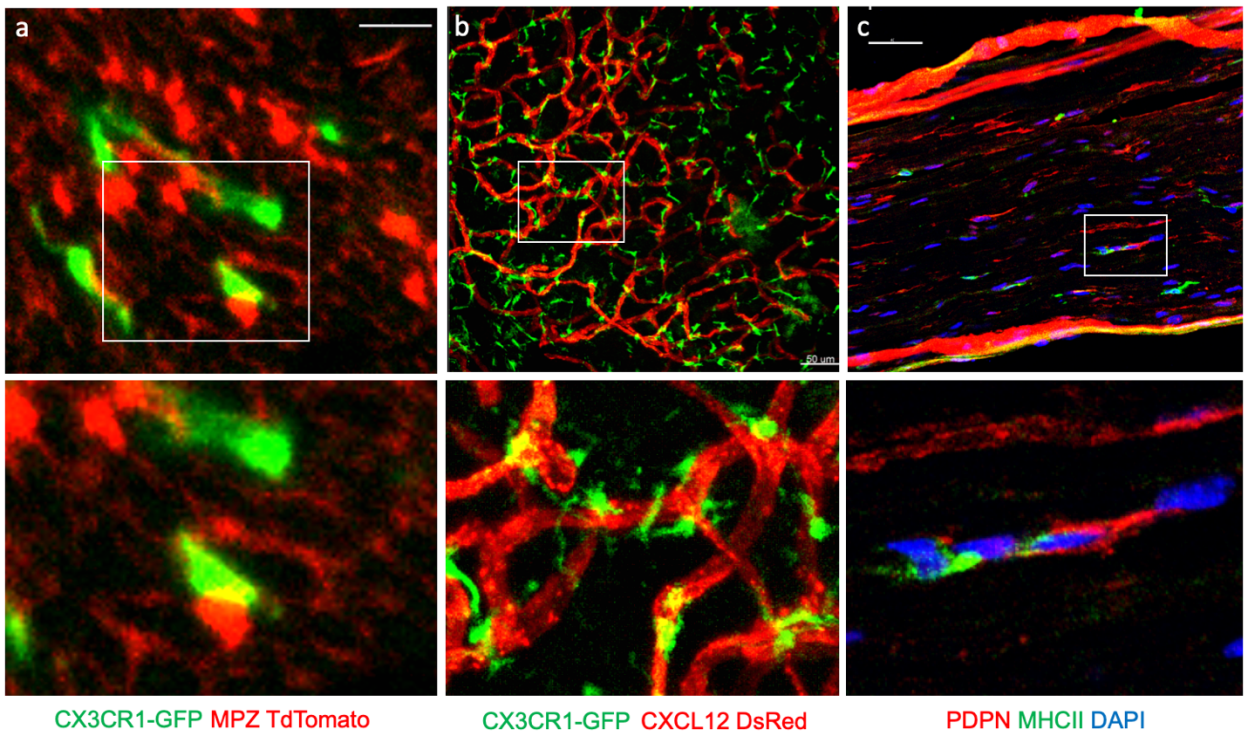

Figure 1. PNS macrophages are in close contact with Schwann cells, vasculature, and endoneurial fibroblasts. a Confocal imaging of PNS macrophages in close contact with Schwann cells in transverse section of sciatic nerve from CX3CR1$^{GFP/+}$MPZ^{tdTomato} mice. b PNS macrophages in close contact with DRG vasculature in CXCL12DsRed mice. c MHCII+ PNS macrophages in contact with PDPN+ fibroblasts in sciatic nerve.

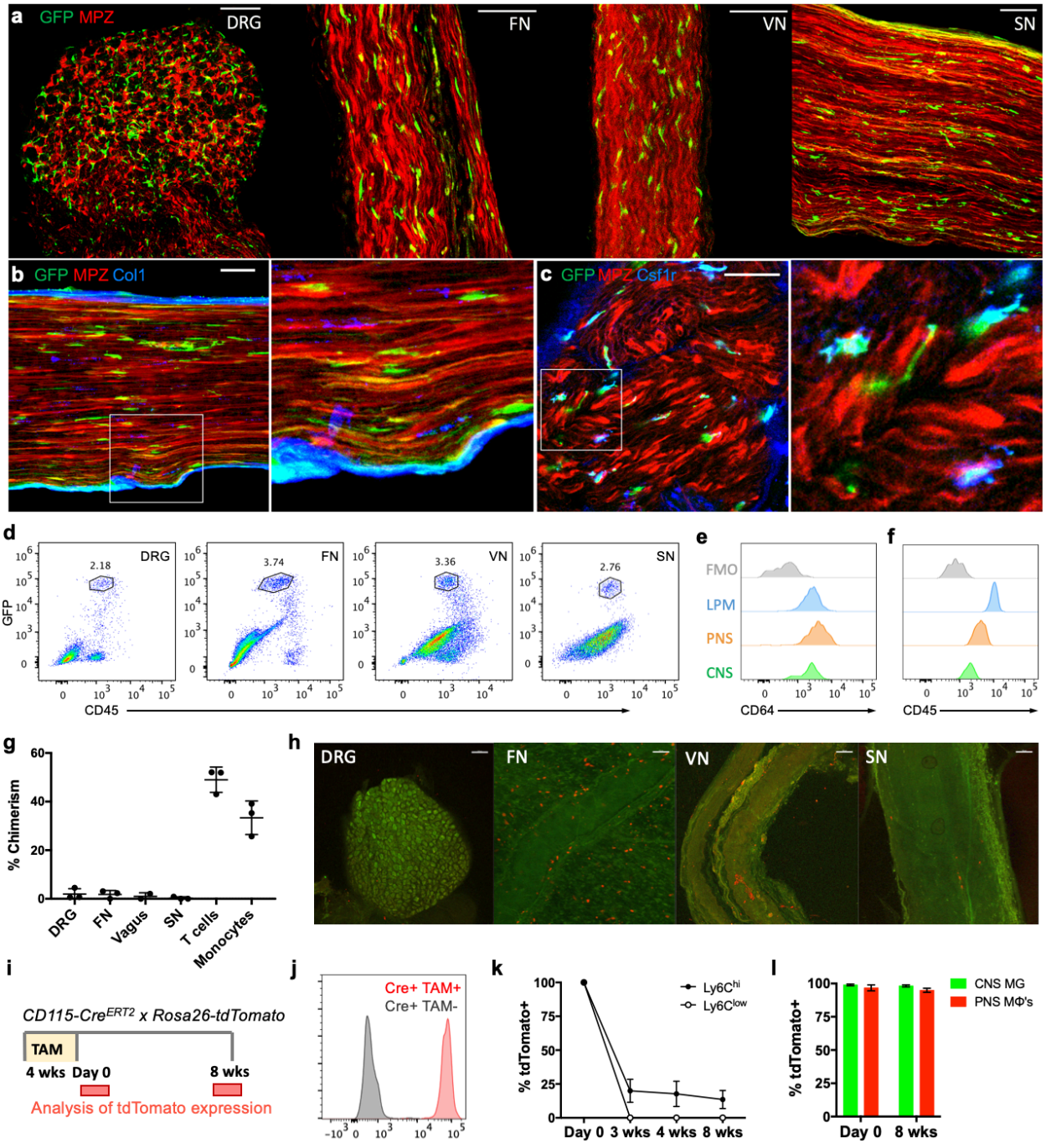

Figure 2. Identification and characterization of PNS resident macrophages. a–c Representative confocal imaging of peripheral nerves from CX3CR1$^{GFP/+}$MPZ^{tdTomato} mice (tomato from MPZ depicted here in blue). **a** Images of whole-mount dorsal root ganglia (DRG), cutaneous fascial (FN), vagal (VN), and sciatic nerves (SN) isolated from CX3CR1$^{GFP/+}$ MPZ^{tdTomato} mice. Scale bars are 50 μm. **b** Endoneurial localization of GFP+ cells in longitudinal sections of sciatic nerves from CX3CR1$^{GFP/+}$ MPZ^{tdTomato} mice. **c** CSF1R (red) and CX3CR1^{GFP} (green) colocalization in sciatic nerve

cross sections. Scale bars are 50 μm. **d** Flow cytometric gating of CX3CR1$^{GFP/+}$ cells from peripheral nerve tissues. **e**, **f** Representative expression of CD64 and CD45 in CX3CR1$^{GFP/+}$ cells compared with brain microglia, large peritoneal macrophages (LPMs), and fluorescence minus one (FMO) control. **g** Flow cytometric quantification of CD45.1 and CD45.2 chimerism in blood (total T cells or total monocytes) and nerves from three pairs of wild-type (CD45.1) and Lyz2Cre tdTomato (CD45.2) parabionts 10 weeks after joining. **h** Representative imaging in peripheral nerves from wild-type parabiont; Scale bars are 100 μm. **i–l** Analysis of tdTomato expression in tamoxifen-pulsed CSF1R$^{Mer\text{-}iCre\text{-}Mer}$ × Rosa26-tdTomato mice. **i** Tamoxifen delivery schematic for fate mapping. Mice were given tamoxifen diet for 4 weeks and analyses for PNS macrophages and CNS microglia were performed at 0 days and 8 weeks after tamoxifen diet removal. **j** tdTomato expression by genotype from combined peripheral nerves in tamoxifen-fed mice. **k** Flow cytometric quantification of Ly6c high and Ly6C low monocytes from mice bled at 0 days, 3 weeks, 4 weeks, and 8 weeks after tamoxifen removal. **l** Flow cytometric quantification of CNS microglia (brain and spinal cord) and PNS macrophages (pooled from DRG, fascial nerve, vagus nerve, and sciatic nerve to increase yield in analysis) 0 days and 8 weeks following tamoxifen removal. Data are mean ± SEM ($n = 3$ mice per time point). Source data are available as a Source Data file.

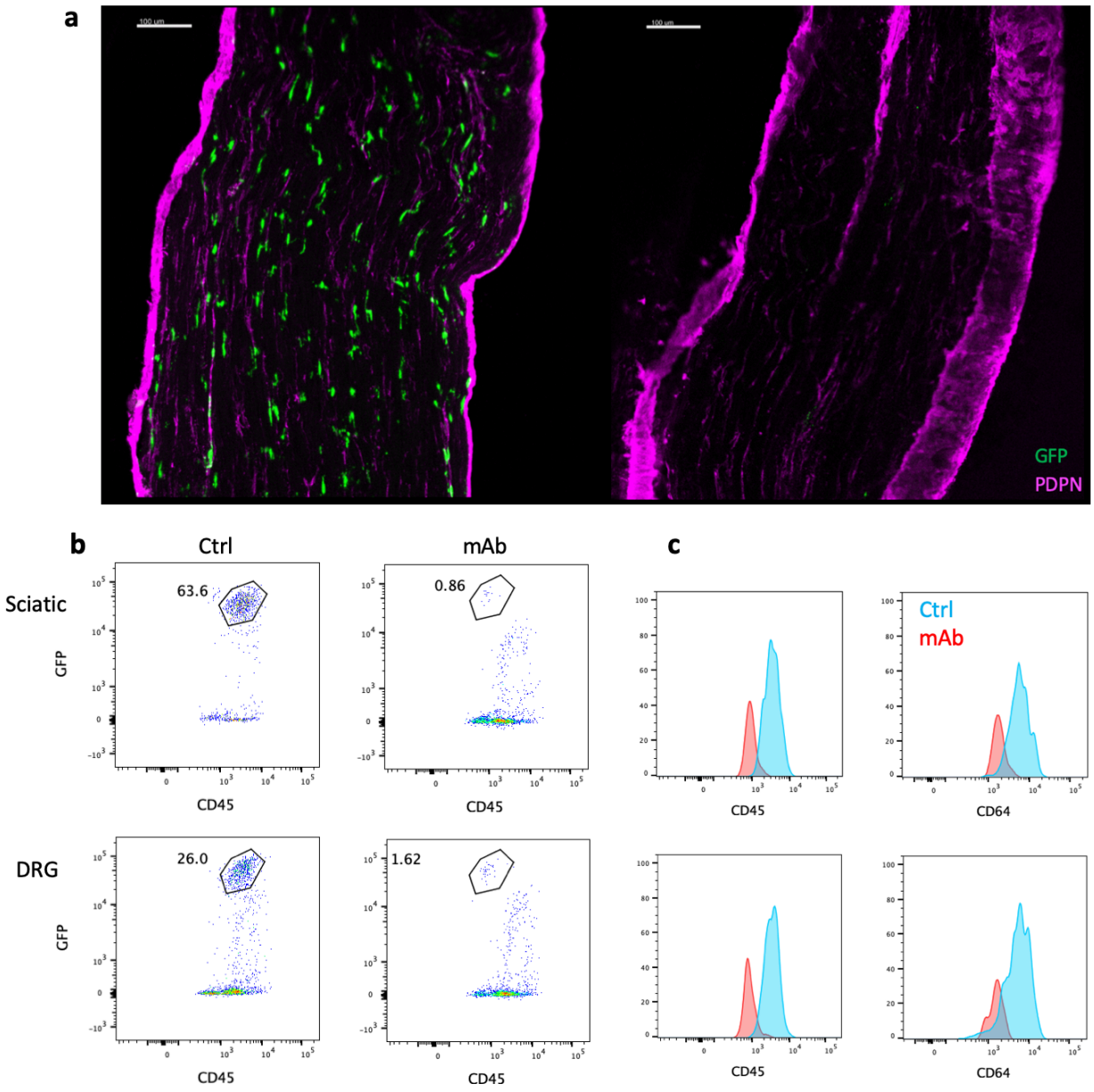

Figure 3. PNS macrophage depletion with anti-CSF1R monoclonal antibody. a Confocal imaging of PNS macrophages in normal (left) and antibody treated (right) sciatic nerves from $CX3CR1^{GFP/+}MPZ^{tdTomato}$ mice 10 days after i.p. injection. **b** Flow cytometric analysis of sciatic nerve and DRG macrophage depletion. **c** Expression of CD45 and CD64 in normal and remaining cells after CSF1R mAb depletion.

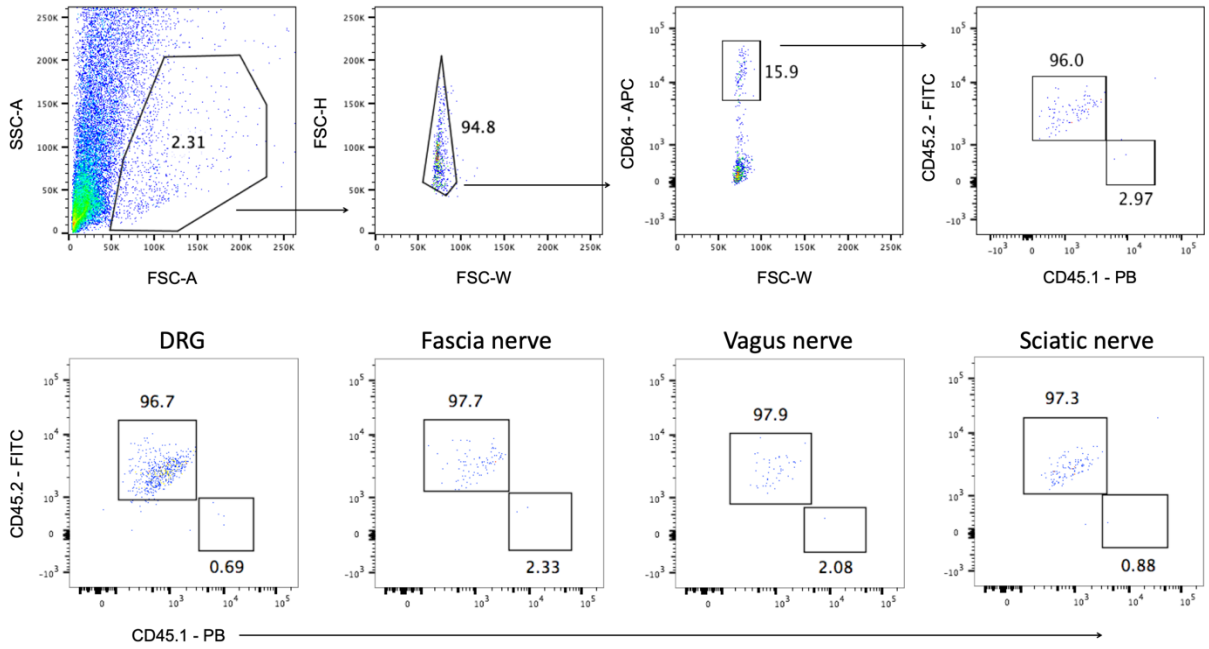

Figure 4. Analysis of resident macrophage chimerism in CD45.1 wild type and CD45.2 Lyz2-Cre tdTomato parabionts. Gating scheme (top) and representative flow plots of CD45.1 and CD45.2 expression in nerve macrophages from CD45.2 parabiont (bottom).

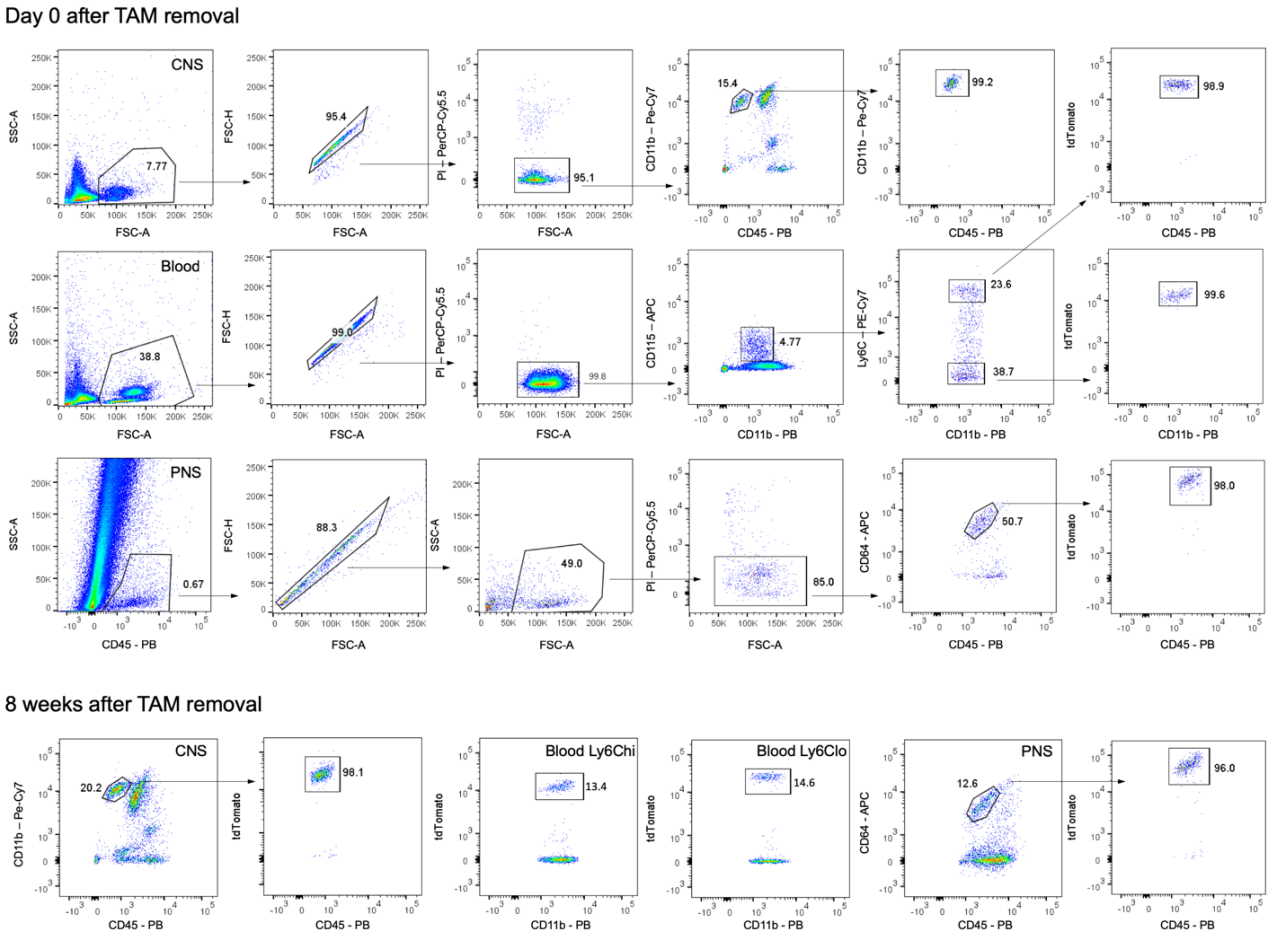

Figure 5. Flow cytometric analysis of blood and neural resident macrophages in pulse chase experiment. Gating strategy and representative flow plots of CNS microglia, blood monocytes, and PNS macrophages at day 0 and 8 weeks after tamoxifen removal.

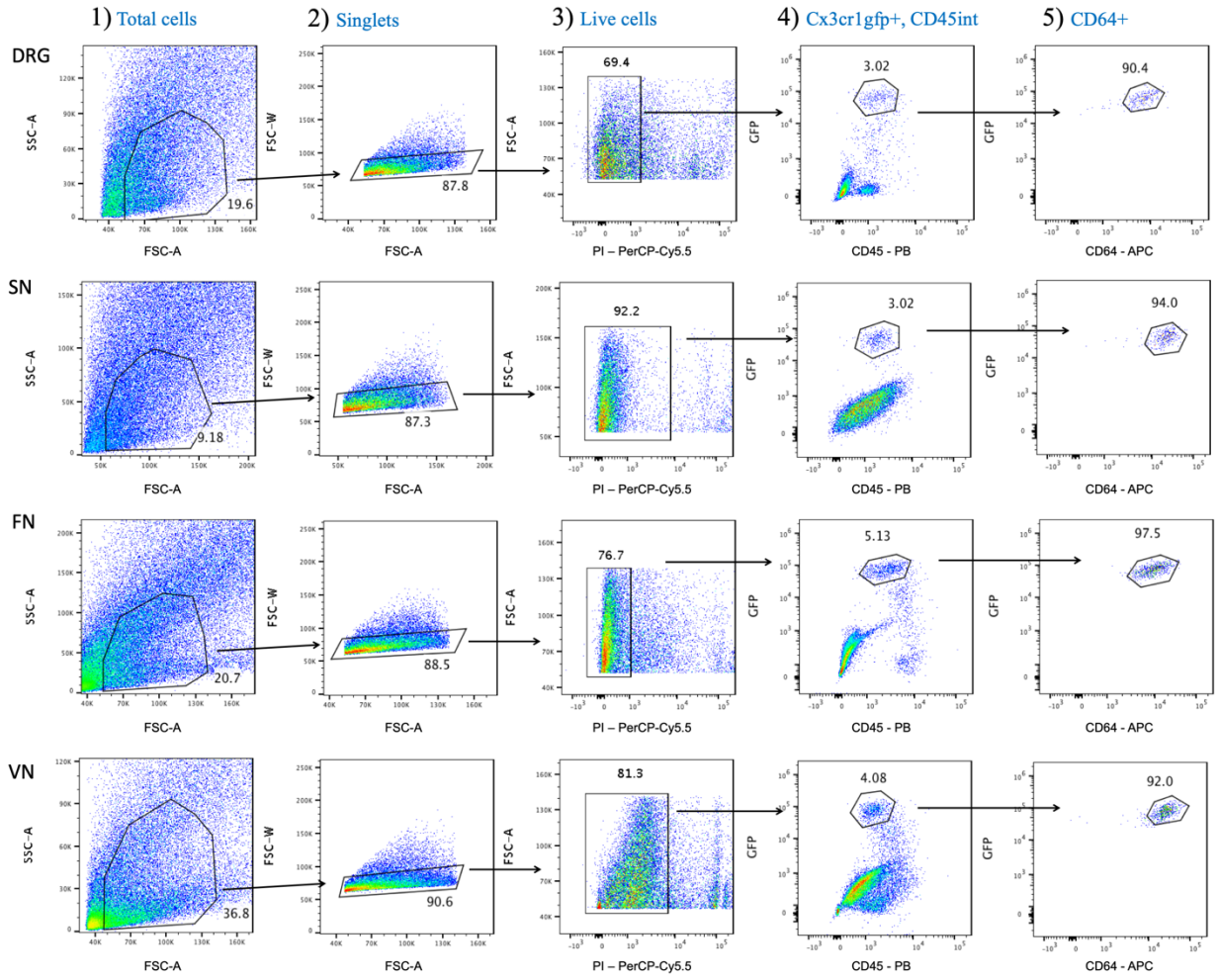

Figure 6. Gating strategy for identifying PNS macrophages and for double-sorted populations used in bulk-RNA sequencing. Representative gating schematic for flow cytometric identification and sorting of CX3CR1-GFP+, CD45 intermediate, CD64+ PNS macrophages in DRG, SN, FN, and VN .

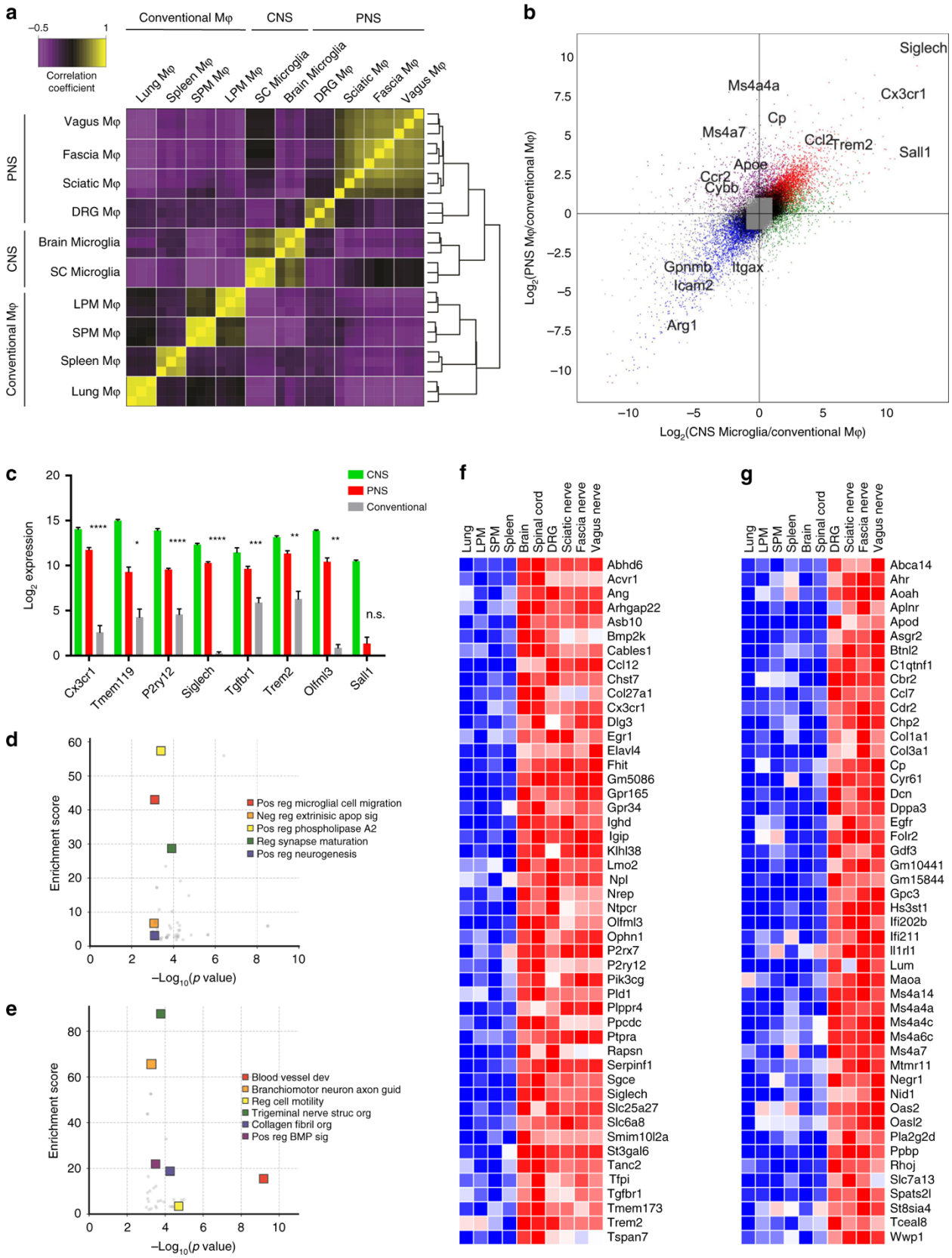
a
−0.5
1
Correlation coefficient
Conventional Mφ
CNS
PNS
Lung Mφ
Spleen Mφ
SPM Mφ
LPM Mφ
SC Microglia
Brain Microglia
DRG Mφ
Sciatic Mφ
Fascia Mφ
Vagus Mφ
PNS
CNS
Conventional Mφ
b
Siglech
Ms4a4a
Cx3cr1
Cp
Ms4a7
Ccl2
Trem2
Sall1
Apoe
Ccr2
Cybb
Gpnmb
Itgax
Icam2
Arg1
Log2(PNS Mφ/conventional Mφ)
Log2(CNS Microglia/conventional Mφ)
c
CNS
PNS
Conventional
Log2 expression
n.s.
Cx3cr1
Tmem119
P2ry12
Siglech
Tgfbr1
Trem2
Olfml3
Sall1
d
Enrichment score
−Log10(p value)
Pos reg microglial cell migration
Neg reg extrinisic apop sig
Pos reg phospholipase A2
Reg synapse maturation
Pos reg neurogenesis
e
Enrichment score
−Log10(p value)
Blood vessel dev
Branchiomotor neuron axon guid
Reg cell motility
Trigeminal nerve struc org
Collagen fibril org
Pos reg BMP sig
f
Lung
LPM
SPM
Spleen
Brain
Spinal cord
DRG
Sciatic nerve
Fascia nerve
Vagus nerve
Abhd6
Acvr1
Ang
Arhgap22
Asb10
Bmp2k
Cables1
Ccl12
Chst7
Col27a1
Cx3cr1
Dlg3
Egr1
Elavl4
Fhit
Gm5086
Gpr165
Gpr34
Ighd
Igip
Klhl38
Lmo2
Npl
Nrep
Ntpcr
Olfml3
Ophn1
P2rx7
P2ry12
Pik3cg
Pld1
Plppr4
Ppcdc
Ptpra
Rapsn
Serpinf1
Sgce
Siglech
Slc25a27
Slc6a8
Smim10l2a
St3gal6
Tanc2
Tfpi
Tgfbr1
Tmem173
Trem2
Tspan7
g
Lung
LPM
SPM
Spleen
Brain
Spinal cord
DRG
Sciatic nerve
Fascia nerve
Vagus nerve
Abca14
Ahr
Aoah
Aplnr
Apod
Asgr2
Btnl2
C1qtnf1
Cbr2
Ccl7
Cdr2
Chp2
Col1a1
Col3a1
Cp
Cyr61
Dcn
Dppa3
Egfr
Folr2
Gdf3
Gm10441
Gm15844
Gpc3
Hs3st1
Ifi202b
Ifi211
Il1rl1
Lum
Maoa
Ms4a14
Ms4a4a
Ms4a4c
Ms4a6c
Ms4a7
Mtmr11
Negr1
Nid1
Oas2
Oasl2
Pla2g2d
Ppbp
Rhoj
Slc7a13
Spats2l
St8sia4
Tceal8
Wwp1

Figure 7. PNS macrophages express microglial transcripts as well as a unique signature. a Sample correlation plot showing global transcriptomic analysis and hierarchical clustering of resident macrophages from PNS, CNS, and conventional macrophages. Each box represents one replicate. Three replicates comprising up to 20 mice per replicate were included for each population. **b** Visualization of PNS macrophage unique transcripts (upper quadrant), CNS microglia unique transcripts (right quadrant), shared transcripts between PNS macrophages and CNS microglia (diagonal, top right quadrant), and conventional macrophages (bottom right quadrant). **c** Expression of microglial core transcripts in combined PNS macrophages compared with combined conventional macrophages. Multiple *t*-tests. Data are mean ± SEM. **P* < 0.05, ***P* < 0.01, ****P* < 0.001, *****P* < 0.0001. **d** GO analysis of genes enriched in PNS macrophages and CNS microglia. **e** GO analysis of genes enriched in PNS macrophages. **f** Transcripts expressed at least fourfold higher in PNS macrophages and CNS microglia than conventional tissue-resident macrophages ($p \leq 0.05$). **g** Transcripts expressed at least fourfold higher in PNS macrophages than CNS microglia or conventional macrophages ($p \leq 0.05$). **f**, **g** Each box represents average of three replicates. Abbreviations: LPM, large peritoneal macrophage; SPM, small peritoneal macrophage. Source data are available as a Source Data file.

Table 1. Gene ontology analysis of enriched transcripts shared by CNS microglia and PNS macrophages.

GO term	Description	P-value	FDR q-value	Enrichment (N, B, n, b)
GO:0050804	modulation of chemical synaptic transmission	3.01E-09	4.02E-05	5.92 (9205,247,107,17)
GO:0099177	regulation of trans-synaptic signaling	3.20E-09	2.14E-05	5.90 (9205,248,107,17)
GO:0048870	cell motility	2.24E-06	9.97E-03	3.41 (9205,480,107,19)
GO:0040011	locomotion	2.30E-06	7.67E-03	3.26 (9205,528,107,20)
GO:0016477	cell migration	1.43E-05	3.82E-02	3.26 (9205,448,107,17)
GO:0048247	lymphocyte chemotaxis	1.84E-05	4.09E-02	14.83 (9205,29,107,5)
GO:0023051	regulation of signaling	3.52E-05	6.72E-02	1.88 (9205,1741,107,38)
GO:0008347	glial cell migration	4.66E-05	7.77E-02	19.12 (9205,18,107,4)
GO:0006935	chemotaxis	5.00E-05	7.41E-02	4.70 (9205,183,107,10)
GO:0048167	regulation of synaptic plasticity	5.09E-05	6.79E-02	6.04 (9205,114,107,8)
GO:0042330	taxis	5.74E-05	6.96E-02	4.63 (9205,186,107,10)
GO:0030334	regulation of cell migration	5.78E-05	6.43E-02	2.81 (9205,551,107,18)
GO:0051272	positive regulation of cellular component movement	6.01E-05	6.17E-02	3.38 (9205,356,107,14)
GO:0040012	regulation of locomotion	6.39E-05	6.10E-02	2.69 (9205,608,107,19)
GO:0030595	leukocyte chemotaxis	6.41E-05	5.71E-02	6.92 (9205,87,107,7)
GO:0051270	regulation of cellular component movement	6.83E-05	5.70E-02	2.68 (9205,611,107,19)
GO:0010646	regulation of cell communication	7.32E-05	5.75E-02	1.84 (9205,1729,107,37)
GO:0040017	positive regulation of locomotion	7.64E-05	5.66E-02	3.31 (9205,364,107,14)
GO:2000145	regulation of cell motility	9.16E-05	6.44E-02	2.71 (9205,571,107,18)
GO:0072676	lymphocyte migration	1.17E-04	7.79E-02	10.24 (9205,42,107,5)
GO:0048246	macrophage chemotaxis	1.22E-04	7.75E-02	28.68 (9205,9,107,3)
GO:0090128	regulation of synapse maturation	1.22E-04	7.40E-02	28.68 (9205,9,107,3)
GO:0060326	cell chemotaxis	1.36E-04	7.89E-02	5.25 (9205,131,107,8)
GO:0002687	positive regulation of leukocyte migration	1.55E-04	8.64E-02	6.02 (9205,100,107,7)
GO:0030335	positive regulation of cell migration	1.63E-04	8.68E-02	3.26 (9205,343,107,13)
GO:2000147	positive regulation of cell motility	1.93E-04	9.91E-02	3.20 (9205,349,107,13)
GO:0006928	movement of cell or subcellular component	2.01E-04	9.92E-02	2.47 (9205,663,107,19)

GO:0001934	positive regulation of protein phosphorylation	2.03E-04	9.69E-02	2.64 (9205,554,107,17)
GO:0010562	positive regulation of phosphorus metabolic process	2.19E-04	1.01E-01	2.53 (9205,612,107,18)
GO:0045937	positive regulation of phosphate metabolic process	2.19E-04	9.77E-02	2.53 (9205,612,107,18)
GO:1905517	macrophage migration	2.35E-04	1.01E-01	23.46 (9205,11,107,3)
GO:0042327	positive regulation of phosphorylation	3.63E-04	1.52E-01	2.51 (9205,582,107,17)
GO:0032879	regulation of localization	3.98E-04	1.61E-01	1.81 (9205,1524,107,32)
GO:0032430	positive regulation of phospholipase A2 activity	3.99E-04	1.57E-01	57.35 (9205,3,107,2)
GO:0071310	cellular response to organic substance	4.34E-04	1.66E-01	2.25 (9205,763,107,20)
GO:0051966	regulation of synaptic transmission, glutamatergic	4.83E-04	1.79E-01	10.75 (9205,32,107,4)
GO:0050921	positive regulation of chemotaxis	6.05E-04	2.18E-01	5.74 (9205,90,107,6)
GO:0050900	leukocyte migration	6.10E-04	2.14E-01	4.82 (9205,125,107,7)
GO:0072677	eosinophil migration	6.28E-04	2.15E-01	17.21 (9205,15,107,3)
GO:0048245	eosinophil chemotaxis	6.28E-04	2.10E-01	17.21 (9205,15,107,3)
GO:0032103	positive regulation of response to external stimulus	6.60E-04	2.15E-01	3.74 (9205,207,107,9)
GO:0051897	positive regulation of protein kinase B signaling	7.39E-04	2.35E-01	6.94 (9205,62,107,5)
GO:1904141	positive regulation of microglial cell migration	7.91E-04	2.46E-01	43.01 (9205,4,107,2)
GO:0050769	positive regulation of neurogenesis	8.05E-04	2.44E-01	3.10 (9205,305,107,11)
GO:2001237	negative regulation of extrinsic apoptotic signaling pathway	8.55E-04	2.54E-01	6.72 (9205,64,107,5)
GO:0045860	positive regulation of protein kinase activity	9.11E-04	2.65E-01	3.28 (9205,262,107,10)
GO:0008284	positive regulation of cell proliferation	9.46E-04	2.69E-01	2.48 (9205,520,107,15)
GO:0050920	regulation of chemotaxis	9.63E-04	2.68E-01	4.46 (9205,135,107,7)

Table 2. Gene ontology analysis of enriched transcripts in PNS macrophages.

GO term	Description	P-value	FDR q-value	Enrichment (N, B, n, b)
GO:0001568	blood vessel development	6.64E-10	8.87E-06	15.47 (9203,85,70,10)
GO:0051271	negative regulation of cellular component movement	1.04E-05	6.96E-02	6.36 (9203,186,70,9)
GO:0040013	negative regulation of locomotion	1.40E-05	6.24E-02	6.13 (9203,193,70,9)
GO:2000145	regulation of cell motility	1.93E-05	6.43E-02	3.45 (9203,571,70,15)
GO:0032879	regulation of localization	2.62E-05	7.01E-02	2.24 (9203,1525,70,26)
GO:0001525	angiogenesis	3.45E-05	7.68E-02	6.34 (9203,166,70,8)
GO:0040012	regulation of locomotion	4.02E-05	7.66E-02	3.24 (9203,608,70,15)
GO:0051270	regulation of cellular component movement	4.25E-05	7.10E-02	3.23 (9203,611,70,15)
GO:0030199	collagen fibril organization	5.48E-05	8.12E-02	18.78 (9203,28,70,4)
GO:0030334	regulation of cell migration	5.53E-05	7.38E-02	3.34 (9203,551,70,14)
GO:0070208	protein heterotrimerization	8.83E-05	1.07E-01	32.87 (9203,12,70,3)
GO:0032102	negative regulation of response to external stimulus	1.16E-04	1.29E-01	5.34 (9203,197,70,8)
GO:0043589	skin morphogenesis	1.70E-04	1.75E-01	87.65 (9203,3,70,2)
GO:0021637	trigeminal nerve structural organization	1.70E-04	1.62E-01	87.65 (9203,3,70,2)
GO:0030336	negative regulation of cell migration	1.72E-04	1.53E-01	5.90 (9203,156,70,7)
GO:2000146	negative regulation of cell motility	2.34E-04	1.96E-01	5.61 (9203,164,70,7)
GO:0009653	anatomical structure morphogenesis	2.86E-04	2.24E-01	2.72 (9203,724,70,15)
GO:0030510	regulation of BMP signaling pathway	3.03E-04	2.25E-01	12.23 (9203,43,70,4)
GO:0048646	anatomical structure formation involved in morphogenesis	3.16E-04	2.22E-01	3.42 (9203,423,70,11)
GO:0030513	positive regulation of BMP signaling pathway	3.17E-04	2.11E-01	21.91 (9203,18,70,3)
GO:0032489	regulation of Cdc42 protein signal transduction	3.39E-04	2.15E-01	65.74 (9203,4,70,2)
GO:0021785	branchiomotor neuron axon guidance	3.39E-04	2.06E-01	65.74 (9203,4,70,2)
GO:0071230	cellular response to amino acid stimulus	3.94E-04	2.28E-01	11.43 (9203,46,70,4)
GO:1902531	regulation of intracellular signal transduction	5.37E-04	2.99E-01	2.37 (9203,942,70,17)
GO:0006930	substrate-dependent cell migration, cell extension	5.62E-04	3.00E-01	52.59 (9203,5,70,2)

GO:0048820	hair follicle maturation	5.62E-04	2.89E-01	52.59 (9203,5,70,2)
GO:0043200	response to amino acid	6.31E-04	3.12E-01	10.11 (9203,52,70,4)
GO:0009966	regulation of signal transduction	6.86E-04	3.27E-01	1.97 (9203,1538,70,23)
GO:0043062	extracellular structure organization	7.34E-04	3.38E-01	5.52 (9203,143,70,6)
GO:0060976	coronary vasculature development	7.61E-04	3.38E-01	16.43 (9203,24,70,3)
GO:0048568	embryonic organ development	8.26E-04	3.56E-01	6.78 (9203,97,70,5)
GO:0090263	positive regulation of canonical Wnt signaling pathway	8.37E-04	3.49E-01	9.39 (9203,56,70,4)
GO:0003214	cardiac left ventricle morphogenesis	8.39E-04	3.39E-01	43.82 (9203,6,70,2)
GO:0021612	facial nerve structural organization	8.39E-04	3.29E-01	43.82 (9203,6,70,2)
GO:0032101	regulation of response to external stimulus	9.63E-04	3.67E-01	2.99 (9203,483,70,11)

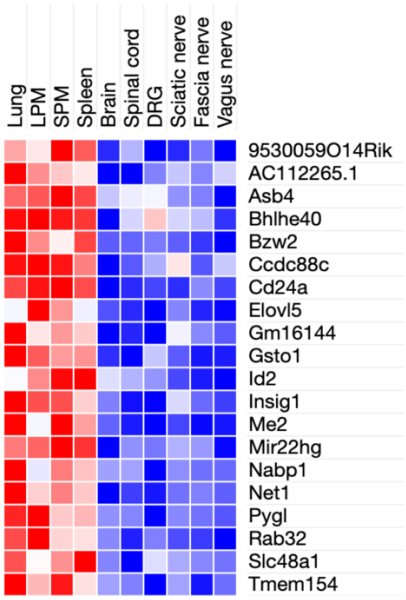

Figure 8. Uniquely downregulated genes in neural resident macrophages. Heat map of mRNA transcripts fourfold or more downregulated in CNS microglia and PNS macrophages compared to conventional tissue-resident macrophages. Each box represents average of three replicates.

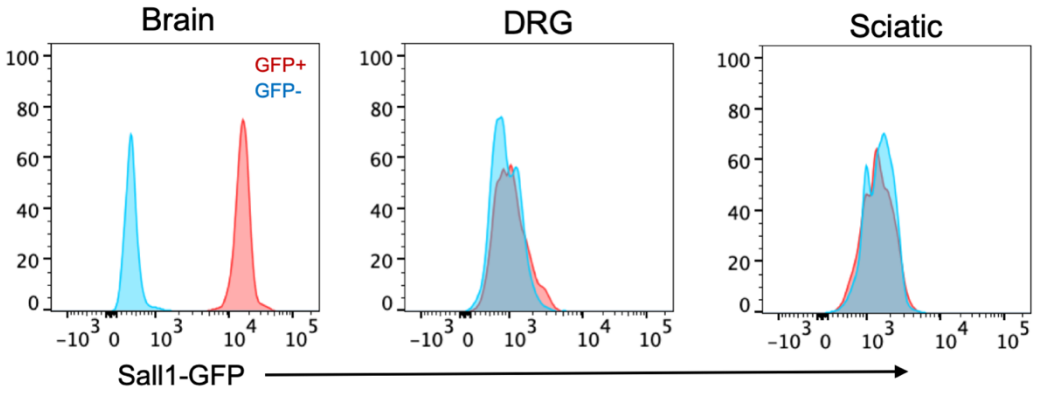

Figure 9. Examination of Sall1 expression in PNS macrophages. Flow cytometry analysis of GFP expression in brain microglia, DRG macrophages, and sciatic nerve macrophages isolated from Sall1-GFP/+ mice (red) and wild type controls (blue).

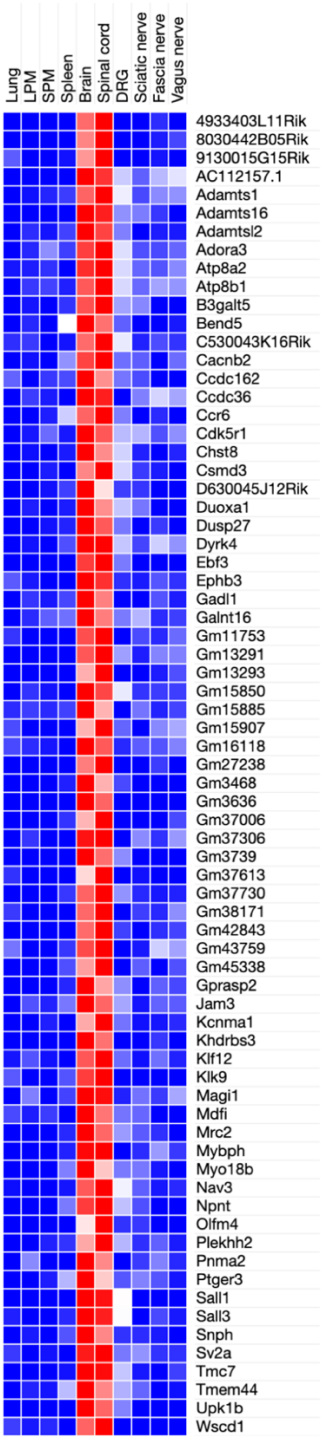

Figure 10. Identification of unique signatures in CNS microglia. Heat map of transcripts selectively enriched fourfold or more in brain and spinal cord microglia compared to PNS and conventional macrophages. Each box represents average of three replicates.

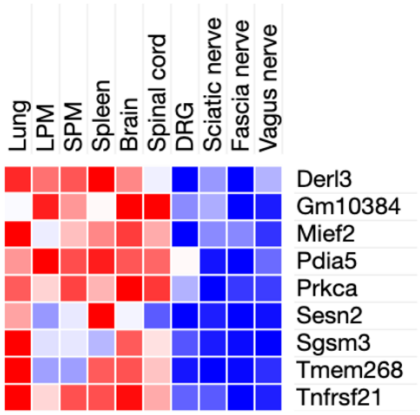

Figure 11. Downregulated genes in PNS macrophages. Heat map of genes that are downregulated fourfold or more in PNS macrophages compared to all other populations combined. Each box represents average of three replicates.

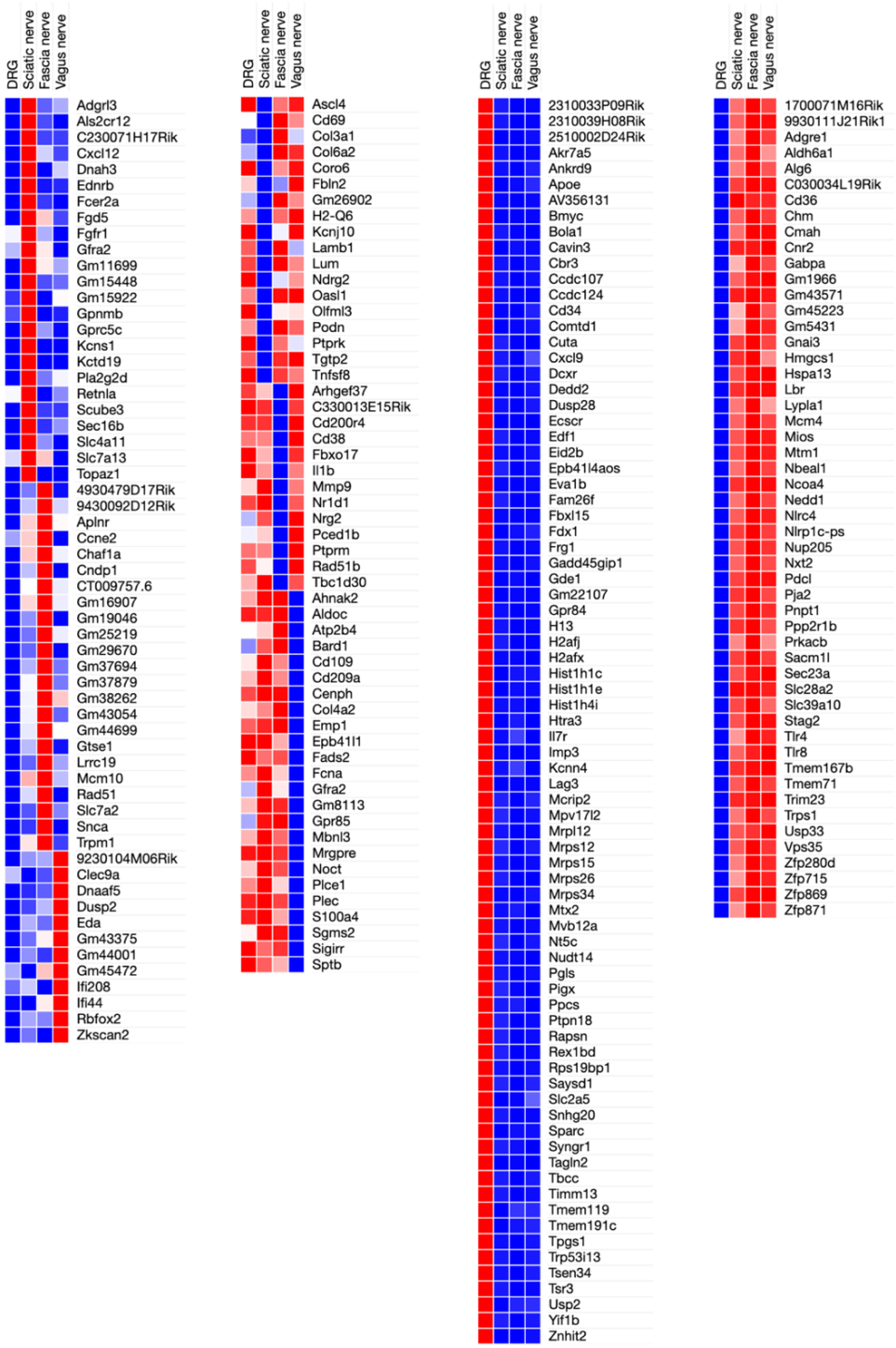

Figure 12. Unique gene expression patterns in individual PNS macrophage populations. Heat map of upregulated and downregulated mRNA transcripts in single PNS macrophage populations by fourfold or more in sciatic, fascial, and vagal nerves and eightfold or more in DRG relative to their expression in the remaining three populations combined. Each box represents average of three replicates.

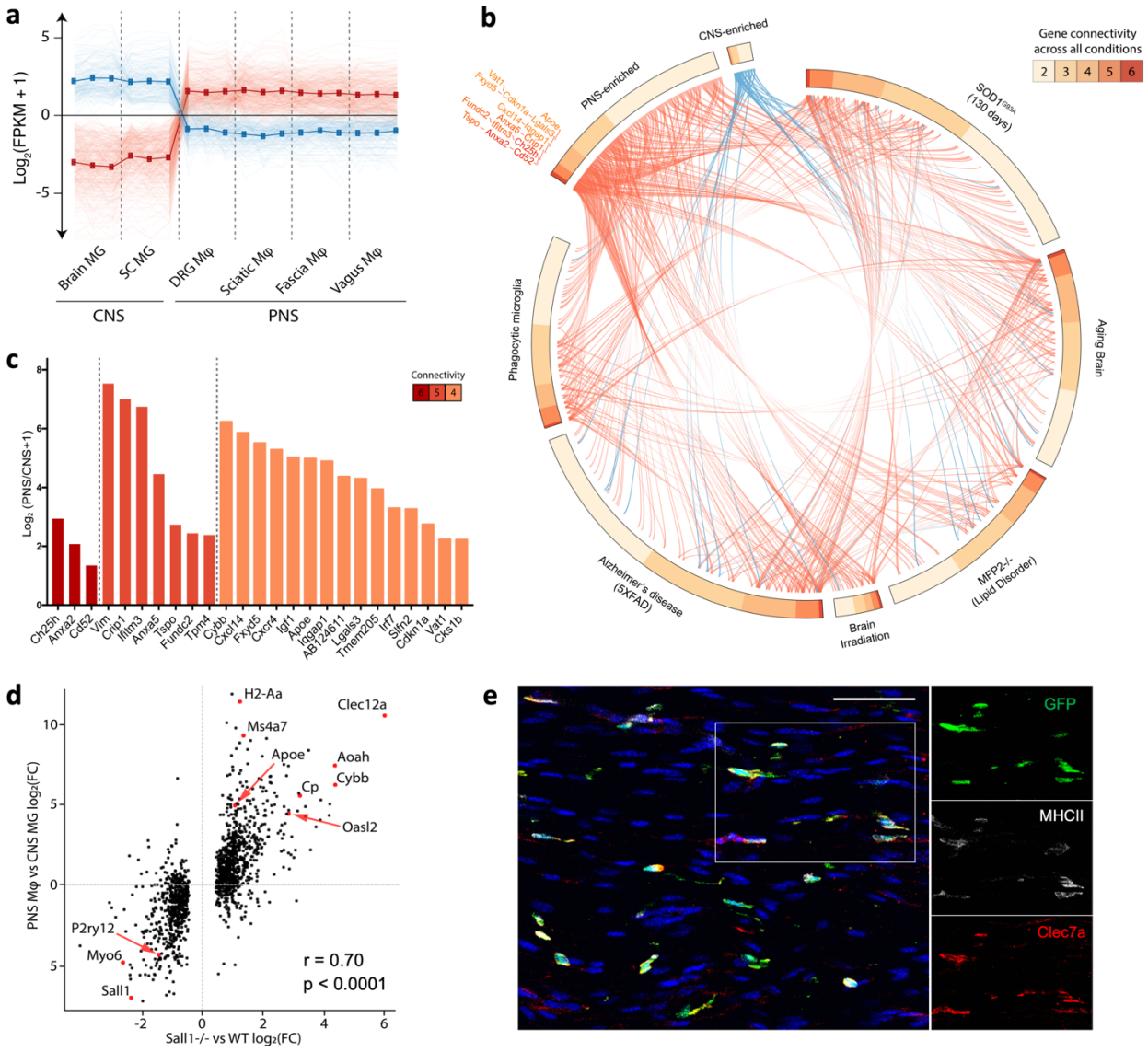

Figure 13. PNS macrophages constitutively express transcripts associated with activated microglia. **a** Expression pattern of DEGs defined as PNS-enriched (red) or CNS-enriched (blue). CNS microglia includes brain and spinal cord and PNS macrophages include DRG, vagal, fascial, and sciatic nerves. **b** Circos plot showing the number of connections (gene connectivity) between GSEA-scored genes from microglia in 6 neurodegenerative and aging-associated conditions as defined in Krasemann et al.[6] and neural macrophage-enriched genes from either PNS macrophages (red) or CNS microglia (blue). **c** PNS-enriched genes from connectivity groups 6–4 expressed as Log_2 fold change (PNS

macrophages/CNS microglia). **d** Expression plot comparing PNS macrophage-enriched genes (expressed as PNS macrophage/CNS microglia Log2FC) and Sall1$^{-/-}$ microglia-enriched genes (expressed as Sall1$^{-/-}$/wild-type microglia Log2FC) from Buttgereit et al.; *r*, correlation coefficient; *p*, *p*-value for linear regression analysis. **e** Representative immunohistochemistry in sciatic nerves of CX3CR1$^{GFP/+}$ mice showing DAPI (blue), GFP (green), MHCII (white), and Clec7a (red). Scale bar, 50 μm. Source data are available as a Source Data file.

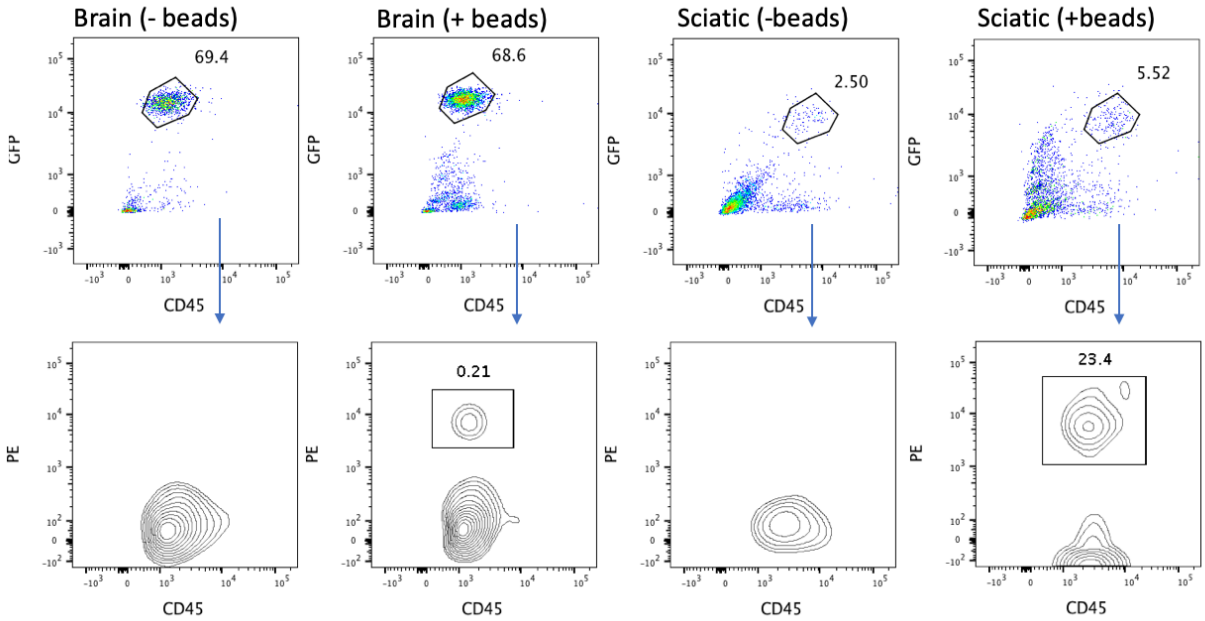

Figure 14. Comparison of phagocytic capacity in brain microglia and sciatic nerve macrophages. Flow cytometric analysis of fluorescent bead uptake by brain microglia and sciatic nerve macrophages during 30 minute incubation period.

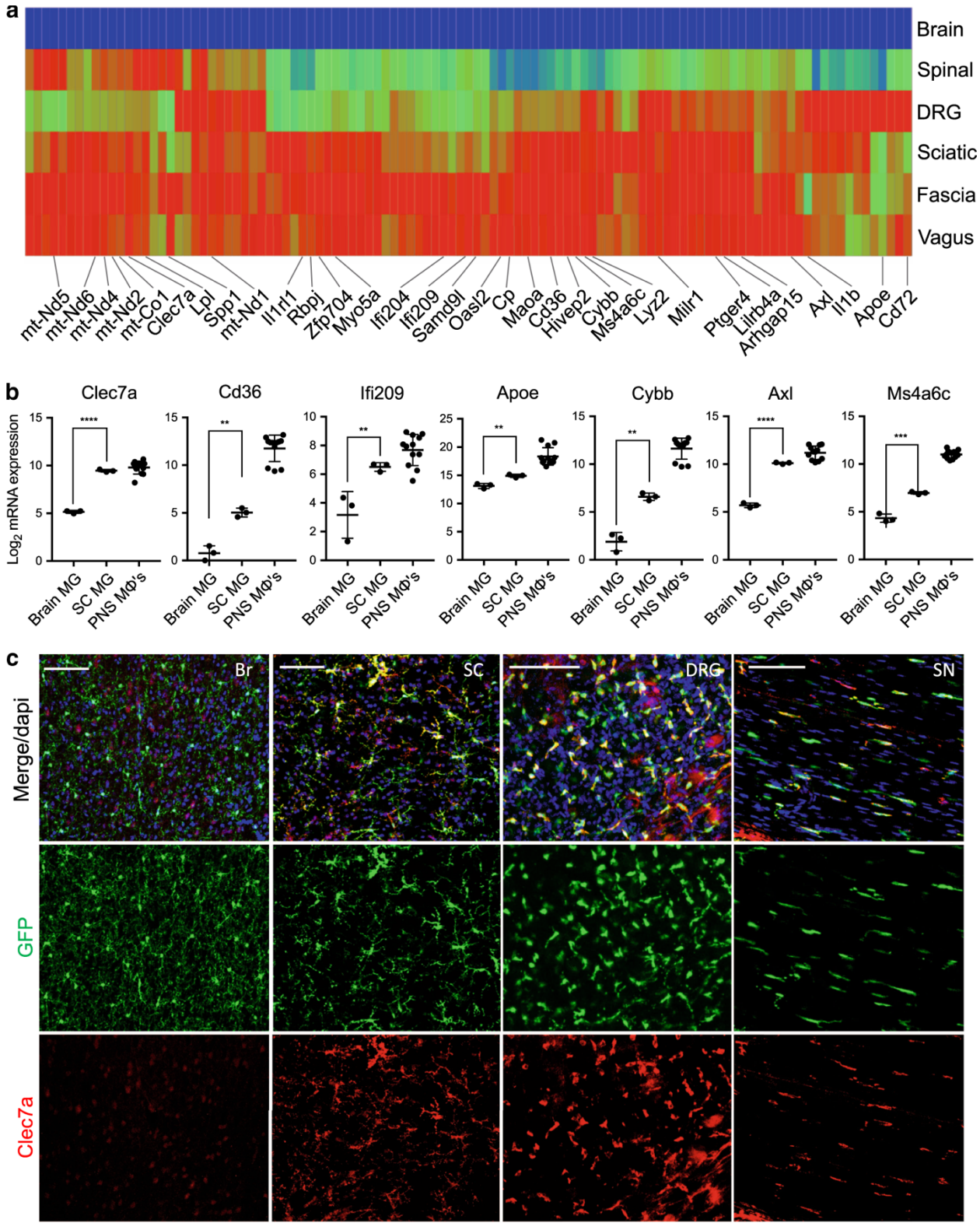
a
Brain
Spinal
DRG
Sciatic
Fascia
Vagus
mt-Nd5
mt-Nd6
mt-Nd4
mt-Nd2
mt-Co1
Clec7a
Lpl
Spp1
mt-Nd1
Il1rl1
Rbpj
Zfp704
Myo5a
Ifi204
Ifi209
Samd9l
Oasl2
Cp
Maoa
Cd36
Hivep2
Cybb
Ms4a6c
Lyz2
Milr1
Ptger4
Lilrb4a
Arhgap15
Axl
Il1b
Apoe
Cd72
b
Clec7a
Cd36
Ifi209
Apoe
Cybb
Axl
Ms4a6c
Log2 mRNA expression
Brain MG
SC MG
PNS Mφ's
c
Br
SC
DRG
SN
Merge/dapi
GFP
Clec7a

Figure 15. Zonation of PNS macrophage-enriched transcripts in neural resident macrophages. **a** Heat map showing genes corresponding to PNS to CNS zonation pattern (PNS macrophages high, spinal cord microglia high/intermediate, brain microglia low). Each box represents average from three replicates. **b** Gene expression analysis of individual genes following PNS to CNS zonation pattern. Each dot represents one replicate. Unpaired *t*-test. Data are mean ± SD. **P* < 0.05, ***P* < 0.01, ****P* < 0.001, *****P* < 0.0001. **c** Representative Clec7a staining in brain (Br), spinal cord (SC), dorsal root ganglia (DRG), and sciatic nerve (SN) of $CX3CR1^{GFP/+}$ mice. Scale bars are 100 μm. Source data are available as a Source Data file.

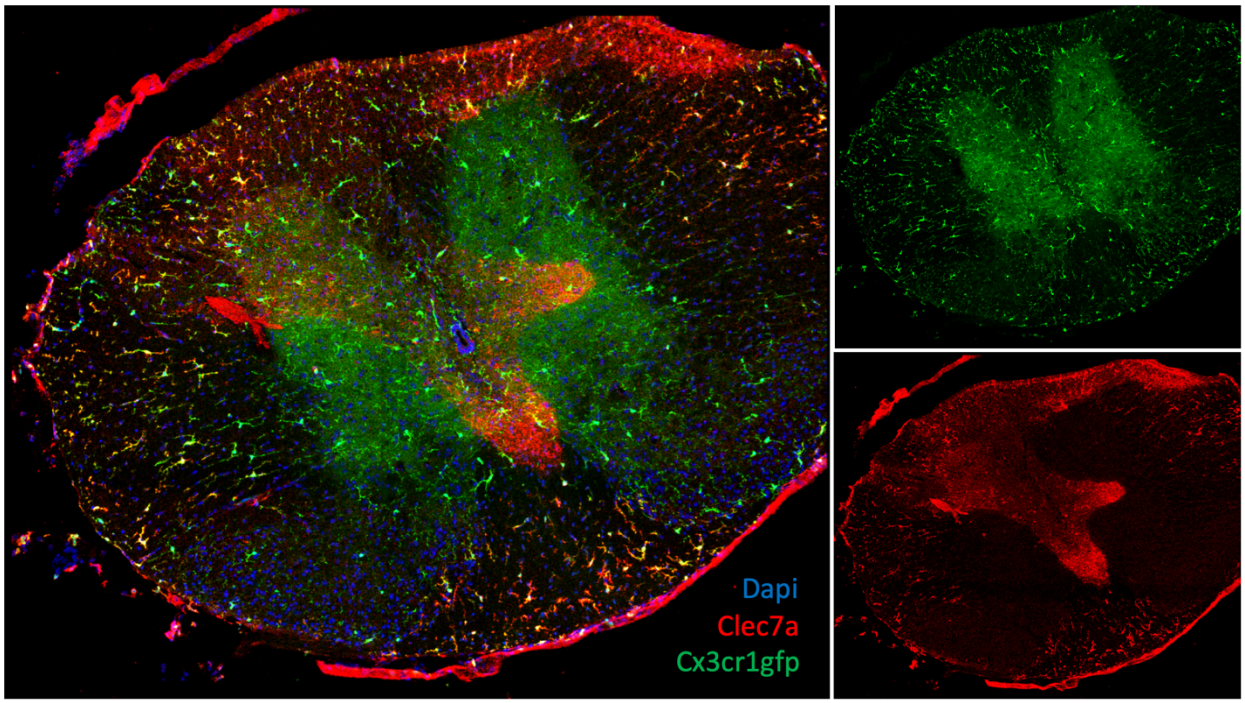

Figure 16. Clec7a+ microglia localization in spinal cord. IHC analysis of CLEC7A expression by microglia in spinal cord transverse sections of CX3CR1GFP/+ mice.

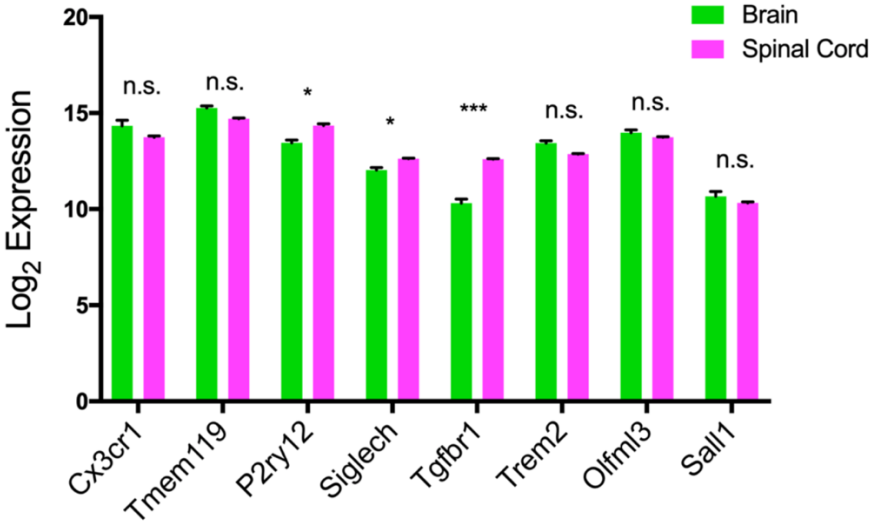

Figure 17. Expression of microglial homeostatic genes in spinal cord and brain microglia. Log_2 expression of microglial homeostatic genes in brain (green) and spinal cord (magenta) microglia. Multiple t tests. Data are mean of three replicates +/- SEM with adjusted p-value shown. * $P < 0.05$, ** $P < 0.01$, *** $P < 0.001$.

3. Ontogeny of peripheral nerve resident macrophages

The work described in this chapter was published in the journal *Nature Communications* under the following citation:

Wang PL, Yim AKY, Kim KW, Avey D, Czepielewski RS, Colonna M, Milbrandt J, Randolph GJ. Peripheral nerve resident macrophages share tissue-specific programming and features of activated microglia. *Nat Commun*. 2020 May 21;11(1):2552.

AUTHOR CONTRIBUTIONS: P.L.W. purified macrophage populations, designed, and performed the experiments, analyzed data, and wrote the manuscript. A.Y. analyzed RNA-seq data and helped with experiments and writing of the manuscript. K.K. purified macrophage populations and discussed results. D.A. and R.C. helped with experiments and discussed results. M.C. provided conceptual feedback and the IL-34$^{-/-}$ strain. G.J.R. and J.M. designed and supervised the experiments, acquired funding, and edited the manuscript. The Immunological Genome Project set standards for data acquisition, conducted sequencing, QC, and generation of raw data for bulk RNA samples.

3.1 Introduction

While all tissue resident macrophages arise from erythro-myeloid progenitors (EMP) that form in the embryonic yolk sac by embryonic day E8.5 (YS), only CNS microglia are thought to remain predominantly YS-derived in throughout life, without contribution from the fetal liver or definitive hematopoiesis [1-3]. In all other known tissues, including lung, liver, pancreas, kidney, and heart, YS precursors are mostly or entirely replaced by fetal liver monocytes before birth [1]. In some tissues, such as gut and dermis, fetal liver monocytes are further replaced by bone marrow monocytes in a CCR2-dependent manner before and during adulthood [1,4].

The realization that macrophages arise from different sources raises key questions about macrophage replacement in disease contexts. For example, could dysfunctional or overly inflammatory microglia in CNS diseases be replaced, and if so, from which source? Studies to address this question have found that when hematopoietic stem cell (HSC)-derived macrophage precursors were transplanted into the brains of mice that lack resident microglia, these cells took on a more activated transcriptional signature compared to normal microglia [5,6]. Notably, these cells also expressed microglial homeostatic signatures, but not to the extent of their YS-derived counterparts [5]. While the beneficial or detrimental effects of microglial transplantation still remain to be worked out, these observations suggest that both developmental source and brain environment mediates the expression of microglial signatures.

Considering the growing interest in how tissue environment and ontogeny contribute to microglial identity and function in neurological diseases, we investigated these questions in PNS macrophages for the first time. We found that PNS macrophages originate from both embryonic and hematopoietic sources in mice. Peripheral nerves were fully populated by macrophages at birth and included a subpopulation of YS-derived cells. PNS macrophages also exhibit partial

dependence on IL-34, an alternative ligand for colony-stimulating factor 1 receptor (CSF1R) that is important for the development and maintenance of microglia [7,8], and do not depend on CCR2 signaling to seed peripheral nerves. With the exception of *Ccr2* expression, transcriptional signatures in PNS macrophage were largely similar between embryonic and hematopoietic sources, suggesting that nerve environment controls their identity at steady state.

3.2 Results

3.2.1 Identification of embryonic- and HSC-derived PNS resident macrophages

In addition to microenvironmental cues, ontogeny may also play an important role for specifying microglial identity and function. Specifically, it has been shown that, compared to naturally occurring microglia with yolk sac origin, monocyte- and hematopoietic stem cell (HSC)-derived microglia display a more activated signature [5,6]. Thus, we sought to determine PNS macrophage ontogeny by examining Flt3Cre × LSL-YFP$^{fl/fl}$ reporter mice (Fig. 18a), a strain that labels fetal monocyte and adult HSC-derived hematopoietic multipotent progenitors and their progeny [2,9]. We found that ~26% of PNS macrophages across nerve types appeared to be embryonically derived (YFP−) and 74% of PNS macrophages were HSC-derived (YFP+) (Fig. 18b and Fig. 19).

To further examine the contribution of embryonic precursors to PNS macrophages, we performed fate mapping using CSF1R$^{Mer\text{-}iCre\text{-}Mer}$ × tdTomato$^{fl/fl}$ × CX3CR1$^{GFP/+}$ double reporter mice, which allows simultaneous visualization of tamoxifen-pulsed CSF1R-expressing macrophages and resident Cx3cr1+ macrophages. After giving tamoxifen at embryonic day 8.5

(E8.5), a developmental time point that labels yolk-sac derived macrophages, we checked newborn pups for labeling. The PNS was fully populated with CX3CR1$^{GFP/+}$ macrophages at birth. In line with previous observations [10], we observed partial labeling in 42% of brain microglia (Fig. 18c, d). Labeling in PNS macrophages was 8% from SN and DRG, or roughly one-fifth of the entire PNS macrophage population when normalized to microglia (Fig. 18c, d). Less than 1% of macrophages were tdTomato+ in spleen, kidney, and blood, and only 3% of lung macrophages were tdTomato+ (Fig. 18c, d and Fig. 20). These results demonstrate that the PNS is fully populated by macrophages at the time of birth and that a subset of these cells are derived from yolk sac progenitors.

3.2.2 PNS macrophage seeding depends on IL-34 but not CCR2

Although monocyte entry into injured nerves depends on CCR2 [11,12], it is not known whether CCR2 is required for seeding or maintaining the PNS macrophage niche. To address this question, we quantified CSF1R+ macrophages in SNs of CCR2 knock-in (CCR2$^{GFP/GFP}$) and control (CCR2$^{GFP/+}$) mice. We observed no difference in PNS macrophage numbers between CCR2 knockouts and controls (Fig. 18e-g). However, although GFP+ cells were present in SNs from CCR2$^{GFP/+}$ mice, GFP+ cells were almost entirely absent from CCR2$^{GFP/GFP}$ mice (Fig. 18e, f and Fig. 21). These observations suggest that CCR2-dependent monocyte entry is not required to fill or maintain the PNS macrophage niche, but may contribute to a modest subset of PNS macrophages at steady state.

Given the resemblance between microglia and PNS macrophages, we wondered if IL-34, an alternative ligand for CSF1R that contributes to CNS microglia homeostasis [7,8], likewise governs PNS macrophage numbers. We quantified PNS macrophages of IL-34 deficient mice

(IL-34$^{LacZ/LacZ}$) by flow cytometry and imaging. In the SN, the fraction of CD45^{+} cells in the disaggregated nerve was reduced by a 30% (Fig.18h-i), apparently owing to more than 50% reduction in PNS macrophage density per nerve area, as examined by imaging the intact nerve (Fig. 18j-k). In the DRG, we observed a reduction in macrophage density of more than 35% (Fig. 22), underscoring significant dependence on IL-34 in multiple PNS sites. Indeed, this fraction of loss resembles that observed in the CNS microglial population [7,8].

In the SN, we checked expression of IL-34 mRNA transcripts by in-situ hybridization (ISH). Surprisingly, we found that Prx-expressing myelinating Schwann cells were a source of IL-34 (Fig. 18l). In the absence of IL-34, PNS macrophages in the SN showed increased surface marker expression of CD45 and CD11b, suggesting a shift in phenotype further away from microglial characteristics (Fig. 18m). Taken together, these results reveal shared and unique developmental programs, including instructive cytokines, between PNS macrophages and CNS microglia.

3.2.3 Nerve environment shapes transcriptional identity of PNS macrophages

To investigate the extent to which PNS macrophage identity is specified by ontogeny or nerve environment, we individually sorted YFP− embryonic-derived and YFP+ HSC-derived PNS macrophages from SNs of Flt3Cre LSL-YFP$^{fl/fl}$ mice and performed single-cell RNA-seq (Fig. 23a). We captured a total of 935 YFP− cells and 3186 YFP+ cells. Unsupervised clustering analysis of all 4121 cells revealed 5 separate clusters, with the majority of PNS macrophages belonging to one major group (clusters 1, 2, and 3) and the remainder falling into 2 smaller clusters (4 and 5) (Fig. 23b).

Although we observed a significant overlap of YFP− and YFP+ macrophages in clusters 1, 3, 4, and 5, cluster 2 contained mostly YFP+ macrophages (Fig. 23b). Interestingly, cluster 2 was defined by *Ccr2* expression, which is consistent with this subset arising from circulating precursors (Fig. 23c). Indeed, we confirmed by flow cytometry that CCR2+ PNS macrophages were only found in the YFP+ fraction (Fig. 23f and Fig. 24). We also observed varying heterogeneity between the overlapping clusters (Fig. 23c). For instance, cluster 5 was easily distinguished by proliferation genes *Mki67* and *Top2a*. Cluster 4 was also relatively distinct and showed enrichment for *Ly6e*, *Ninj1*, *Retnla*, and *Wfdc17*, potentially representing a previously undescribed activation state. Cluster 3 selectively expressed early activation genes *Fos*, *Jun*, and *Egr1*. Cluster 1 was slightly enriched for *Lyve1* expression compared to cluster 2 (Fig. 23c). We confirmed Lyve1 expression in a subset of PNS macrophages by immunostaining (Fig. 23g). Interestingly, we also saw axonal expression of YFP in Flt3-Cre LSL-YFP mice (Fig. 23g), which is in accordance with previous findings that Flt3 is expressed in neurons and may play a role in neural stem cell proliferation and survival [13].

Despite the identification of separate clusters in our data, we observed no obvious difference in the expression of PNS macrophage-enriched or microglial activation-associated transcripts between the main clusters. Specifically, Apoe, Cp, H2-Aa, Cd74, Ms4a6c, Ifitm3, Anxa5, Cybb, and Cd52 were nearly identical between clusters 1, 2, and 3 (Fig. 23d). We also observed no difference in *Cx3cr1* and *Trem2* between these clusters. Importantly, all of these genes were similarly expressed between YFP− and YFP+ macrophages (Fig 23e). We conclude that embryonic- and HSC-derived PNS macrophages are transcriptionally similar and that the nerve environment confers a predominant effect over developmental origin on PNS macrophage identity.

3.3 Discussion

Here we demonstrate that both embryonic and HSC-derived PNS macrophages exist as transcriptionally similar populations in adult nerves regardless of origin, thus suggesting a more important role for nerve environment than ontogeny in programming neural resident macrophages at steady state. While these results imply that there exists a subset of PNS macrophages that more closely resembles microglia by way of embryonic origin, future experiments are needed to determine if this more primitive subset behaves differently compare with HSC-derived macrophages in the PNS. Interestingly, we and others have found that a subset of macrophages similar in proportion to those which are embryonic-derived remains in peripheral nerves after lethal irradiation and bone marrow transfer [14,15]. As microglia are known to be radio-resistant [16], this raises the question of whether embryonic-derived PNS macrophages are more radio-resistant compared with HSC-derived counterparts.

From the observation that PNS macrophages are reduced and more activated in IL-34 KO mice, a similar question that arises is whether IL-34 deficiency specifically depletes embryonic-derived macrophages. Also, is loss of CSF-1 but preservation of IL-34 sufficient to maintain PNS macrophages, and if so, to what extent? By modeling PNS macrophage deficiency, these mouse strains may be further useful for examining the roles of PNS macrophages in development, injury response, and neuroprotection.

Future experiments are also needed to examine whether there are differential roles between embryonic and HSC-derived resident macrophage populations as well as recruited monocytes in neuropathic conditions. Indeed, studies in heart macrophages, which likewise identify CCR2- embryonic and CCR2+ HSC-derived subsets, indicate that these two populations

respond differently after heart injury with CCR2- macrophages facilitating regeneration and CCR2+ macrophages contributing to monocyte recruitment and inflammatory responses [17,18]. These and other models may be useful for dissecting the relative contribution of embryonic- and HSC-derived PNS macrophages after nerve injury.

Lastly, the observation that the majority of PNS macrophage signatures were expressed independent of ontogeny suggests that PNS macrophage signatures are strongly influenced by neuronal environment. This is the subject of the next chapter.

3.4 Materials and methods

Experimental animals

Mouse care and experiments were performed in accordance with protocols approved by the Institutional Animal Care and Use Committee at Washington University in St. Louis under the protocols 20170154 and 20170030. Mice were kept on a 12 h light–dark cycle and received food and water ad libitum. The following strains were used: C57/B6 CD45.1 (stock number 002014), CX3CR1$^{GFP/+}$(Cx3cr1tm1Litt/LittJ; stock number 008451), and CSF1R$^{Mer\text{-}iCre\text{-}Mer}$ mice were obtained from JAX (stock number 019098). Flt3-Cre LSL-YFP$^{fl/fl}$ [9] mice were kindly provided by D. Denardo, CCR2$^{gfp/+}$ (B6(C)-Ccr2$^{tm1.1Cln}$/J, (JAX stock number 027619) mice were kindly provided by K. Lavine, and IL34$^{LacZ/LacZ}$ mice were previously described and generated at Washington University [7].

Immunohistochemistry

For whole-mount imaging, samples were harvested and immediately stored in 4% paraformaldehyde (PFA) containing 40% sucrose overnight. Samples were then washed in

phosphate-buffered saline (PBS), blocked, stained, and imaged. For frozen sections, samples were collected, stored in PFA/sucrose, and embedded into optimal cutting temperature compound. Fifteen-micrometer cuts were made for SNs. Sections were then blocked in 1% bovine serum albumin, stained, and imaged. Antibodies to the following proteins were used: anti-GFP, CSF1R (R&D Systems, accession number P09581), MHCII (IA/IE clone M5/114.15.2), and LYVE1 (ab14917).

Preparation of single-cell suspensions

For blood, mice were bled from the cheek immediately before killing and cells were prepared as previously described. For nerves and all other tissues, mice were killed and perfused with PBS. Nerves were collected and kept on ice until dissociation. Cells were then incubated with gentle shaking for 20 min in digestion media containing collagenase IV, hyaluronidase, and DNAse. Cells were then washed and filtered through 70 μm cell strainers. For brain and spinal cord, myelin was removed using a 40/80% Percoll gradient.

Flow cytometry

Single-cell suspensions were stained at 4 °C. Dead cells were excluded by propidium idodide (PI). Antibodies to the following proteins were used: B220 (clone RA3-6B2), CCR2 (clone SA203G11), CD3e (clone 145-2C11), CD4 (clone RM4-5), CD8 (clone 53-6.7), CD11b (clone M1/70), CD16 (clone 2.4G2), CD45 (clone 30-F11), CD64 (clone X54-5/7.1), CD115 (clone AFS98), GR1 (clone 1A8), and Ly6C (clone HK1.4). Cells were analyzed on a LSRII flow cytometer (Becton Dickinson) and analyzed with FlowJo software.

Cell sorting

For sorting in preparation of the Flt3-Cre LSL-YFP single-cell Seq experiments, SNs from 19 male mice aged 10–12 weeks were combined and CD64+ CD45int macrophages were sorted individually into YFP+ and YFP− groups, yielding 18,000 and 5,000 cells, respectively. Both groups were immediately run on the 10× Genomics Chromium Controller according to the manufacturer's protocol.

Embryonic labeling

Homozygous CX3CR1-GFP female mice were rotated daily with $CSF1R^{Mer\text{-}iCre\text{-}Mer}$ tdTomato male mice and checked for plugs in the morning. Plug-positive females were administered 1.5 mg of 4-Hydroxytamoxifen (Sigma, catalog number H6278) and 1 mg of progesterone (Sigma, catalog number P0130) dissolved in corn oil by oral gavage 8 days following identification of plugs to pulse the embryos at embryonic 8.5 days. Following birth, pups were immediately sacrificed. Blood was collected for flow cytometric analysis and tissues were fixed in PFA/sucrose for imaging.

Cell preparation, 10× single-cell library preparation, sequencing, and analyses

A total of 4500 Flt3-negative and 16,000 Flt3-positive cells were loaded to separate lanes of the 10X Chip for preparation of two single-cell libraries. The library preparation was performed according to the manufacturer's instructions (Chromium Single-cell v2; 10× Genomics, USA). A total of 153 M and 174 M reads were sequenced for Flt3-negative and Flt3-positive libraries, respectively, using Illumina HiSeq2500. Reads were mapped by using the cellranger pipeline v2.1.1 onto the reference genome grcm38/mm10. We filtered cells for those

with ≥50,000 mapped reads, leaving ~1k Flt3-negative and 4k Flt3-positive cells. Downstream analyses were performed by using the package Seurat2 in R.

3.5 References

1. Ginhoux F. and Guilliams M. Tissue-resident macrophage ontogeny and homeostasis. *Immunity* 44, 439-449 (2016).
2. Gomez Perdiguero, E., et al. Tissue-resident macrophages originate from yolk-sac-derived erythro-myeloid progenitors. Nature 518, 547-551 (2015).
3. Ginhoux, F., et al. Fate mapping analysis reveals that adult microglia derive from primitive macrophages. *Science* 330, 841845 (2010).
4. Bain, C., et al. Constant replenishment from circulating monocytes maintains the macrophage pool in the intestine of adult mice. *Nat Immunol* 15**,** 929–937 (2014).
5. Bennett, F. C., et al. A combination of ontogeny and CNS environment establishes microglial identity. *Neuron* 98, 1170-1183 (2018).
6. Cronk, J. C., et al. Peripherally derived macrophages can engraft the brain independent of irradiation and maintain an identity distinct from microglia. *J. Exp. Med.* 215, 1627-1647 (2018).
7. Wang, Y., et al. IL-34 is a tissue-restricted ligand of CSF1R required for the development of Langerhans cells and microglia. *Nat. Immunol.* 13, 753-760 (2012).
8. Greter, M., et al. Stroma-derived interleukin-34 controls the development and maintenance of langerhans cells and the maintenance of microglia. *Immunity* 37, 1050-1060 (2012).
9. Zhu, Y., et al. Tissue-resident macrophages in pancreatic ductal adenocarcinoma originate from embryonic hematopoiesis and promote tumor progression. *Immunity* 47, 597 (2017).
10. Epelman, S., et al. Embryonic and adult-derived resident cardiac macrophages are maintained through distinct mechanisms at steady state and during inflammation. *Immunity* 40, 91-104 (2014).
11. Mueller, M., et al. Macrophage response to peripheral nerve injury: the quantitative contribution of resident and hematogenous macrophages. *Lab. Invest.* 83, 175-185 (2003).

12. Stratton, J. A., et al. Macrophages regulate Schwann cell maturation after nerve injury. *Cell Rep.* 24, 2561-2572 (2018).
13. Brazel, C. Y., et al. The FLT3 tyrosine kinase receptor inhibits neural stem/progenitor cell proliferation and collaborates with NGF to promote neuronal survival. *Mol. Cell. Neurosci.* 18, 381-393 (2001).
14. Monaco, S., et al. MHC-positive, ramified macrophages in the normal and injured rat peripheral nervous system. *J. Neurocytol.* 21, 623-634 (1992).
15. Ydens, E., et al. Profiling peripheral nerve macrophages reveals two macrophage subsets with distinct localization, transcriptome and response to injury. *Nat. Neurosci.* 23**,** 676–689 (2020).
16. Shemer, A., et al. Engrafted parenchymal brain macrophages differ from microglia in transcriptome, chromatin landscape and response to challenge. *Nat. Commun.* 9**,** 5206 (2018).
17. Lavine K.J., et al. Distinct macrophage lineages contribute to disparate patterns of cardiac recovery and remodeling in the neonatal and adult heart. *Proc. Natl. Acad. Sci.* USA. 111, 16029-34 (2014).
18. Bajpai G. et al. Tissue resident CCR2- and CCR2+ cardiac macrophages differentially orchestrate monocyte recruitment and fate specification following myocardial injury. *Circ. Res*. 124, 263-278, (2019).

Figures

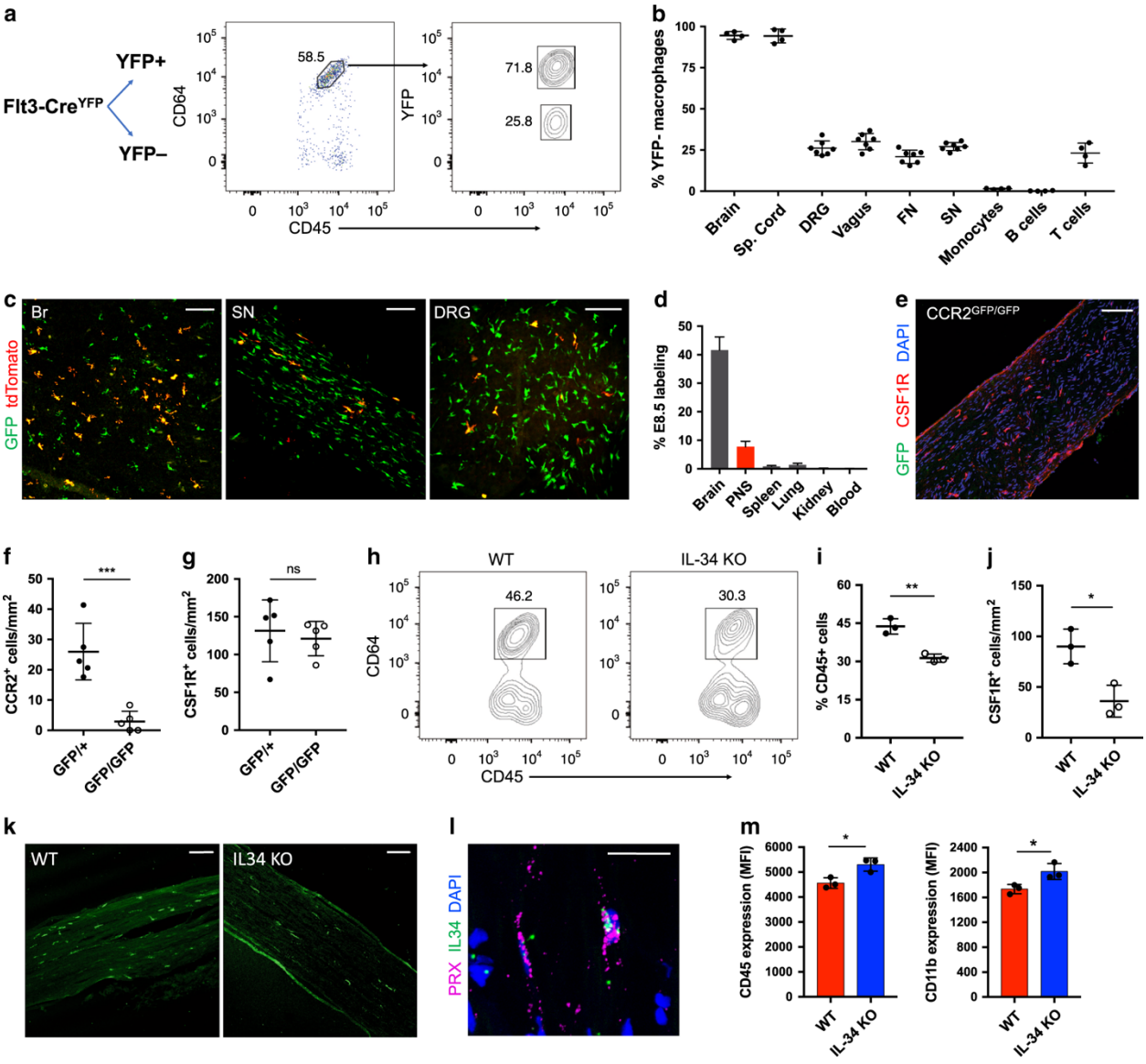

Figure 18. Shared and distinct developmental programs in PNS macrophages. a Schematic and flow cytometric gating for analysis of YFP expression in PNS macrophages from Flt3-Cre LSL-YFP sciatic nerves. **b** Comparison of YFP− macrophage ratios (expressed as % YFP− cells of population) across neural resident macrophage populations, monocytes, B cells, and T cells ($n = 4–7$ mice per group). **c** E8.5 tdTomato labeling and GFP expression in brain (left panel), sciatic nerve (middle panel), and DRG (right panel) of $CSF1R^{Mer\text{-}iCre\text{-}Mer} \times tdTomato^{fl/fl} \times CX3CR1^{GFP/+}$ mice. Scale bar, 100 µm. **d** Quantification of E8.5 tdTomato labeling in brain, PNS, spleen, lungs, kidney, and blood from newborn pups ($n = 2$ mice for blood analysis, $n = 3$ mice for tissue analysis). **e** Histological representation of PNS macrophages in

$CCR2^{GFP/GFP}$ sciatic nerves. Scale bar, 100 μm. **f** Quantification of CCR2+ CSF1R+ macrophages in sciatic nerves in $CCR2^{GFP/+}$ and $CCR2^{GFP/GFP}$ mice ($n = 5$ mice per group). **g** Quantification of total CSF1R+ macrophages in $CCR2^{GFP/+}$ and $CCR2^{GFP/GFP}$ mice ($n = 5$ mice per group). **h** Flow cytometric gating and (**i**) analysis of sciatic nerve macrophages from wild type (WT) and IL-34 knockout (KO) mice ($n = 3$ mice per group). **j** Quantification of sciatic nerve macrophages in WT and IL-34 KO mice ($n = 3$ mice per group). Scale bar, 100 μm. **k** Representative imaging of WT and IL-34 KO sciatic nerves. CSF1R staining in green. Scale bar, 120 μm. **l** In-situ hybridization in WT sciatic nerve showing IL-34 colocalization with Prx-expressing Schwann cell. Scale bar, 50 μm. **m** CD11b and CD45 expression in PNS macrophages from WT (red) and $IL\text{-}34^{LacZ/LacZ}$ (blue) mice. For imaging quantification, at least three images were taken and analyzed from each tissue and averages from each group were plotted. Each dot represents one mouse. All data are mean ± SD. Data comparing wild type and knockouts analyzed by unpaired *t*-test. $*P < 0.05$, $**P < 0.01$, $***P < 0.001$, $****P < 0.0001$; NS, not significant. Source data are available as a Source Data file.

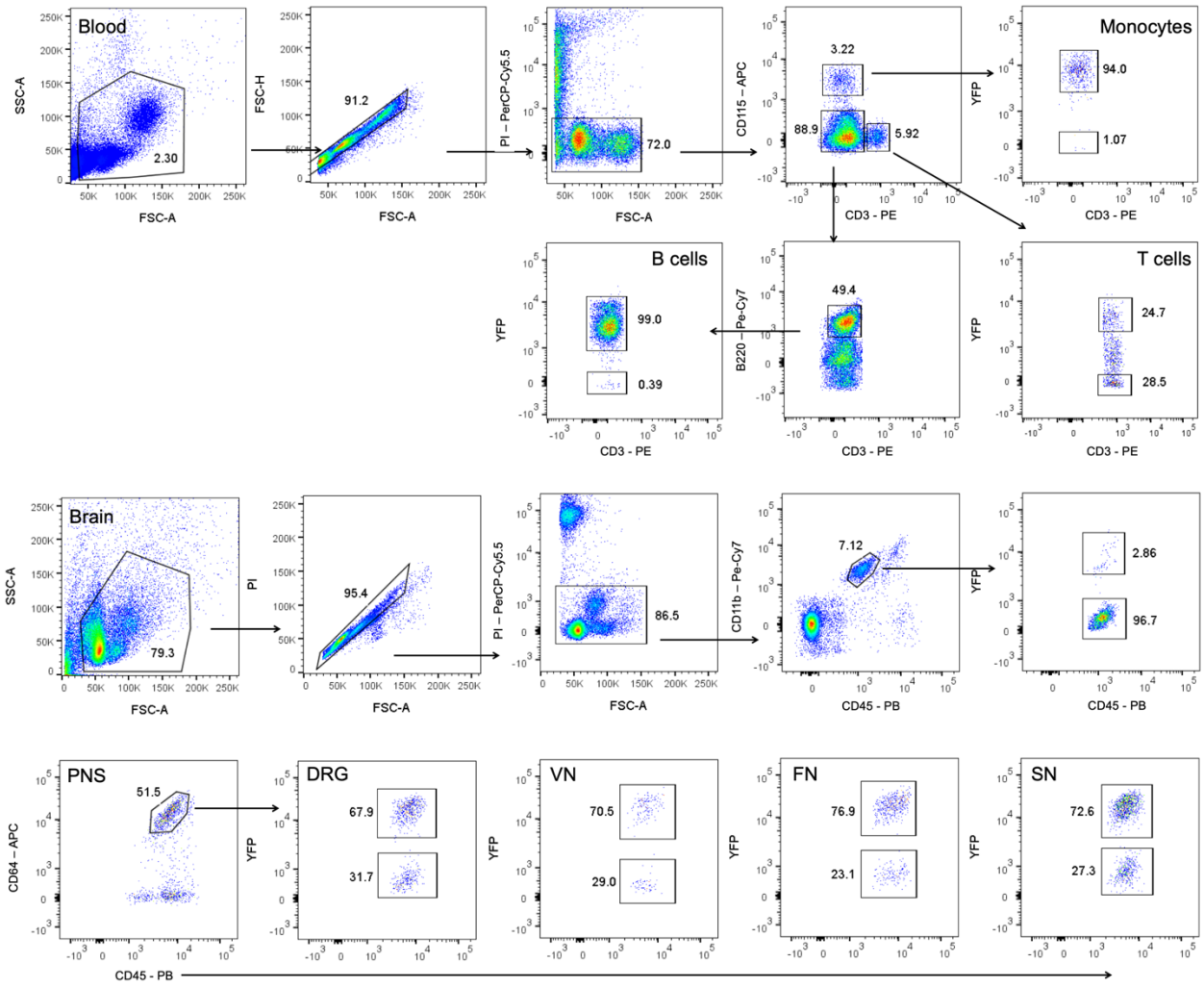

Figure 19. Flow cytometric gating of blood and CNS populations in Flt3-Cre LSL-YFP. Gating strategy for determining YFP- and YFP+ percentages in monocytes, B cells, T cells, brain microglia, and PNS macrophages (related to Figure 5a-b).

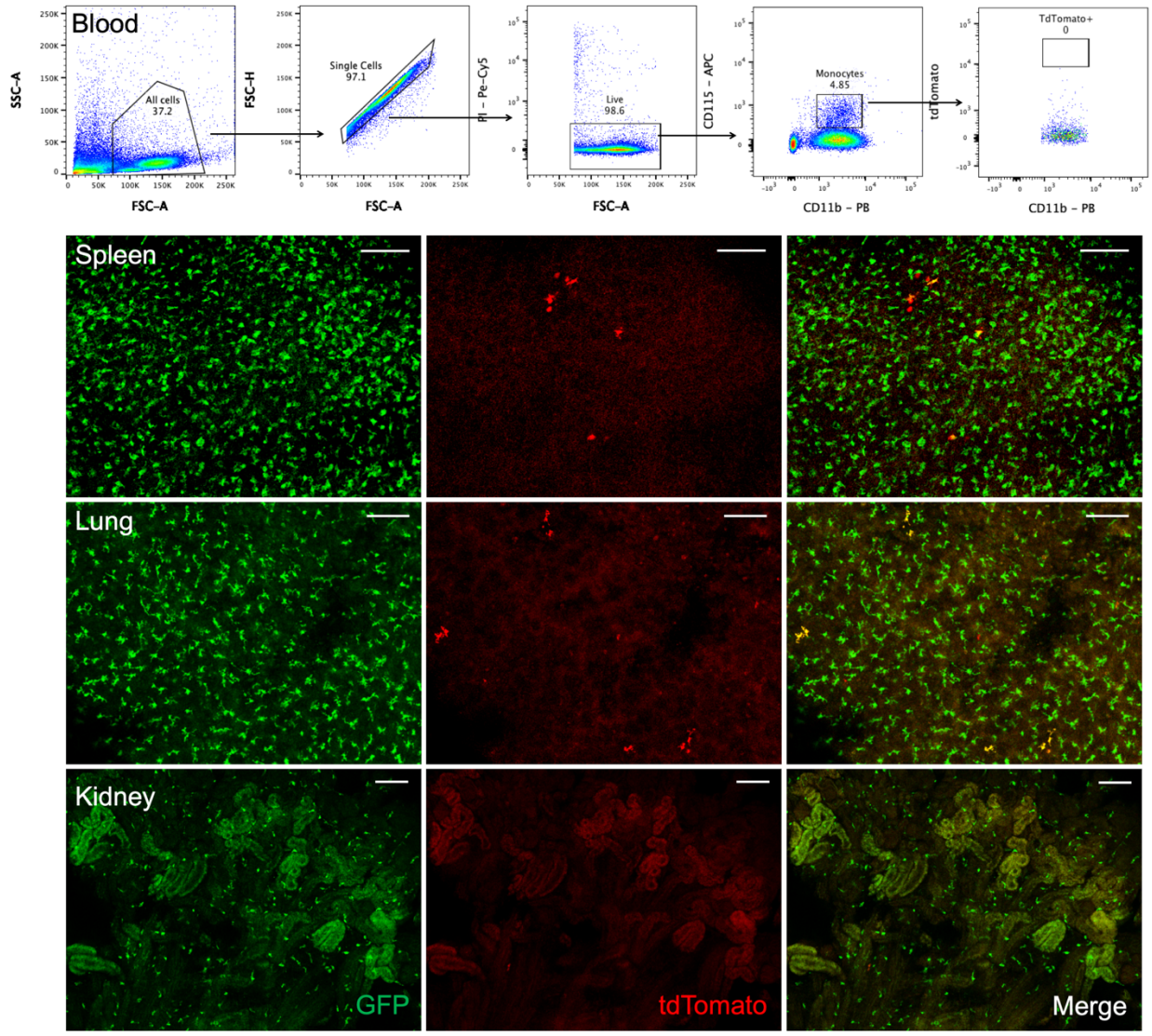

Figure 20. Embryonic day 8.5 labeling in blood and non-neuronal tissues. Flow cytometric gating of tdTomato labeling in blood and representative imaging of spleen, lung, and kidney of CSF1R$^{Mer\text{-}iCre\text{-}Mer}$ x tdTomato$^{fl/fl}$ x CX3CR1-$^{GFP/+}$ newborn pups pulsed with tamoxifen at E8.5. Scale bar, 100 µm.

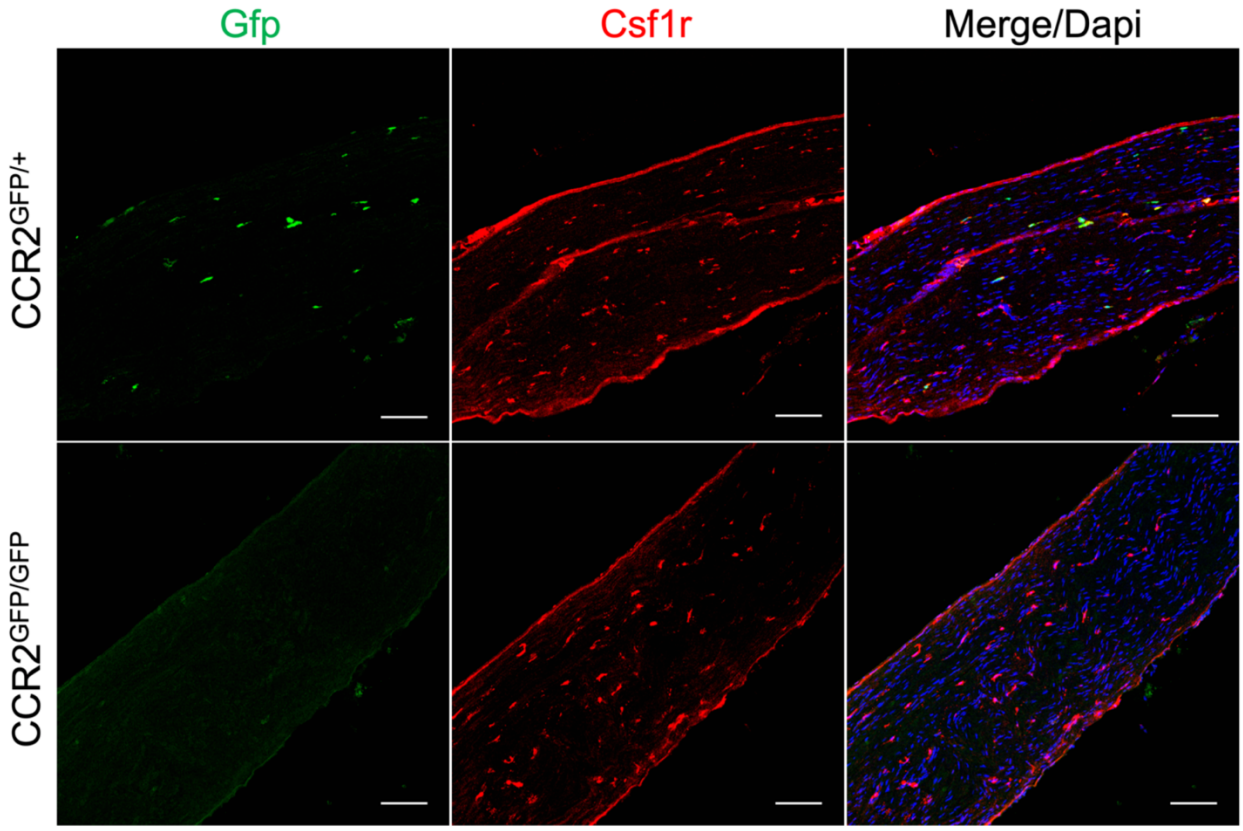

Figure 21. CCR2 is not required for seeding and maintaining PNS macrophages. Representative imaging of total CSF1R+ and CCR2+ macrophages in sciatic nerve sections of $CCR2^{GFP/+}$ and $CCR2^{GFP/GFP}$ mice. Scale bar, 100 μm.

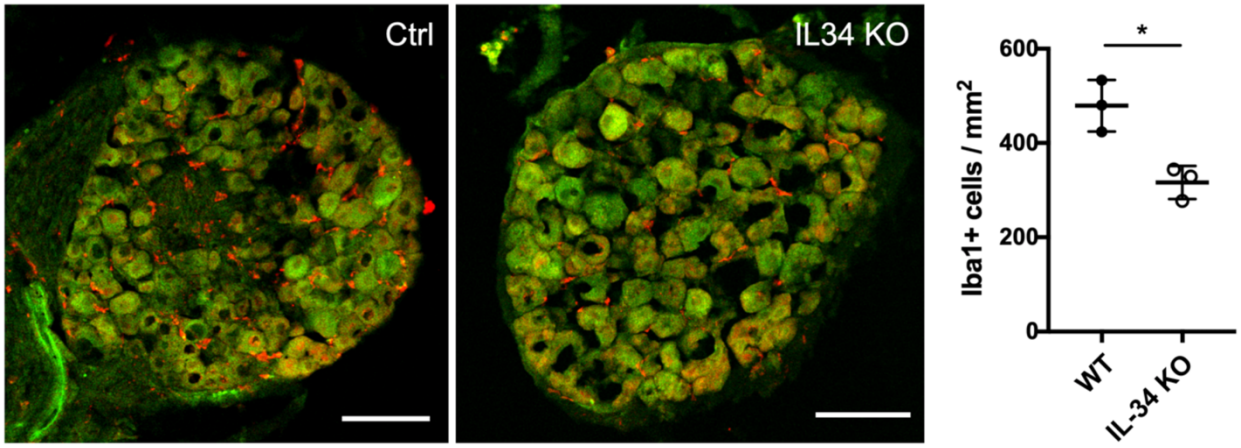

Figure 22. DRG macrophages are reduced in IL-34 KO mice. Representative imaging of Iba1+ macrophages (red) in DRG and quantification of macrophages. At least 3 images were analyzed and averaged for each DRG (n = 3 mice per group). Scale bar, 100 μm. Unpaired t test. Data are mean +/- SD.

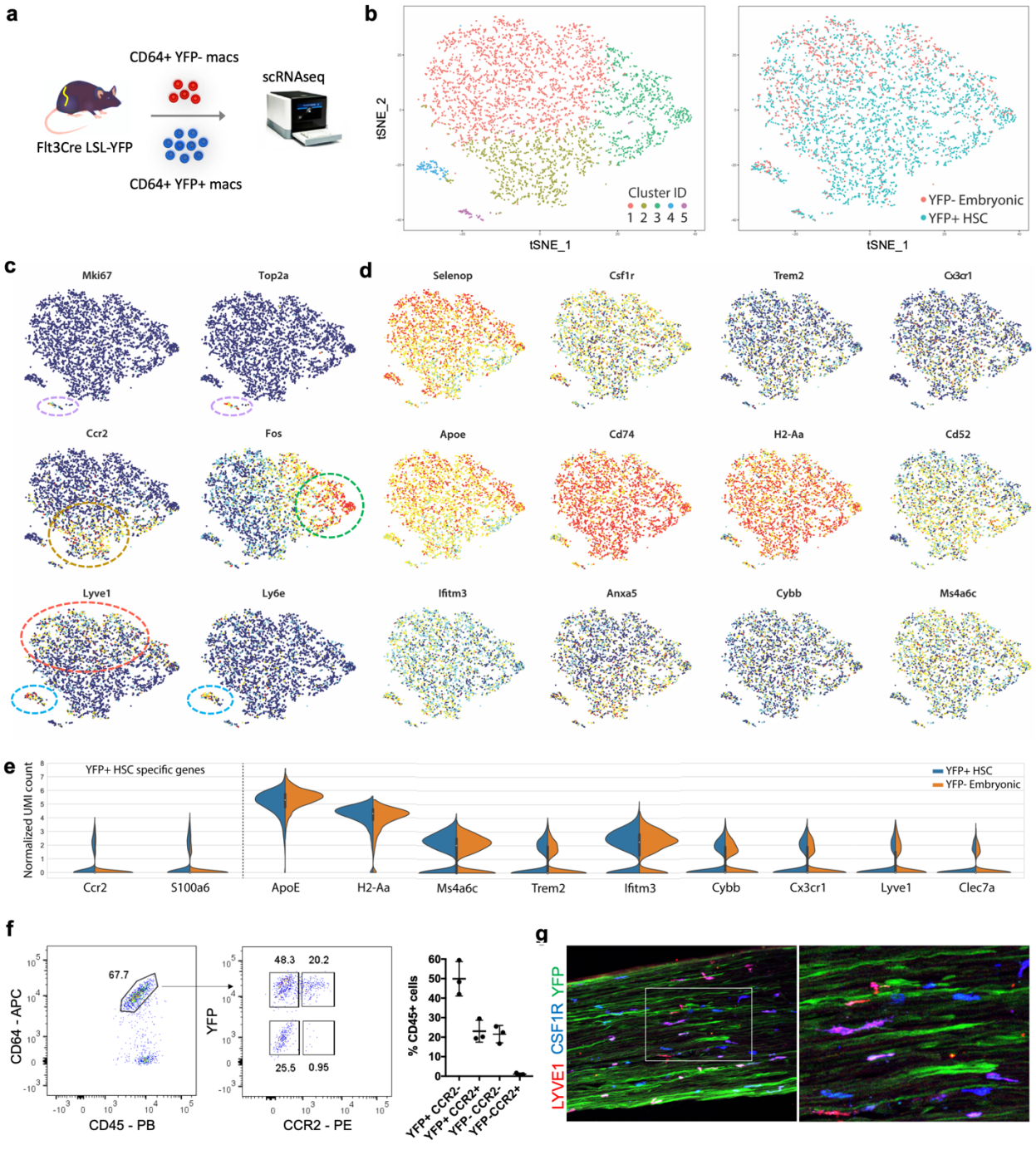

Figure 23. Nerve environment shapes transcriptional identity of PNS macrophages. a Schematic for isolation and separate single-cell RNA sequencing of YFP− embryonic and YFP+ HSC-derived macrophages from sciatic nerves of Flt3-Cre LSL-YFP$^{fl/fl}$ mice. Two single-cell libraries from YFP− and YFP+ macrophages were prepared using the 10× single-cell RNA-seq platform (Chromium Controller image provided by 10× Genomics). **b** t-SNE plot of 4121 CD64+ CD45int cells from pooled sciatic

nerves ($n = 18$) showing unsupervised clustering (left panel) and overlay of YFP− (red) and YFP+ (blue) populations (right panel). **c**, **d** t-SNE plots depicting distribution of (**c**) transcripts relating to clusters in b and (**d**) transcripts associated with microglial activation across combined embryonic and HSC-derived PNS macrophages. **e** Violin plots of marker gene expression in YFP+ HSC-derived and YFP− embryonic groups. **f** Flow cytometric identification of CCR2+ macrophages in a subset of YFP+ macrophages. Gating is representative of at least seven nerves examined over three separate experiments. **G** Representative imaging of a subset of Lyve1+ macrophages in Flt3-Cre LSL-YFP$^{fl/fl}$ mouse sciatic nerve. Scale bar, 100 μm. Source data are available as a Source Data file.

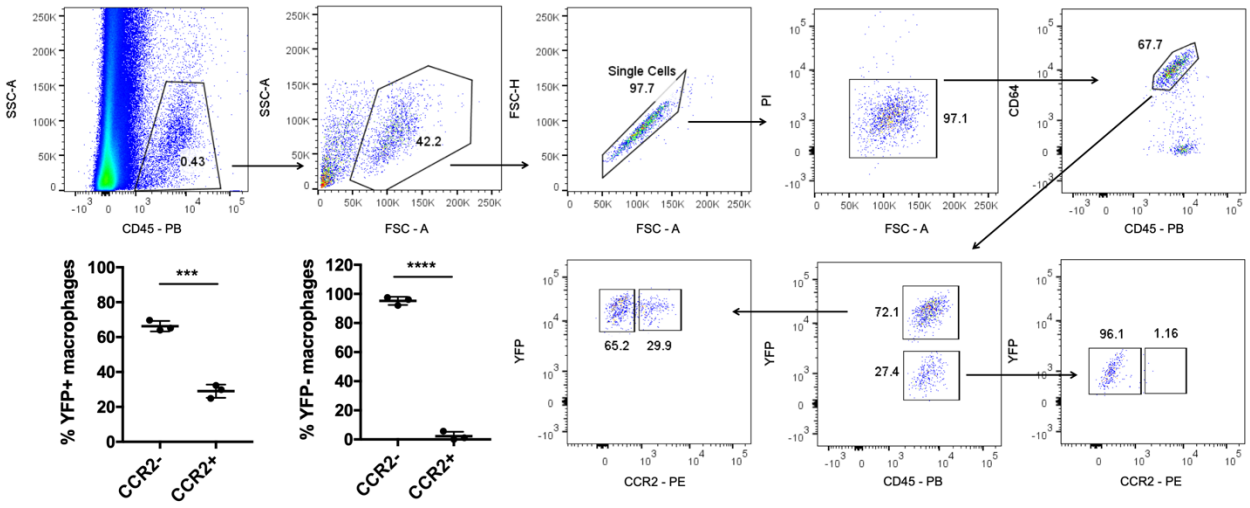

Figure 24. Quantification of CCR2+ subsets in YFP+ and YFP- macrophages in Flt3-Cre LSL-YFP mice. Gating scheme for identification and analysis of CCR2+ and CCR2- macrophages as a percentage of both YFP+ and YFP- macrophages in Flt3-Cre LSL-YFP mice. Data are mean +/- SD (n = 3).

4. Nerve environment influence on PNS macrophages

The work described in this chapter is unpublished.

AUTHOR CONTRIBUTIONS: P.L.W. purified macrophage populations, designed, and performed the experiments, and analyzed data. A.Y. analyzed RNA-seq data and helped with experiments. G.J.R. and J.M. designed and supervised the experiments.

4.1 Introduction

The unique functionality of the nervous system can be attributed to the cells that comprise it. Both the PNS and CNS are made up of neurons, glia, resident macrophages, stromal cells, and endothelial cells, which together determine the nerve environment.

Studies in mice show that CNS microglia rapidly lose their transcriptional signature if taken out of the brain [1,2]. CNS-naïve cells also rapidly take on a microglia signature when transplanted into the brain [2-4]. These findings demonstrate that intrinsic tissue factors critically shape microglial phenotypes. Indeed, a known key regulator for microglia is TGF-β signaling, which not only confers expression of microglial signature genes, but is also required for microglia development and homeostasis [5].

Another intrinsic feature of the nervous system is myelin. Structurally, myelin is comprised of a mixture of proteins and phospholipids that insulate nerve fibers and increase the speed of electrical impulses [6]. In the CNS, myelin is produced by oligodendrocytes, while in the PNS, myelin is produced by Schwann cells. It has been reported that CNS microglia signatures differ between areas of grey matter, which contain mostly neuronal cell bodies and few myelinated axons, and areas of white matter, which contain mostly long-range myelinated axons and few neuronal cell bodies [7]. Microglia in grey matter were shown to have higher expression of type1 interferon genes, while microglia in white matter were enriched for NF-κB pathway genes [8]. Apart from injury conditions, it is currently unclear how myelin affects macrophage biology, either in the CNS or PNS. As the PNS contains diverse glia, including satellite glial cells surrounding the cell bodies of DRG neurons, and both myelinating and non-myelinating Schwann cells surrounding axons, it offers a unique opportunity to study how neural resident macrophages are affected by myelin or other glia-derived factors.

A number of extrinsic factors also contribute to the status of neuronal tissues. One example is neurotropic viruses, or viruses that are capable of infecting nerve cells. Indeed, neurotropic viruses have been common in humans over the course of evolutionary history [9]. These include deadly viruses such as rabies and polio that have been successfully targeted by vaccines over the past century [10]. The more common alpha herpesviruses include herpes simplex virus (HSV) species that primarily infect and either destroy or remain latent in sensory neurons [11]. According to estimates from the World Health Organization (WHO), HSV-1 and HSV-2, which causes oral and genital herpes, respectively infect 67% and 13% of people under the age of 49 worldwide [12]. While HSV primarily infects peripheral neurons, they have been shown in both mice and humans to be able to translocate to the CNS [11,13]. Interestingly, there is a long proposed link between viral infections and neurodegenerative diseases, which spans both peripheral neuropathies such as Guillain Barre syndrome as well as CNS diseases such as multiple sclerosis and Alzheimer's disease [13-15]. Yet, how viral infections affect PNS macrophages and their response in host protection is virtually unknown.

Apart from infections, physical trauma is another highly prevalent and clinically important extrinsic factor that affects the nerve environment. When nerves are cut or crushed, the part of the axon distal to the injury degenerates, a process called Wallerian degeneration [16]. Axon degeneration is followed by myelin sheath degradation and macrophage infiltration. While studies show that after nerve injury, PNS macrophages facilitate debris clearance, angiogenesis, SC maturation, and provide ROS to help with regeneration [17-20], how macrophages are themselves affected by the injured nerve environment is less clear. One clue may come from the basic function of phagocytosis. PNS macrophages have been shown to be critical for debris clearance through phagocytosis, not only of myelin, but also of cells undergoing apoptosis, a

process called efferocytosis [21]. How macrophages process and respond to phagocytic cargo is therefore a topic of interest. Indeed, it has been shown that in both atherosclerotic lesions and CNS lesions, lipid-filled macrophages are important mediators that can decide the difference between pro-regenerative and anti-regenerative outcomes [22-24]. How PNS macrophages accomplish these and the contextual factors that regulate their success or failure will be of interest for strategies aimed at improving regeneration and downstream outcomes.

Here we build on our understanding of PNS macrophages to explore their phenotypes in models with perturbed nerve environments. We explore PNS macrophage responses and transcriptional signatures in nerves with dysregulated Schwann cells as well as in nerve injury. We show that phagocytic PNS macrophages adopt a unique signature associated with lipid-handling that may have implications for neuroinflammation and regeneration.

4.2 Results

4.2.1 Schwann cell dysregulation induces macrophage expansion and reprogramming

To study the link between nerve environment and PNS macrophage signatures, we examined mice lacking TSC2, a prime regulator of mTOR signaling that is often mutated in patients with tuberous sclerosis [25], in Schwann cells. We bred MPZ-Cre mice with TSC2 floxed mice to generate MPZ-Cre $TSC2^{Fl/Fl}$ mice (TSC2-SCKO mice). These mice manifest arrested Schwann cell development at the promyelinating stage and exhibit a massive increase in Sox10+ glia accompanied by severe hypomyelination and loss of nerve conduction [25] (Fig. 25 a,b). To label peripheral nerve macrophages in TSC2-SCKO mice, we crossed them to CX3CR1-GFP

mice. Upon examination of the sciatic nerve, we observed a remarkable 20-fold expansion of PNS macrophages (Fig. 25c). Consistent with the highly specific expression of MPZ in peripheral nerves [26], CNS microglia numbers did not appear to be significantly different (Fig. 25c). These results show that PNS macrophage numbers are highly sensitive to perturbances in Schwann cells.

We next sought to examine gene expression in macrophages from TSC2-SCKO mice. We sorted 1000 CX3CR1-GFP+ $CD45^{int/low}$ cells per replicate from sciatic nerves and brains of TSC2-SCKO and WT mice and performed RNA-seq. Interestingly, TSC2-SCKO macrophages had a significant reduction in previously identified PNS macrophage signatures (*Cbr2*, *Msr1*, *Ms4a7*, *C7bb*, *Clec7a*, and *Aoah*) as well as genes involved in macrophage activation (*Cd68*) and immune response (*Clec7a*, *Mrc1*, *Tlr4*, and *Tlr7*) (Fig. 26a,b). TSC2-SCKO macrophages also had reduced expression of genes associated with endosomal/retromer functions, including several sorting nexin genes that have been shown to promote phagosome maturation [27,28] (Fig. 26b). Upregulated transcripts in TSC2-SCKO macrophages included genes associated with neuronal connectivity/support and gli/hedgehog signaling (Fig. 26b). Surprisingly, microglial homeostatic genes, including *Sall1*, *Tmem119*, *P2ry12*, and *Tgfbr1* were also increased in TSC2-SCKO macrophages (Fig. 26c). Since the expression in microglial signatures, including *Sall1*, has been attributed to TGF-β signaling [1,5], we examined the correlation between *Tgfbr1* and *Sall1* across our samples. Indeed, we found the expression of *Sall1* to be directly correlated with *Tgfbr1* expression across both sciatic nerve macrophage and brain microglia samples (Fig. 26d). Thus, PNS macrophages in TSC2-SCKO mice exhibit a unique transcriptional signature characterized by dysregulated cellular dynamics, reduced activation, and increased TGF-β responsiveness.

To examine macrophage heterogeneity in TSC2-SCKO mice, we performed single cell sequencing on sciatic nerve macrophages from these mice (Fig. 27a). Notably, microglial genes (*Tmem119*, *Hexb*, and *P2ry12*) were ubiquitously expressed in TSC2-SCKO macrophages (Fig. 27b). However, we did observe differential gene expression between two subgroups of macrophages (Fig. 27c). Genes expressed in the first subgroup included *Apoc1* and *Apoc4*, which are associated with monocyte-to-macrophage differentiation and lipid metabolism [29,30], Pf4, which is associated with the inhibition of angiogenesis [31], and *Gas6*, which is involved in the stimulation of cell proliferation and also the regulation of Schwann cell maturation by macrophages after nerve injury (Fig. 27c) [19]. The second group expressed *Il1b*, *Jun*, and *Cxcl12*, which correspond with inflammation, and *Ppp1r15a*, which is associated with stressful growth arrest conditions (Fig. 27c) [32]. Therefore, while most genes are homogeneously expressed in sciatic nerve macrophages in TSC2-SCKO, there is some polarization in genes related to cell cycle, lipid metabolism, and pro-inflammatory response. Taken together, our results suggest that PNS macrophages are uniquely responsive in TSC2-SCKO mice.

4.2.2 PNS macrophage signatures in nerves with different myelin composition

Given the association between increased microglial signatures and reduced myelination in the TSC2-SCKO mice, we sought to determine if myelination could be a significant regulator in the observed shift in gene expression. It has been reported that vagal nerves are less myelinated than sciatic nerves due to vagal nerves containing a higher composition of non-myelinating Schwann cells than myelinating Schwann cells, with the opposite being true in sciatic nerves [33]. Thus, we reasoned that if microglial activation genes are correlated with the

extent of myelination, PNS macrophages in the sciatic should express more activated microglia signature genes and less microglial homeostatic genes.

Using our previously generated data on PNS macrophages [34], we specifically compared gene expression in vagal and sciatic nerve macrophages. While we found 126 genes that were upregulated by 2-fold or more in sciatic nerves macrophages, we did not see any upregulation of microglial activation genes in this population (Fig. 28a). Instead, we found that sciatic nerve macrophages expressed genes related to fatty acid derivative transport (*Anxa1*, *Abcc1*, and *Pla2g2d*), angiogenesis (*Plxnd1*, *Fgfr1*, *Ecm1*, and *Tgfbr3*), and neural cell migration (*Cxcl12*, *Ccdc141*, *Egfr*, and *Ndnf*) (Fig. 28a and Table 1). In vagal nerves macrophages, we found 137 genes that were upregulated by at least 2-fold (Fig. 28b). Remarkably, these included a wide range of genes involved in immune response, including genes involved in interferon response (*Ifi47*, *Ifit2*, *Ifi204*, *Oasl2*, and *Stat1*), antigen presentation (*H2-T24*, *H2-Q4*, *H2-Q7*, and *H2-Q6*), response to biotic stimulus (*Gbp6*, *Peli1*, *Axl*, *Cr2*, and *Herc6*) (Fig. 28b). Indeed, many of the genes that were enriched in vagal nerve macrophages, including *Axl*, *Cp*, *Apoe*, and several interferon response genes have been linked to microglial activation [34]. Interestingly, vagal nerve macrophages also exhibited increased expression of a number of homeostatic microglia genes, including *Olfml3*, *Tmem119*, *Hexb* and *Tgfbr1* (Fig 28b). Taken together, these observations suggest that expression of microglial activation-associated genes in PNS macrophages is uniquely regulated and not simply explained by myelination.

4.2.3 PNS macrophages in HSV infection

Since the activation signature seen in PNS macrophages is highly associated with immune defense against pathogens, we reasoned that PNS macrophages may be responsive to

infections of the nervous system. Thus, we sought to examine the PNS macrophage response to infection with HSV, a highly common neurotropic virus that has evolved alongside humans and is responsible for oral and genital herpes infection. We started by infecting female mice intravaginally, a natural route of infection in humans, with HSV-1 and HSV-2 at a standard dose of 10^4 PFU per mouse [35]. While it is known that both strains spread to sensory neurons of the dorsal root ganglia (DRG) after infection [35], it is unclear what happens in the sciatic nerve. Interestingly, we saw an early increase in sciatic nerve macrophages in both HSV-1 and HSV-2 infected mice at 1 day post infection (Fig 29a). HSV-2 infected mice showed a further increase in sciatic nerve macrophages by day 5 (Fig. 29a). The expanded macrophages in sciatic nerves were highly positive for MHC-II (Fig. 29b). To further determine if virus was present in the sciatic nerve, we infected macrophage-labeled CX3CR1-CreER TdTomato mice with GFP-tagged HSV-1 and imaged whole optically cleared nerves 10 days post infection. Remarkably, we saw strings of ameboid macrophages in proximal and distal sites of infected sciatic nerves containing what appeared to be GFP-positive virus (Fig. 29c). Indeed, this reflects published work on the ability of macrophages to trap HSV in multivesicular bodies to facilitate protection against severe disease [36]. These results show that PNS macrophages are highly responsive to HSV infection and may function to control viral spread by phagocytosing infectious particles.

4.2.4 Phagocytic activation of PNS macrophages after nerve injury

To examine resident macrophage responses following nerve injury, we performed sciatic nerve crush in CX3CR1-CreER tdTomato mice and imaged nerves at different time points. Early crush (day 3) was associated with the appearance of CD68+ lysosomal staining in macrophages at the crush site (Fig. 30a). Interestingly, tdTomato+ resident macrophages appeared on the outer

region of the crush site (Fig. 30a), suggesting that the majority of macrophages at the injury core are monocyte-derived cells. Using CX3CR1-GFP/+ mice treated with anti-CSF1R monoclonal antibody to deplete resident macrophages, we observed that CX3CR1-GFP+ monocytes indeed infiltrate the injury site as well as distal regions of the nerve (Fig 30b). By day 7, CD68+ macrophages that actively phagocytose and degrade myelin in degenerating axons appear in distal regions where GFAP+ reactive SCs can be seen, but remain absent proximal to the crush site (Fig. 30c,d). Thus, phagocytosis and monocyte recruitment after nerve injury follows the spatial dynamics of Wallerian degeneration.

Since phagocytic activation of macrophages after nerve injury was specific to degeneration, we wondered whether nerve breakdown was required for phagocytic activation in nerve macrophages. To test this, we compared the response of PNS macrophages to sciatic nerve transection in WT mice versus Sarm1-KO mice, which are resistant to axonal degeneration due to loss of SARM1, an enzyme that controls axon death via NAD+ depletion [37]. We found that at 14 days following transection, PNS macrophages became ameboid and were highly phagocytic in WT nerves, whereas in Sarm1KO nerves macrophages remained elongated and non-phagocytic (Fig. 31a). Indeed, there appeared to be no significant myelin breakdown in Sarm1KO mice while WT mice exhibited a high degree of breakdown (Fig. 31b). These results suggest that phagocytic activation in PNS macrophages is tightly controlled by axonal destruction.

4.2.5 Polarization of lipid metabolism and pro-inflammatory genes in PNS macrophages

To examine gene expression in PNS macrophages after injury, we performed single cell RNA-sequencing on injured nerves 4 days after nerve crush (Fig. 32). Focusing only on macrophages, we observed a small population (cluster 2) that was highly enriched for genes related to lipid metabolism (*Fabp5*, *Pld3*, *Gpnmb*, *Plin2*, and *Trem2*). Since our lab has recently identified several of these lipid-related markers to be upregulated in "foamy" macrophages in atherosclerotic plaques [38], we reasoned that cluster 2 macrophages may be similarly lipid-laden foam cells. To confirm this, we performed flow cytometry on nerves 3 weeks after injury and probed for lipid content using BODIPY dye. BODIPY+ macrophages were identified in the injured nerve and exhibited increased side scatter, indicating increased cellular granularity (Fig. 33a,b).

We also observed the expression of pro-inflammatory cytokines *Cxcl2* and *Il1b*, which were distinct from the highly specific foamy macrophages in cluster 2, but were instead part of the *Ccr2*+ population. Indeed, macrophages in cluster 2 were notably negative for *Ccr2* expression, suggesting that they are either resident macrophages or recruited cells that have lost *Ccr2* expression. Interestingly, there was some overlap in *Abca1*, *Plin2* and *Trem2* with the *Ccr2*+ pro-inflammatory subset. Thus, while there is a distinct separation between non-inflammatory *Ccr2*- foamy macrophages and *Ccr2*+ inflammatory monocytes/macrophages, there seems to be a shared region where some lipid-associated genes are co-expressed with pro-inflammatory markers, perhaps reflecting a gradient of macrophage differentiation (Fig. 32).

Given the unique activation response observed after nerve injury, we were interested to see how lipid-associated and pro-inflammatory genes of interest are expressed in other conditions of nerve dysregulation. We thus combined our SC-RNA-sequencing data from sciatic nerve crush injury, TSC2-SCKO, and steady state nerves to generate a combined single cell atlas

containing macrophages and other immune cells from the three conditions (Fig. 34a,b). Interestingly, macrophages from both crush injury and TSC2-SCKO showed a similar pattern of separation between cells expressing the lipid-associated gene *Trem2* and cells expressing *Ccr2* (Fig. 34c). Moreover, macrophages enriched for *Trem2* in injury also uniquely expressed the pro-regenerative gene *Arg1* and microglia activation-associated gene *Spp1* (Fig. 34c). These results suggest that macrophages in both crush injury and TSC2-SCKO are uniquely polarized with a lipid-associated *Ccr2*- subset representing a pro-regenerative state that is distinct from pro-inflammatory *Ccr2*+ monocytes/macrophages.

4.2.6 Targeting lipid metabolism in PNS macrophages may influence nerve regeneration

We next wanted to assess whether targeting lipid-associated genes in nerve macrophages affects nerve regeneration. Since APOE has been linked to foam cells in atherosclerosis via its role in reverse cholesterol transport [39], we sought to examine injury response in APOE-KO mice using an inverted screen test, which measures the ability of mice to hang onto an inverted screen. As expected, all mice lost their ability to hang onto the screen during the first and second week following injury (Fig. 35a). However, by the third week, two mice (1 in each genotype) regained performance (Fig. 35a). Interestingly, improvements in performance were correlated with macrophage numbers, including BODIPY+ foam cells, regardless of genotype (Fig. 35b). While the number of mice was insufficient to determine significance, Apoe genotype did not appear to affect performance on the inverted screen test after injury.

Another gene that is functionally associated with APOE and also has been shown to regulate lipid handling is TREM2 [40,41]. Interestingly, the ability for TREM2 to regulate microglia activation responses in neurodegeneration also seems to be important for the regulation of cholesterol metabolism after myelin phagocytosis [41]. Indeed, it appears that TREM2 signaling contributes to cholesterol efflux, which is essential for microglia metabolism after phagocytic challenge [41,42]. To assess recovery after sciatic nerve crush in TREM2-KO versus WT mice, we measured the sciatic functional index (SFI) in both groups up to 3 weeks after injury (Fig 36a). While there appeared to be a slight trend of reduced SFI in TREM2-KO mice, no significant difference in regeneration was found.

To further assess both TREM2-KO and APOE-KO mice with an additional screening method, we performed nerve conductance velocity (NCV) testing after sciatic nerve crush injuries (Fig. 36b). We again saw an apparent trend in reduced NCV in TREM2-KO mice early after injury, but observed no significant difference in regeneration between the groups over time (Fig 36b). These results suggest that APOE and TREM2 are not critical for the recovery of peripheral nerve function after injury in adult mice.

Although we did not observe any difference in regeneration with our genetic models for disrupting lipid metabolism, we reasoned that environmental factors could perhaps mediate regeneration through foam cells. Indeed, Berghoff and colleagues have shown that dietary cholesterol can improve repair of demyelinated brain lesions by glial cells in adult mice [43]. This prompted us to test whether increasing dietary cholesterol by high fat diet (HFD) feeding could affect the regeneration response after injury. We started HFD two weeks prior to injury and maintained it throughout the course of NCV testing. Remarkably, HFD-fed WT mice exhibited a significant increase in NCV, reaching nearly normal levels of nerve conductance by 2 weeks

after injury (Fig. 36c). HFD-fed TREM2-KO mice also showed improved NCV compared to chow-fed controls (Fig. 36c). Since TREM2 is highly specific to macrophages, this suggests a partial dependence on macrophages for HFD-enhanced regeneration after injury. To examine whether HFD enhances regeneration when macrophage numbers are significantly reduced, we performed nerve crush in CCR2-KO mice, in which monocyte recruitment is diminished, and administered HFD directly after injury. Indeed, CCR2-KO mice also showed a significant improvement in NCV after HFD feeding (Fig 36d). Therefore, we suspect that dietary lipids facilitate regeneration through both macrophages and peripheral glia, which likely possess compensatory roles for restoring nerve signaling after injury.

4.3 Discussion

Here we find strong evidence that the nerve environment shapes PNS macrophage signatures. Specifically, we show that Schwann cells, the major myelinating cell type in the PNS, have an important influence on nerve macrophages. While it is apparent that macrophages expand significantly in TSC2-SCKO mice, the mechanism by which this occurs remains a mystery. One interesting observation is the expression of genes associated with development, cell cycle dysregulation, and growth arrest, which raises questions about the differentiation state of PNS macrophages in this model. If PNS macrophages exist in a state that is not fully differentiated in this model, their expansion could perhaps be a remnant from earlier developmental processes. Further experiments are needed to determine whether PNS macrophage expansion occurs during development and whether immature PNS macrophages express similar genes as TSC2-SCKO macrophages.

Future experiments should also examine signaling pathways between Schwann cell precursors and PNS macrophages in TSC2-SCKO mice. Could macrophage numbers be "tuned" according to Schwann cell precursor density, which is increased by at least 10-fold in TSC2-SCKO [25]? Indeed, a similar effect has been reported between macrophages and fibroblasts, with in vivo experiments showing that cell cultures containing only fibroblasts and macrophages will reach a stable 1:1 ratio by 15 days regardless of starting ratio [44]. This two-cell circuit effect can be attributed to local growth factors, including PDGF and CSF1 that are secreted by macrophages and fibroblasts, respectively, to support the survival of the other [44]. Interestingly, endoneurial fibroblasts are known to arise from the neural crest and share a precursor state with Schwann cells. Future experiments should examine potential signaling pathways between Schwann cell precursor populations and macrophages in TSC2-SCKO mice. Findings from such studies may have clinical implications for diseases such as glioma, which similarly exhibit an increase in glial progenitor-like cells [45]. It will be interesting to consider if enhancing the activation of PNS macrophages, perhaps by *Sall1* or *Tgfbr* knockdown, increases phagocytosis of expanded glia in these models.

The elevation of microglial genes, including *Sall1*, and reduction of PNS macrophage genes in TSC2-SCKO mice further demonstrates that there are underlying similarities between CNS microglia and PNS macrophages. At the molecular level, the shift in microglial signatures may be explained by increased TGF-β signaling. Indeed, the >2-fold increase in whole nerve expression of *Tgfb1* and *Tgfb2*, and the parallel increase in *Tgfbr1* in sciatic nerve macrophages in TSC2-SCKO mice strongly supports the role of TGF-β in this model. In a separate project involving single nuclei sequencing in peripheral nerves, we observe that many PNS cell types, including endothelial cells, stromal cells, macrophages, and Schwann cells, express *Tgfb1* during

steady state. Future studies should investigate which cells are producing TGF-β in TSC2-SCKO and whether TGF-β also has a proliferative effect on PNS macrophages.

While we hypothesized that microglial activation genes would be reduced in vagal nerve macrophages due to the relatively reduced myelination of vagal nerves compared to sciatic nerves [33], we were surprised to see instead the significant upregulation of interferon-related and antigen presentation genes in vagal nerve macrophages. We previously missed these genes when we included fascial nerves in our analysis, since fascial nerve macrophages also expressed elevated immune defense genes [34]. It is interesting to consider whether the upregulation of immune defense genes is due to the presence of microbiota in the innervation targets of vagal and fascial nerves, which innervate the respiratory/digestive tract and skin, respectively. This raises the possibility that downstream molecules may travel up the nerve, perhaps via fluid drainage channels. Since interferon-related genes are also apparently enriched in grey matter microglia [7], it is possible that there is indeed a link between macrophage signatures and myelination. It is also interesting that vagal nerve macrophages expressed higher homeostatic microglia genes. This could be attributed to the fact that the vagus nerve is a cranial nerve that is directly connects to the brain. The vagus is also unique in that it is primarily comprised of parasympathetic fibers, which are not present in the sciatic, and may provide unique signals [33]. Whether microglial homeostatic or activation-associated genes are associated with a proximal to distal or distal to proximal gradient in vagal nerves is also interesting to consider.

Since herpesvirus infection of the nervous system is a common occurrence with potentially dangerous complications [13], it is important to examine the role of PNS macrophages in the context of HSV infection. While we infected mice by an intravaginal route, we were surprised to see a robust effect on macrophage numbers in the sciatic nerve. One explanation

could be that infection of shared DRG neurons innervating both the vagina and sciatic nerve leads to anterograde travel of HSV-1 down to the sciatic. Indeed, we saw apparent viral particles being engulfed by phagocytic macrophages in the sciatic and even further down near the distal portion. If true, this could have novel implications for chronic pain conditions such as sciatica. Additionally, there may be implications for CNS neurodegenerative diseases. Given the ability of HSV to translocate into the CNS in both mouse models and in humans, there has been a longstanding interest in HSV infection and neurodegenerative diseases such as AD [13-15]. Remarkably, mice expressing humanized APOE4, which encodes the APOE isoform most highly associated with Alzheimer's disease risk, have higher rates of CNS translocation [46]. Future work should examine the role of APOE and PNS macrophages in herpesvirus infection, including their implications for virus-induced nerve pain and HSV translocation to the CNS.

Our observations in nerve injury indicate that CD68+ foamy PNS macrophages represent a sensitive marker for neurodegeneration that specifically localizes to areas of axonal breakdown. Others have also shown CD68 staining to be associated with activated microglia in the brain [47]. Spatial studies in both CNS and PNS may therefore utilize CD68 as a marker to detect regions of degeneration. Since we also found a high degree of specificity between cells expressing high levels of *Cd68* and cells expressing high levels of foam cell genes, including *Trem2*, *Fabp5*, and *Gpnmb*, we speculate that macrophage activation beginning with early myelin engulfment leads to downstream lipid metabolic processes and eventual resolution of inflammatory responses. Indeed, our single cell RNA-seq experiments show that as early as 4 days after crush, foam cells express Arg1, which is associated with immunosuppression in macrophages [48]. Future experiments should examine macrophage signatures further out after

injury to determine whether pro-inflammatory cells transition into anti-inflammatory cells and whether this occurs through lipid uptake and efflux.

The pairing of lipid efflux with inflammatory resolution in PNS macrophages warrants further exploration. Indeed, evidence from studies in atherosclerosis and CNS demyelination suggests that lipid efflux may be critical for mediating disease outcomes [49,50]. Lipid efflux has also been suggested as a mechanism to transport lipids to directly support remyelination, particularly in early stages following CNS injury. In these studies, Berghoff and colleagues show that while microglia were important contributors to early remyelination in CNS demyelinating conditions, oligodendrocytes and their precursors were more important for remyelination in later stages [24]. This could perhaps explain why we did not observe an effect for TREM2 or APOE in regeneration, as Schwann cells may be able to facilitate their own remyelination. Future experiments should examine these and other genetic regulators in aged mice, which show deficits in regeneration. Studies that target lipid metabolism in PNS macrophages, whether through diet or other methods, may reveal new strategies for remyelination and reducing inflammation in peripheral neuropathies.

4.4 Materials and methods

Experimental animals

Mouse care and experiments were performed in accordance with protocols approved by the Institutional Animal Care and Use Committee at Washington University in St. Louis under the protocols 20170154 and 20170030. Mice were kept on a 12 h light–dark cycle and received food and water ad libitum. The following strains were used: C57/B6 CD45.1 (stock number 002014), CX3CR1$^{GFP/+}$(Cx3cr1tm1Litt/LittJ; stock number 008451), and Rosa$^{Lsl\text{-}Tomato}$ (stock

number 007905) mice were purchased from Jackson Laboratory (JAX) and bred at Washington University. APOE-KO, TREM2-KO mice were previously described and generated at Washington University, and Sall1-^{GFP}mice were kindly provided by M. Rauchman.

Sciatic nerve injuries

For all injuries, mice were anesthetized with Avertin. Then the left sciatic nerve was exposed and crushed for 30 seconds or transected above the branching point but below the sciatic notch. Mice were then given subcutaneous analgesic and monitored for three days.

Nerve conductance velocity testing

NCV was done using Viking machine. Mice were anesthetized with isoflourane and electrodes were placed in the sciatic notch and footpad or in the ankle and footpad. Velocities and latency were determined with the software.

High Fat diet

HFD (42% fat Envigo TD.88137) was given prior to injuries for 2 weeks. Mice were weighed before the administration of HFD and in 2 week increments after HFD.

Immunohistochemistry

For whole-mount imaging, samples were harvested and immediately stored in 4% paraformaldehyde (PFA) containing 40% sucrose overnight. Samples were then washed in phosphate-buffered saline (PBS), blocked, stained, and imaged. For frozen sections, samples were collected, stored in PFA/sucrose, and embedded into optimal cutting

temperature compound. Fifteen-micrometer cuts were made for SNs. Sections were then blocked in 1% bovine serum albumin, stained, and imaged. Antibodies to the following proteins were used: CSF1R (R&D Systems, accession number P09581), MHCII (IA/IE clone M5/114.15.2), CD68, GFAP, PDPN, and LYVE1 (ab14917).

Preparation of single-cell suspensions

For blood, mice were bled from the cheek immediately before killing and cells were prepared as previously described. For nerves and all other tissues, mice were killed and perfused with PBS. Nerves were collected and kept on ice until dissociation. Cells were then incubated with gentle shaking for 20 min in digestion media containing collagenase IV, hyaluronidase, and DNAse. Cells were then washed and filtered through 70 μm cell strainers. For brain and spinal cord, myelin was removed using a 40/80% Percoll gradient.

Flow cytometry

Single-cell suspensions were stained at 4 °C. Dead cells were excluded by propidium idodide (PI). Antibodies to the following proteins were used: B220 (clone RA3-6B2), CCR2 (clone SA203G11), CD3e (clone 145-2C11), CD4 (clone RM4-5), CD8 (clone 53-6.7), CD11b (clone M1/70), CD16 (clone 2.4G2), CD45 (clone 30-F11), CD64 (clone X54-5/7.1), CD115 (clone AFS98), GR1 (clone 1A8), and Ly6C (clone HK1.4). Cells were analyzed on a LSRII flow cytometer (Becton Dickinson) and analyzed with FlowJo software.

Cell sorting

For bulk RNA-seq, cells from 6-week-old male mice were double sorted on a FACSAria II (Becton Dickinson) for a final count of 1000 cells into lysis buffer according to the ImmGen Consortium standard operating protocol. Tissues were collected into culture medium on ice and subsequently digested with collagenase IV, hyaluronidase, and DNAse. Following digestion, samples were washed and kept on ice until sorting. The sort was repeated so that all macrophages were sorted twice, with a minimum of 1000 cells recovered. During the second round, cells were sorted directly into 5 µl TCL buffer (Qiagen) containing 5% beta-mercaptoethanol. Samples were kept at −80 °C until further processing. For sorting in preparation of the Flt3-Cre LSL-YFP single-cell Seq experiments, SNs from 19 male mice aged 10–12 weeks were combined and CD64+ CD45int macrophages were sorted individually into YFP+ and YFP− groups, yielding 18,000 and 5,000 cells, respectively. Both groups were immediately run on the 10× Genomics Chromium Controller according to the manufacturer's protocol.

RNA-seq and data analyses

Library preparation, RNA-seq, data generation and quality-control was conducted by the ImmGen Consortium according to the consortium's standard protocols (https://www.immgen.org/Protocols/ImmGenULI_RNAseq_methods.pdf). In short, the reads were aligned to the mouse genome GRCm38/mm10 primary assembly and gene annotation vM16 using STAR 2.5.4a. The raw counts were generated by using featureCounts (http://subread.sourceforge.net/). Normalization was performed using the DESeq2 package from Bioconductor. Differential gene expression analysis was performed using edgeR 3.20.9 in a pairwise manner among all conditions, and a total of 12,240 DEGs were defined with a *p*-

value ≤ 0.001 and ≥4-fold difference. To construct the correlation plot, Euclidean distance among samples were calculated based on the differential expression matrix and clustering was performed using the ward.D2 algorithm in R. CNS/PNS shared, PNS-specific, and CNS-specific genes were determined by subclustering the DEGs based on the expression pattern with a refined *k*-mean clustering using R followed by manual curations. For neuronal microenvironment analysis, only the transcriptome profile of macrophages and microglia from PNS and CNS were used and analyzed through the same pipeline as mentioned above.

4.5 References

1. Gosselin, D. et al. An environment-dependent transcriptional network specifies human microglia identity. *Science* 356, (2017).
2. Bennett, F. C., et al. A combination of ontogeny and CNS environment establishes microglial identity. *Neuron* 98, 1170-1183 (2018).
3. Cronk, J. C., et al. Peripherally derived macrophages can engraft the brain independent of irradiation and maintain an identity distinct from microglia. *J. Exp. Med.* 215, 1627-1647 (2018).
4. Shemer, A., et al. Engrafted parenchymal brain macrophages differ from microglia in transcriptome, chromatin landscape and response to challenge. *Nat. Commun.* 9**,** 5206 (2018).
5. Butovsky, O., et al. Identification of a unique TGF-beta-dependent molecular and functional signature in microglia. *Nat. Neurosci.* 17, 131-143 (2014).
6. Nave K.A., and Werner, H.B. Myelination of the nervous system: mechanisms and functions. Annu. Rev. Cell. Dev. Biol. 30, 503-33 (2014).
7. Lee, J., et al. Heterogeneity of microglia and their differential roles in white matter pathology. *CNS neuroscience & therapeutics* 25, 1290-1298 (2019).
8. van der Poel, M., et al. Transcriptional profiling of human microglia reveals grey–white matter heterogeneity and multiple sclerosis-associated changes. *Nat. Commun.* 10, 1139 (2019).

9. Kaján, G.L., et al. Virus–host coevolution with a focus on animal and human DNA viruses. *J. Mol. Evol.* 88, 41–56 (2020).
10. Hajj Hussein, I., et al. Vaccines through centuries: major cornerstones of global health. *Front. Public. Health.* 3, (2015).
11. Koyuncu O.O., et al. Virus infections in the nervous system. *Cell Host Microbe* 13, 279-93 (2013).
12. James, C., et al. Herpes simplex virus: global infection prevalence and incidence estimates, 2016. *Bull. World Health Organ.* 98, 315-329 (2020).
13. Marcocci, M.E., et al. Herpes simplex virus-1 in the brain: the dark side of a sneaky infection. *Trends in microbiology* 28, 808-820 (2020).
14. Krauer, F., et al. Zika virus infection as a cause of congenital brain abnormalities and Guillain-Barré syndrome: systematic review. *PLoS Med.* 14, (2017).
15. Gilden, D.H. Infectious causes of multiple sclerosis. *The Lancet Neurology* 4, 195-202 (2005).
16. Conforti, L., et al. Wallerian degeneration: an emerging axon death pathway linking injury and disease. *Nat. Rev. Neurosci.* 15, 394–409 (2014).
17. Klein, D. and R. Martini. Myelin and macrophages in the PNS: an intimate relationship in trauma and disease. *Brain Res.* 1641, 130-138 (2016).
18. Cattin, A. L., et al. Macrophage-induced blood vessels guide Schwann cell-mediated regeneration of peripheral nerves. *Cell* 162,1127-1139 (2015).
19. Stratton, J. A., et al. Macrophages regulate Schwann cell maturation after nerve injury. *Cell Rep.* 24, 2561-2572 (2018).
20. Hervera, A., et al. Reactive oxygen species regulate axonal regeneration through the release of exosomal NADPH oxidase 2 complexes into injured axons. *Nat. Cell Biol.* 20, 307–319 (2018).
21. Kalinski, A.L., et al. Analysis of the immune response to sciatic nerve injury identifies efferocytosis as a key mechanism of nerve debridement. *eLife* 9, (2020).
22. Zimmer, S., et al. Cyclodextrin promotes atherosclerosis regression via macrophage reprogramming. *Sci. Transl. Med.* 8 (2016).
23. Cantuti-Castelvetri, Ludovico et al. "Defective cholesterol clearance limits remyelination in the aged central nervous system." *Science (New York, N.Y.)* vol. 359,6376 (2018): 684-688.

24. Berghoff, S.A., et al. Microglia facilitate repair of demyelinated lesions via post-squalene sterol synthesis. *Nat. Neurosci.* 24, 47–60 (2021).
25. Beirowski, B., et al. mTORC1 promotes proliferation of immature Schwann cells and myelin growth of differentiated Schwann cells. *Proc. Natl. Acad. Sci. USA*. 114, E4261-E4270 (2017).
26. Feltri, M. L., et al. P0-Cre transgenic mice for inactivation of adhesion molecules in Schwann cells. *Ann. NY Acad. Sci*. 883, 116-123 (1999).
27. Lou, J., et al. SNX10 promotes phagosome maturation in macrophages and protects mice against *Listeria monocytogenes* infection. *Oncotarget* 8, 53935-53947 (2017).
28. Klose, M., et al. SNX3 drives maturation of Borrelia phagosomes by forming a hub for PI(3)P, Rab5a, and galectin-9. *J. Cell. Biol.* 218, 3039–3059 (2019).
29. Fuior, E.V., and Gafencu, A.V. Apolipoprotein C1: Its pleiotropic effects in lipid metabolism and beyond." *Int. J. Mol. Sci.* 20, 5939 (2019).
30. Xu, S., et al. The association of APOC4 polymorphisms with premature coronary artery disease in a Chinese Han population." *Lipids Health Dis.* 14, (2015).
31. Bikfalvi, A. Platelet factor 4: an inhibitor of angiogenesis. *Semin. Thromb. Hemost.* 30, 379-85 (2004).
32. Morton, E., et al. Identification of the growth arrest and DNA damage protein GADD34 in the normal human heart and demonstration of alterations in expression following myocardial ischaemia. *Int. J. Cardiol.* 107, 126-9 (2006).
33. Howe, J. R. and Ritchie, J. M. Sodium currents in Schwann cells from myelinated and non-myelinated nerves of neonatal and adult rabbits. *J. Physiol.* 425, 169-210 (1990).
34. Wang, P.L., et al. Peripheral nerve resident macrophages share tissue-specific programming and features of activated microglia. *Nat. Commun.* 11, 2552 (2020).
35. Lee, A.G., et al. T cell response kinetics determines neuroinfection outcomes during murine HSV infection. *JCI Insight* 5, (2020).
36. Lang, J., et al. Acid ceramidase of macrophages traps herpes simplex virus in multivesicular bodies and protects from severe disease. *Nat. Comm.* 11, (2020).
37. Gerdts, J., et al. Sarm1-mediated axon degeneration requires both SAM and TIR interactions. *J. Neurosci.* 33, 13569-80 (2013).

38. Kim, K., et al. Transcriptome analysis reveals nonfoamy rather than foamy plaque macrophages are proinflammatory in atherosclerotic murine models. *Circ. Res*. 123, 1127-42 (2018).
39. Martel, C., et al. Lymphatic vasculature mediates macrophage reverse cholesterol transport in mice. *J. Clin. Invest*. 123, 1571-9 (2013).
40. Krasemann, S., et al. The TREM2-APOE pathway drives the transcriptional phenotype of dysfunctional microglia in neurodegenerative diseases. *Immunity* 47, 566-581 (2017).
41. Nugent, A.A., et al. TREM2 regulates microglial cholesterol metabolism upon chronic phagocytic challenge. *Neuron* 105, 837-854 (2020).
42. Ulland, T.K., et al. TREM2 maintains microglial metabolic fitness in Alzheimer's disease. *Cell* 170, 649-663 (2017).
43. Berghoff, S., et al. Dietary cholesterol promotes repair of demyelinated lesions in the adult brain. *Nat. Commun.* 8, 14241 (2017).
44. Zhou, X., et al. Circuit design features of a stable two-cell system. *Cell* 172, 744-757 (2018).
45. Ilkhanizadeh, S., et al. Glial progenitors as targets for transformation in glioma. *Adv. Cancer Res*. 121, 1-65 (2014).
46. Burgos, J.S., et al. Effect of apolipoprotein E on the cerebral load of latent herpes simplex virus type 1 DNA. *J. Virol*. 80, 5383-7 (2006).
47. Marschallinger, J., et al. Lipid-droplet-accumulating microglia represent a dysfunctional and proinflammatory state in the aging brain. *Nat. Neurosci.* 23, 194–208 (2020).
48. Mills, C.D., et al. M-1/M-2 macrophages and the Th1/Th2 paradigm. *J. Immunol.* 164, 6166-73 (2000).
49. Zimmer, S., et al. Cyclodextrin promotes atherosclerosis regression via macrophage reprogramming. *Sci. Transl. Med*. 8, (2016).
50. Cantuti-Castelvetri, L., et al. Defective cholesterol clearance limits remyelination in the aged central nervous system. *Science* 359, 684-88 (2018).

Figures

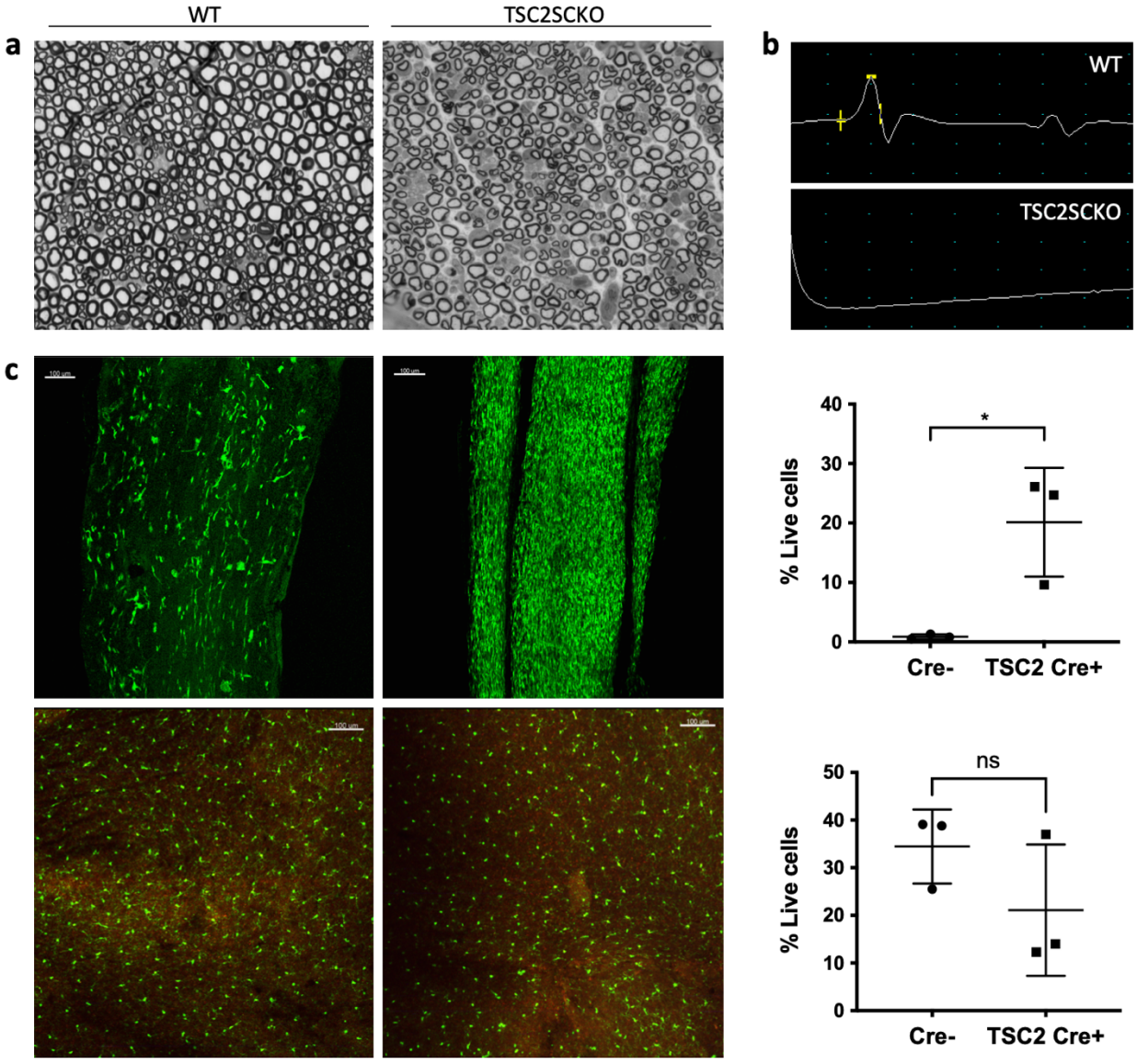

Figure 25. PNS macrophage expansion in TSC2-SCKO mice with dysmyelinated nerves. a. light microscopy of sciatic nerves from WT control and TSC2-SCKO mice at age P28 reveals dysmyelinated nerves in the mutant. b. Nerve conductance velocity (NCV) plot showing representative signals from WT an TSC2-SCKO mutant sciatic nerves. c. Confocal imaging and flow cytometric quantification of GFP+ macrophages in sciatic nerves (top) and brains (bottom) in CX3CR1-GFP/+ control mice and CX3CR1-GFP/+ TSC2-SCKO mutant mice.

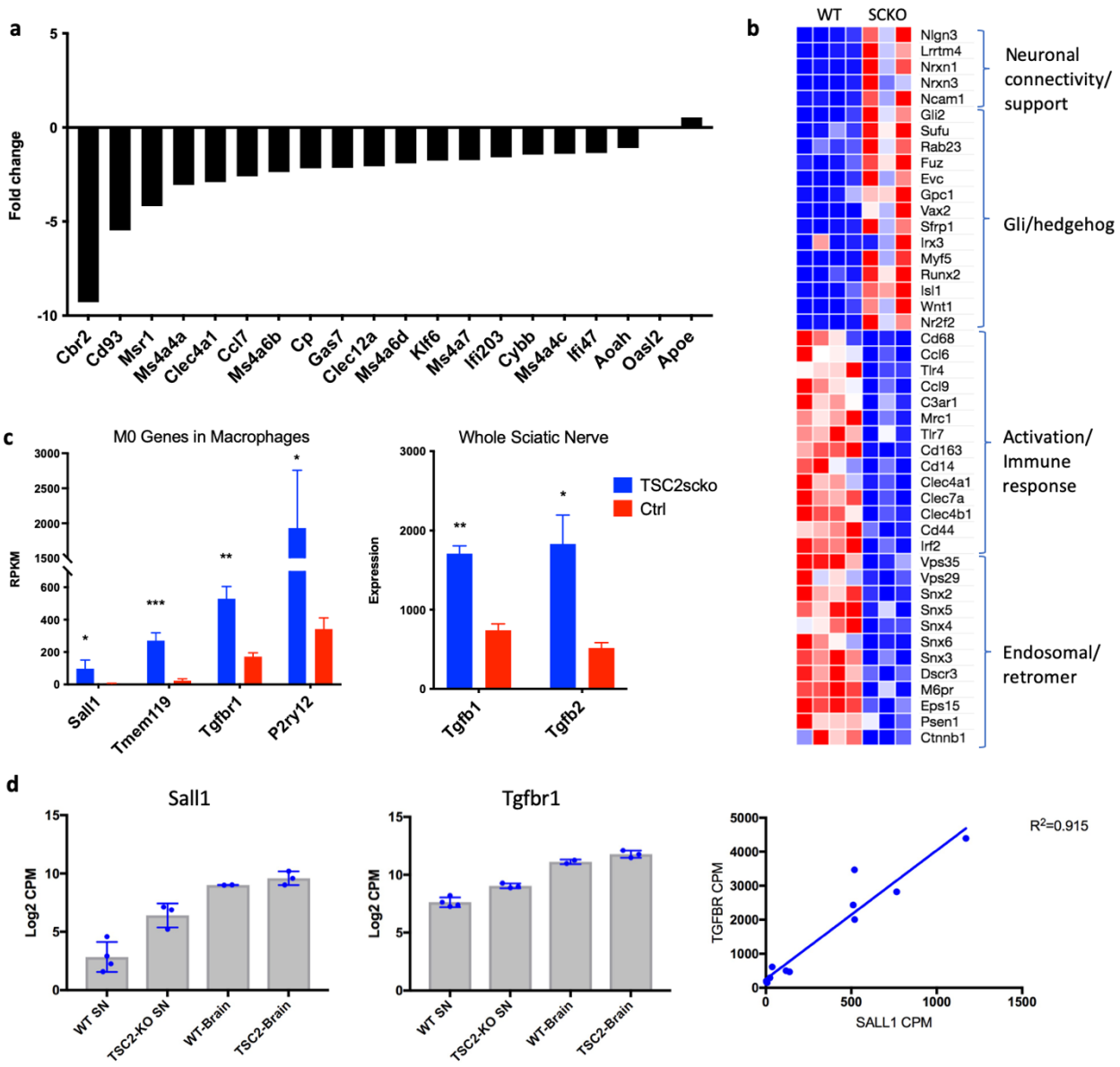

Figure 26. Gene expression analysis of TSC2-SCKO mice reveals upregulation of microglial genes and downregulation of PNS macrophage genes. a. Fold change in previously identified PNS macrophage-enriched genes. b. Differential expression of genes related to neuronal connectivity/support, gli/hedgehog, activation/immune response, and endosomal/retromer functions in WT and TSC2-SCKO macrophages. c. Upregulation of homeostatic microglia (M0) genes in PNS macrophages from TSC2-SCKO (left) and upregulation of Tgfb1 and Tgfb2 expression in whole sciatic nerves of TSC2-SCKO mice. d. Correlation between Sall1 expression and Tgfbr1 expression in sciatic nerve macrophages and brain microglia from WT and TSC2-SCKO mice.

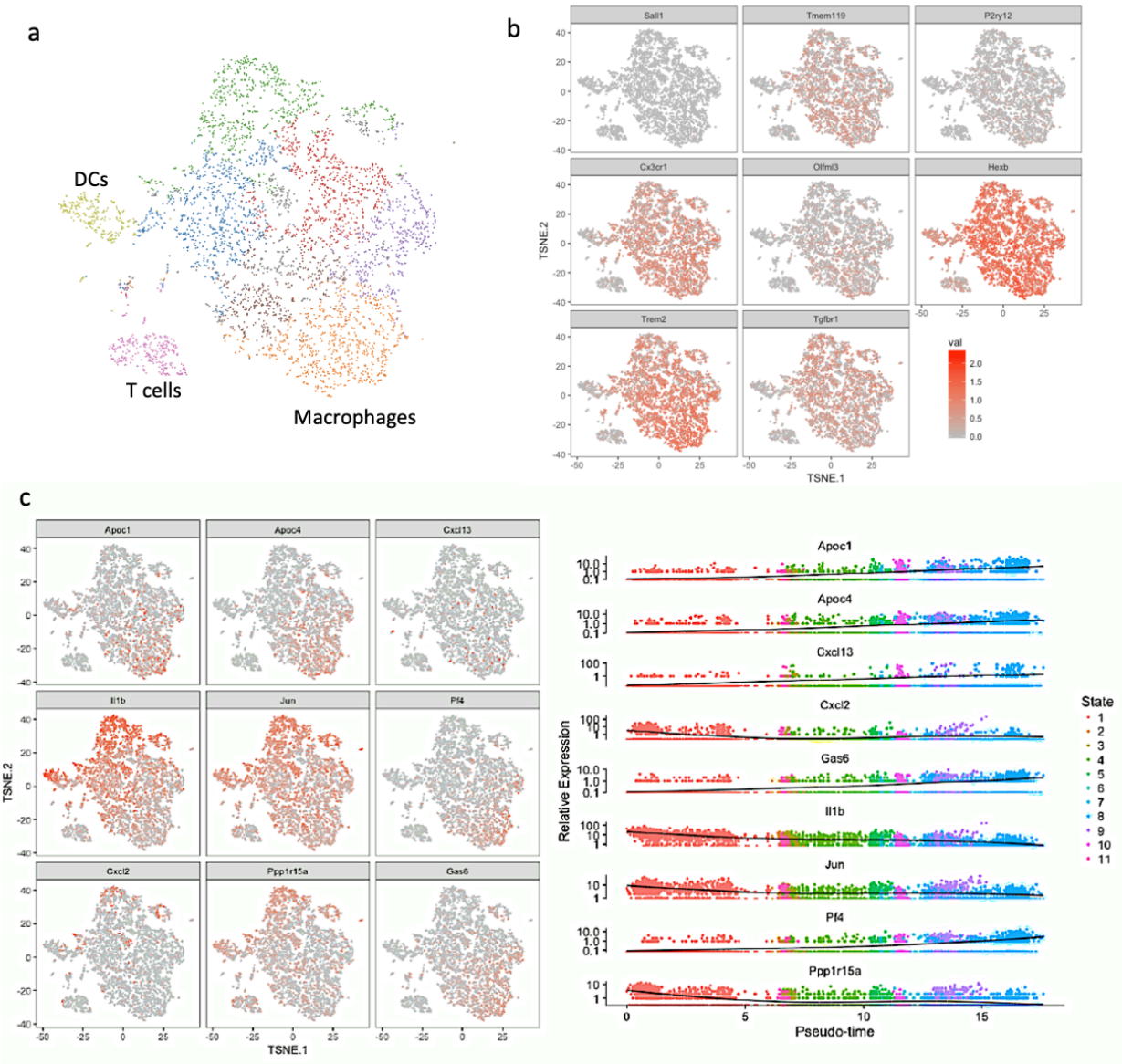

Figure 27. Single cell analysis of PNS macrophage heterogeneity in TSC2-SCKO. a. Clustering of CD45+ immune cells from TSC2-SCKO sciatic nerves. b. Expression of microglial genes in TSC2-SCKO macrophages. c. Polarization of differentially expressed genes in TSC2-SCKO macrophages.

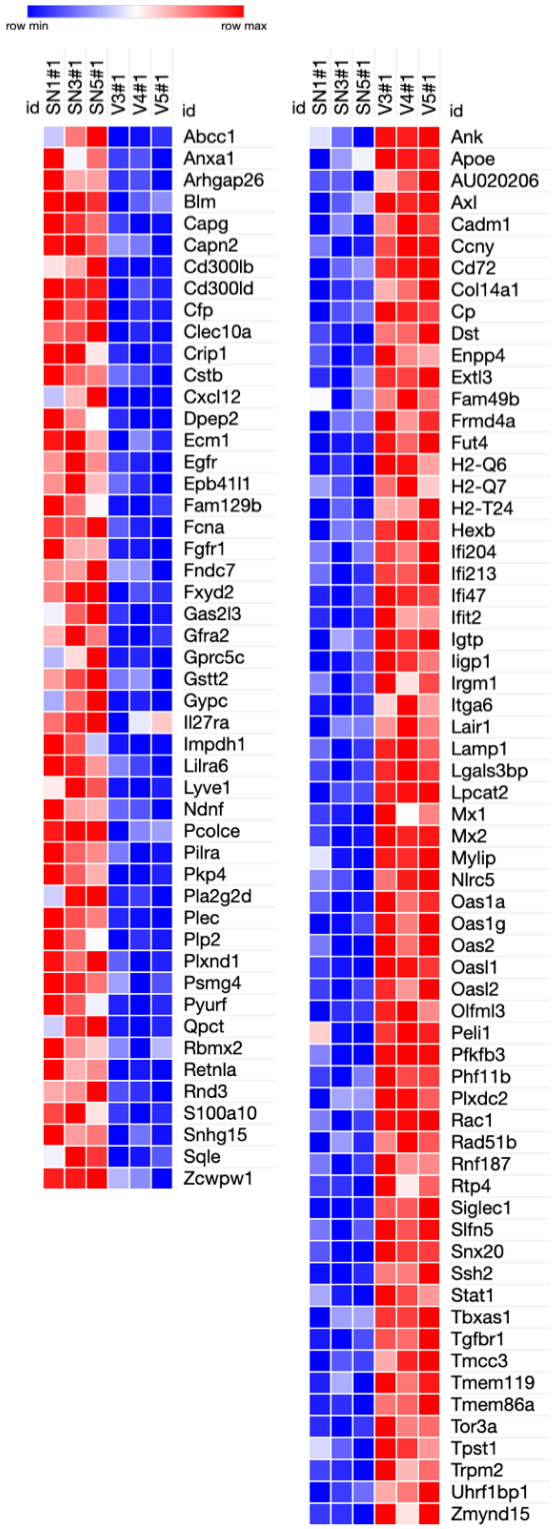

Figure 28. Differential expression of steady state genes associated with myelinated and unmyelinated nerves. Genes enriched in macrophages from sciatic nerves (left) containing predominantly myelinated axons, and vagal nerves (right) containing predominantly unmyelinated axons.

Table 3. Gene ontology analysis of genes enriched in sciatic nerve macrophages.

GO term	Description	P-value	FDR q-value	Enrichment N, B, (n, b)
GO:0022029	telencephalon cell migration	1.56E-4	1E0	14.54 (12726,35,100,4)
GO:0021885	forebrain cell migration	1.74E-4	1E0	14.14 (12726,36,100,4)
GO:0001525	angiogenesis	2E-4	9.51E-1	4.99 (12726,204,100,8)
GO:0060045	positive regulation of cardiac muscle cell proliferation	2.96E-4	1E0	22.46 (12726,17,100,3)
GO:0071715	icosanoid transport	3.53E-4	1E0	21.21 (12726,18,100,3)
GO:1901571	fatty acid derivative transport	3.53E-4	8.37E-1	21.21 (12726,18,100,3)
GO:0098609	cell-cell adhesion	5.8E-4	1E0	4.26 (12726,239,100,8)
GO:0007435	salivary gland morphogenesis	6.02E-4	1E0	50.90 (12726,5,100,2)

Table 4. Gene ontology analysis of genes enriched in vagal nerve macrophages.

GO term	Description	P-value	FDR q-value	Enrichment N, B, (n, b)
GO:0060700	regulation of ribonuclease activity	1.14E-9	1.63E-5	91.82 (12726,11,63,5)
GO:0035458	cellular response to interferon-beta	2.81E-8	2E-4	31.89 (12726,38,63,6)
GO:0001912	positive regulation of leukocyte mediated cytotoxicity	1.2E-7	4.29E-4	25.25 (12726,48,63,6)
GO:0002376	immune system process	1.22E-7	2.91E-4	3.56 (12726,1190,63,21)
GO:0043207	response to external biotic stimulus	1.8E-7	3.2E-4	5.00 (12726,606,63,15)
GO:0051607	defense response to virus	4.8E-7	6.22E-4	11.30 (12726,143,63,8)
GO:0050792	regulation of viral process	2.03E-6	2.07E-3	9.34 (12726,173,63,8)
GO:0043903	regulation of symbiosis, encompassing mutualism through parasitism	3.49E-6	2.76E-3	8.69 (12726,186,63,8)
GO:0001916	positive regulation of T cell mediated cytotoxicity	4.5E-6	3.21E-3	35.13 (12726,23,63,4)
GO:0045071	negative regulation of viral genome replication	4.52E-6	3.06E-3	20.20 (12726,50,63,5)
GO:0048525	negative regulation of viral process	4.87E-6	3.15E-3	13.62 (12726,89,63,6)
GO:0098542	defense response to other organism	2.06E-5	1.13E-2	5.85 (12726,311,63,9)
GO:0002486	antigen processing and presentation of endogenous peptide antigen via MHC class I via ER pathway, TAP-independent	2.46E-5	1.3E-2	50.50 (12726,12,63,3)

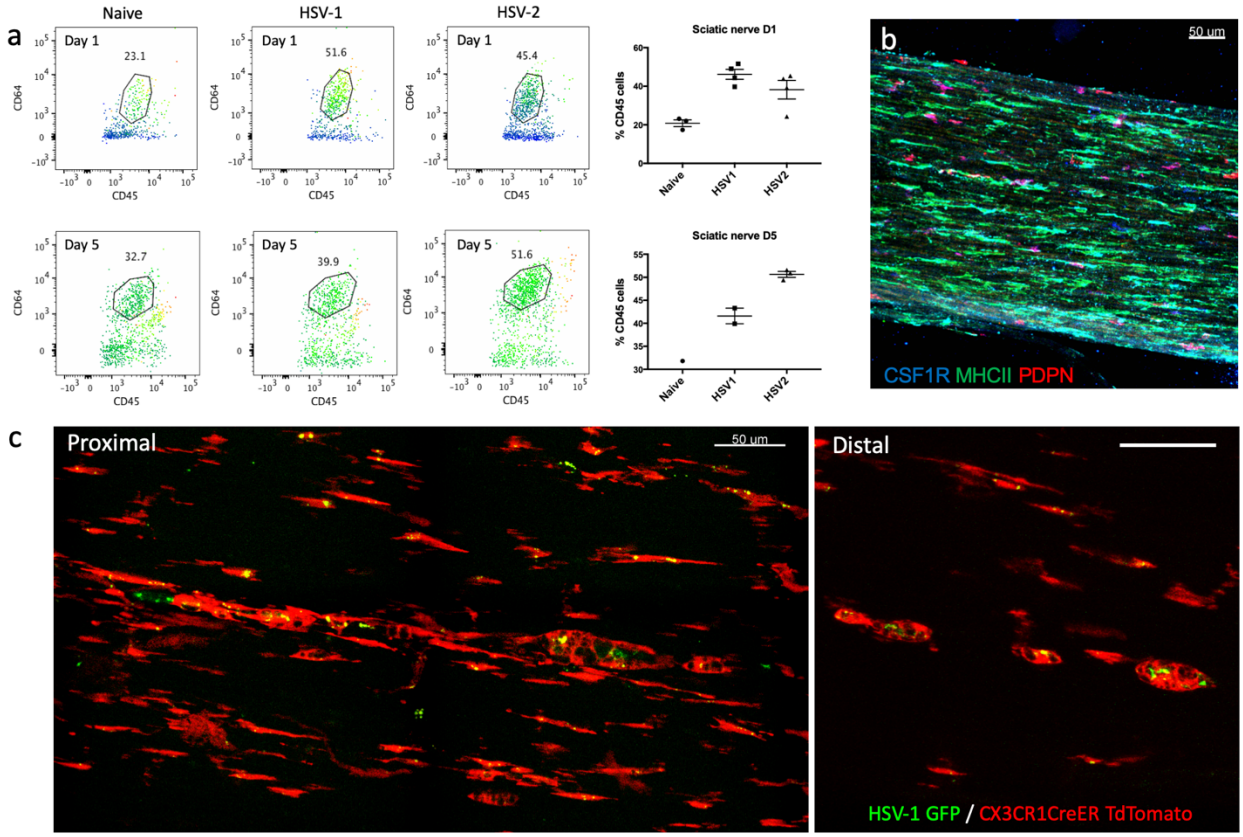

Figure 29. PNS macrophage response to HSV infection. a. Flow cytometric analysis of sciatic nerve macrophages in naïve mice and mice infected intravaginally with HSV-1 and HSV-2 at days 1 and 5 post infection. b. Confocal imaging of HSV-2 infected sciatic nerve (day 2) with MHC-II+ macrophages and PDPN+ fibroblasts. c. Confocal imaging of proximal and distal sciatic nerves in CX3CR1CreER tdTomato mice infected with GFP-tagged HSV-1.

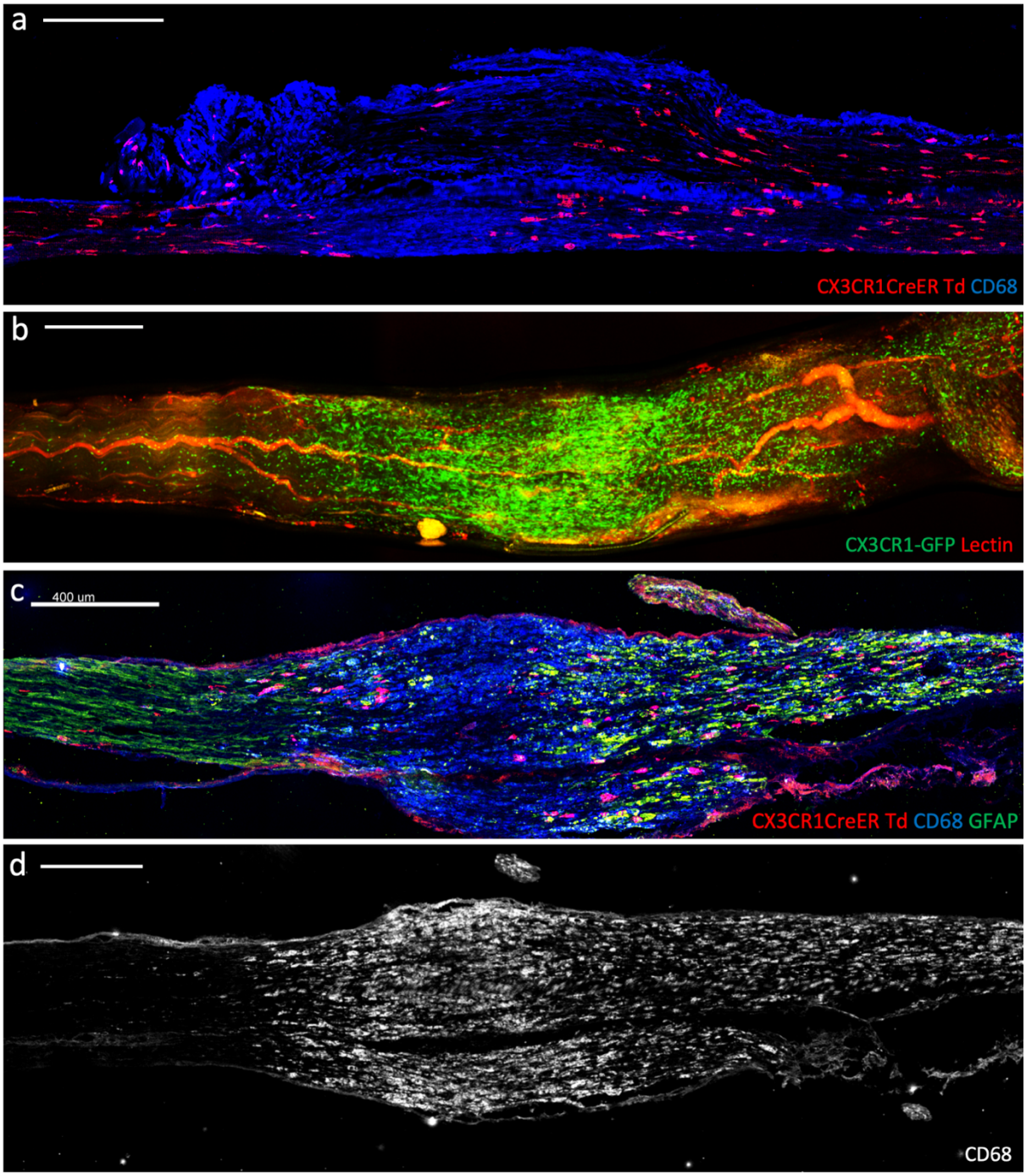

Figure 30. PNS macrophage activation and monocyte recruitment following nerve crush injury. a-d. Confocal imaging of sciatic nerves after crush injury showing proximal region (left), crush site (middle), and distal region of nerves (right). a. Resident (red) and recruited (blue) macrophages 3 days post crush. b. Recruited monocytes in CSF1R mAb-depleted mice 3 days post crush with lectin-stained blood vasculature. c. Resident (red) and recruited (blue) macrophages 7 days post crush with GFAP+ reactive Schwann cells. d. CD68+ activated phagocytic macrophage distribution 7 days post crush.

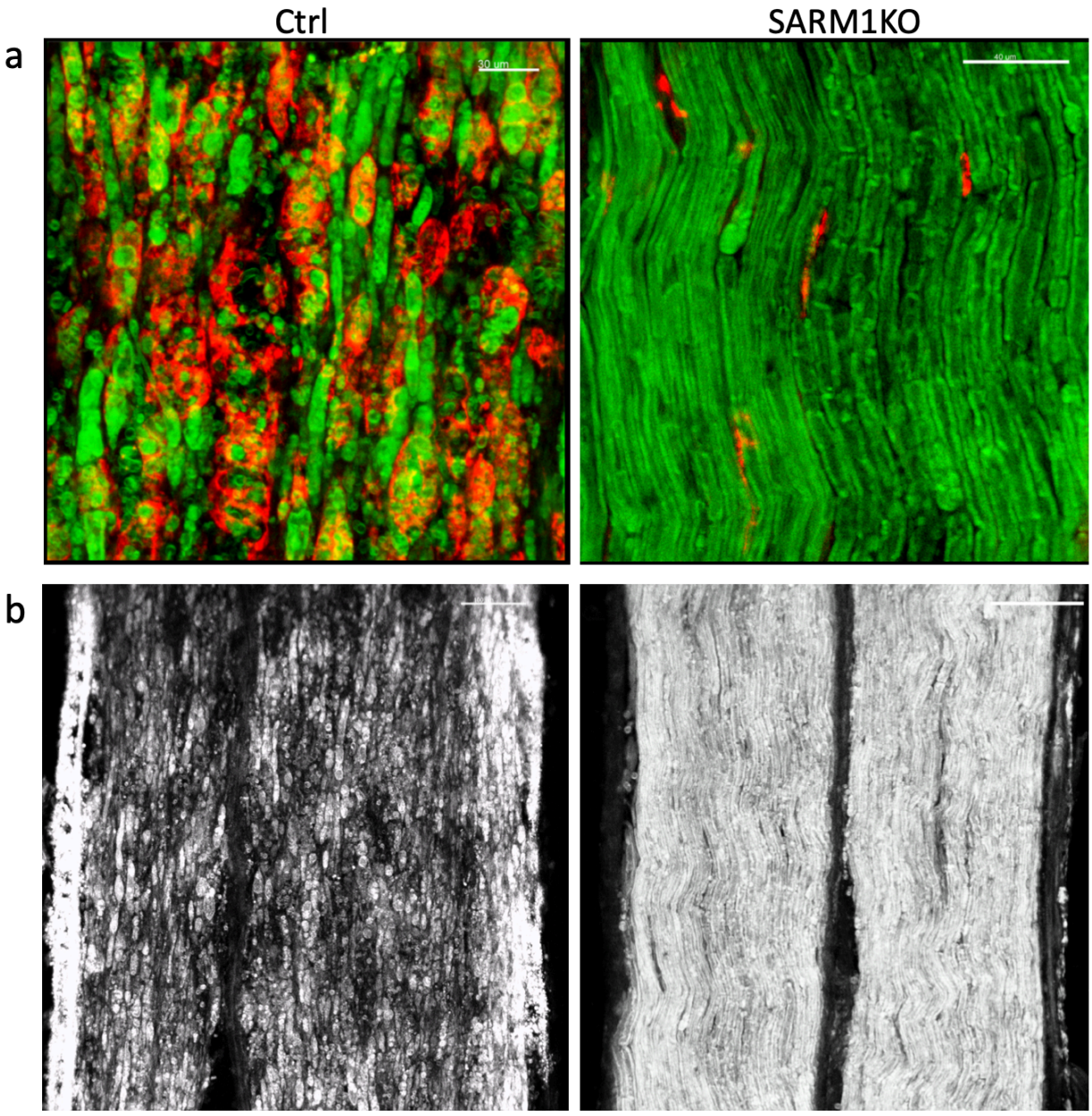

Figure 31. Phagocytic activity in PNS macrophages after nerve transection requires nerve breakdown. a,b. Confocal imaging of distal portion of transected sciatic nerves in WT and SARM1-KO mice 7 days after transection. a. CD68+ phagocytic macrophages (red) and BODIPY+ Schwann cells (green) in WT (left) and SARM1-KO (right) transected nerves. B. Myelin integrity revealed by BODIPY staining (white) in WT (left) and SARM1-KO (right) transected nerves.

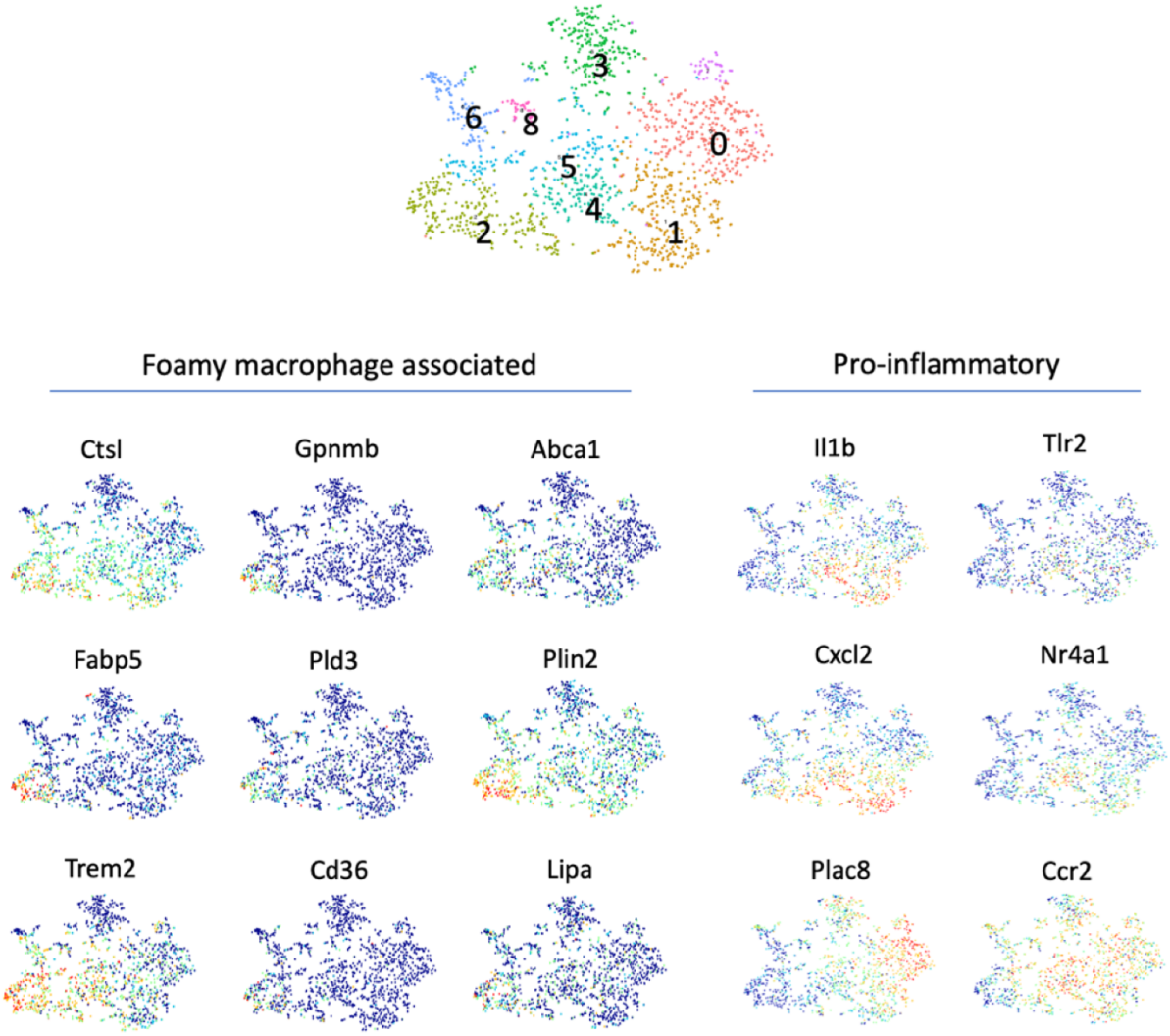

Figure 32. Single cell analysis of macrophage heterogeneity after crush injury. (Top) Subclustering in Csf1r+ macrophages isolated from CD45+ immune cells 4 days after injury. (Bottom left) Distribution of foamy macrophage-associated genes (from Kim. et al 2019). (Bottom right) Distribution of pro-inflammatory and monocyte-associated genes.

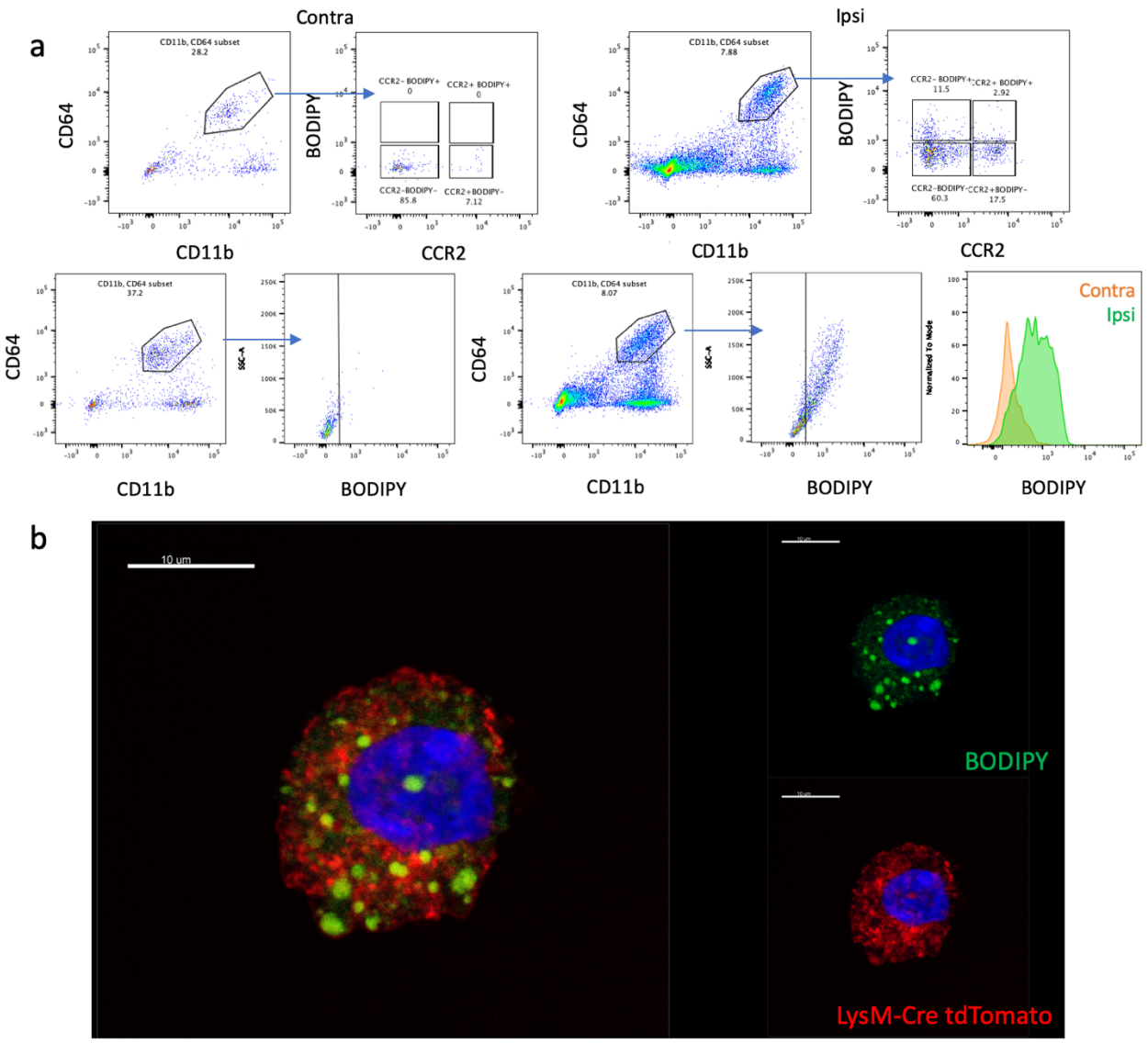

Figure 33. Identification of lipid-laden macrophages after sciatic nerve crush injury. a. Flow cytometric characterization of BODIPY+ macrophages 21 days after crush injury. b. Confocal imaging of BODIPY+ macrophage sorted from sciatic nerves 21 days after crush injury.

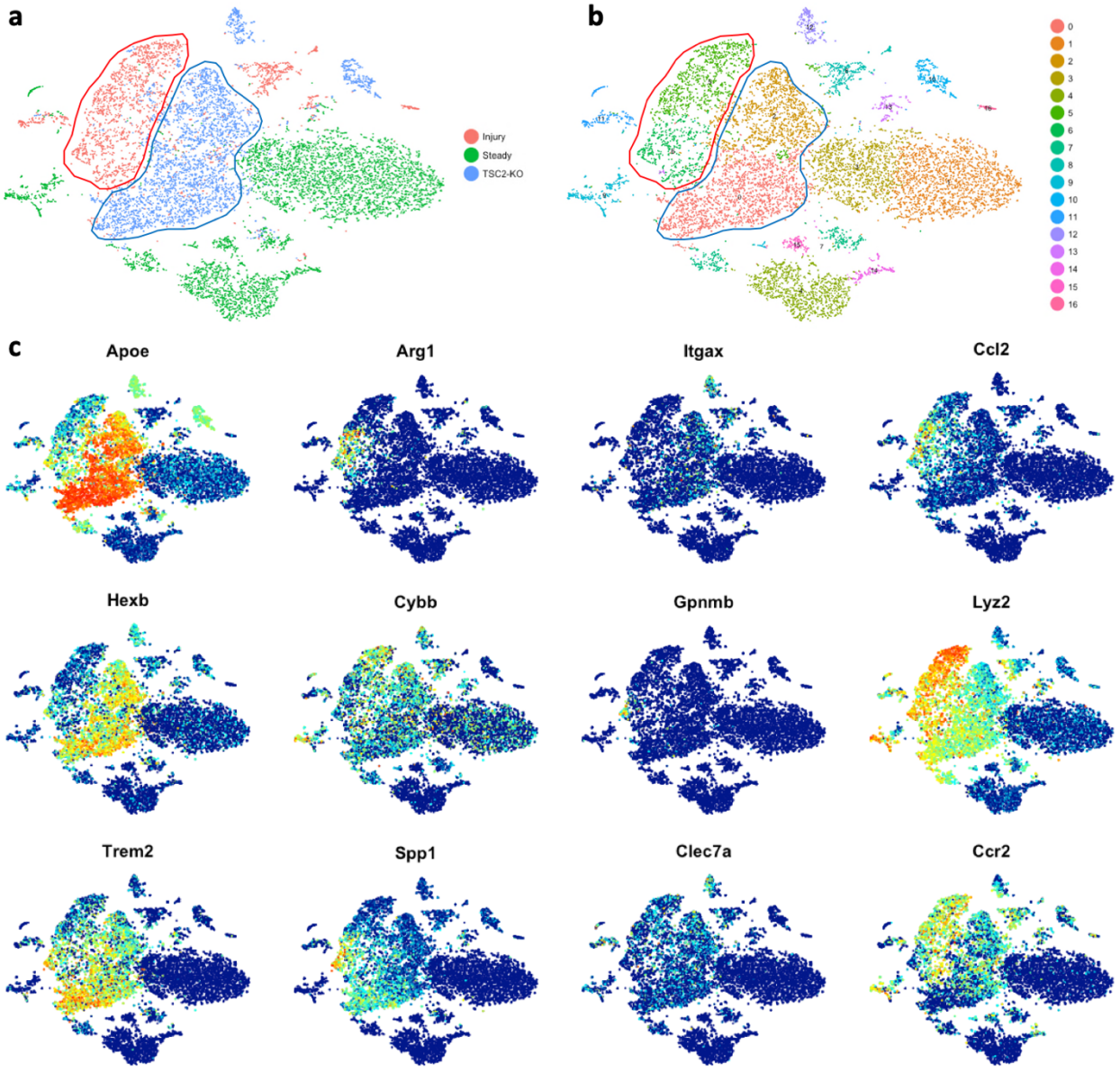

Figure 34. Combined peripheral nerve immune atlas reveals shared patterns of macrophage polarization. a. Clustering analysis of single cell RNA-seq data combined from injury (day 4 injury), TSC2-SCKO, and steady state CD45+ cells. b. Subclustering analysis of combined populations. Circles represent macrophages from injury (red) and TSC2-SCKO (blue). c. Distribution of differentially-expressed genes of interest in combined populations.

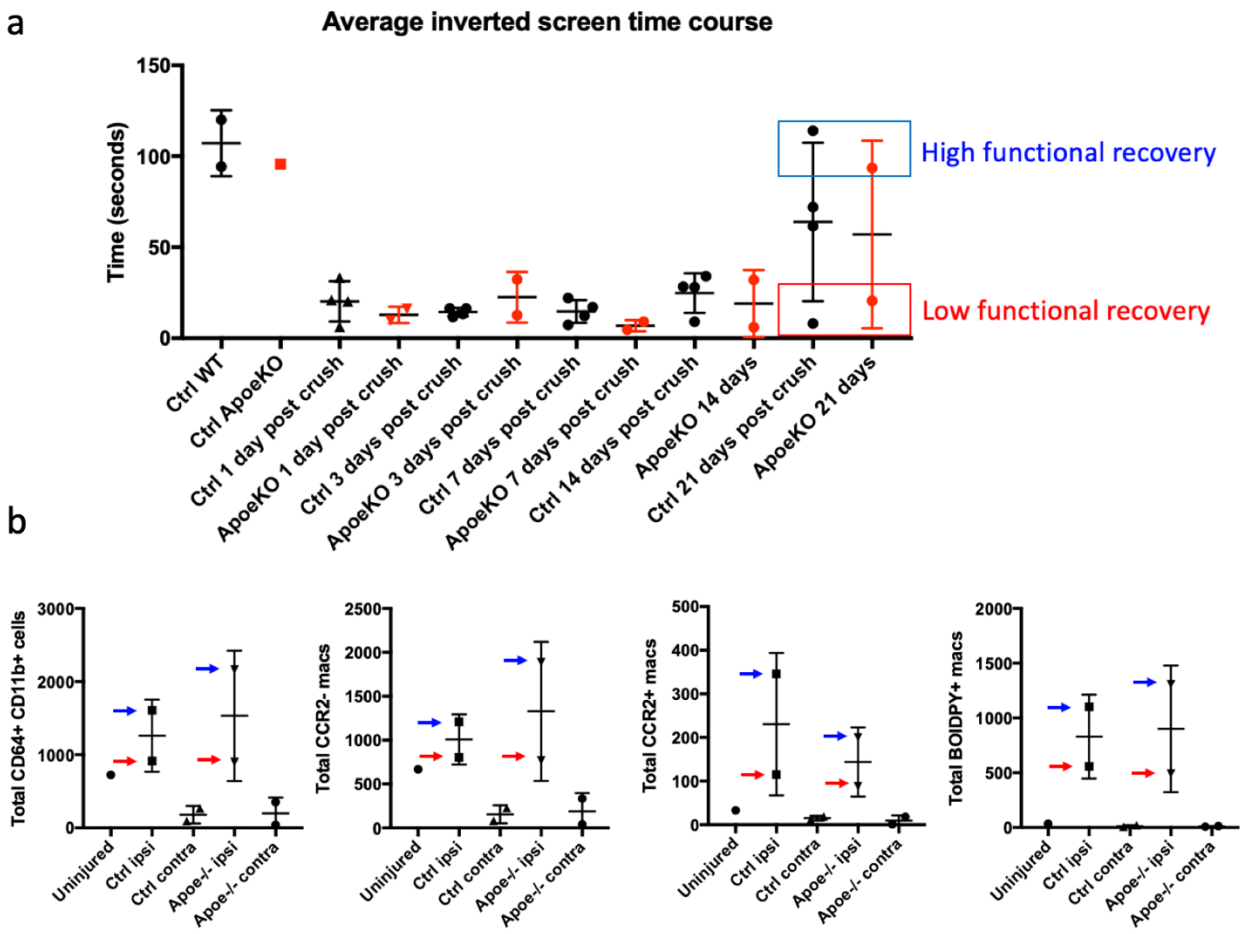

Figure 35. Macrophage numbers correlate with functional recovery after sciatic nerve crush injury. a. Inverted screen test scores across time in WT and APOE-KO mice after crush injury identifies mice with high and low functional recovery by 3 weeks after injury. b. Flow cytometric analysis of mice with high and low functional recovery.

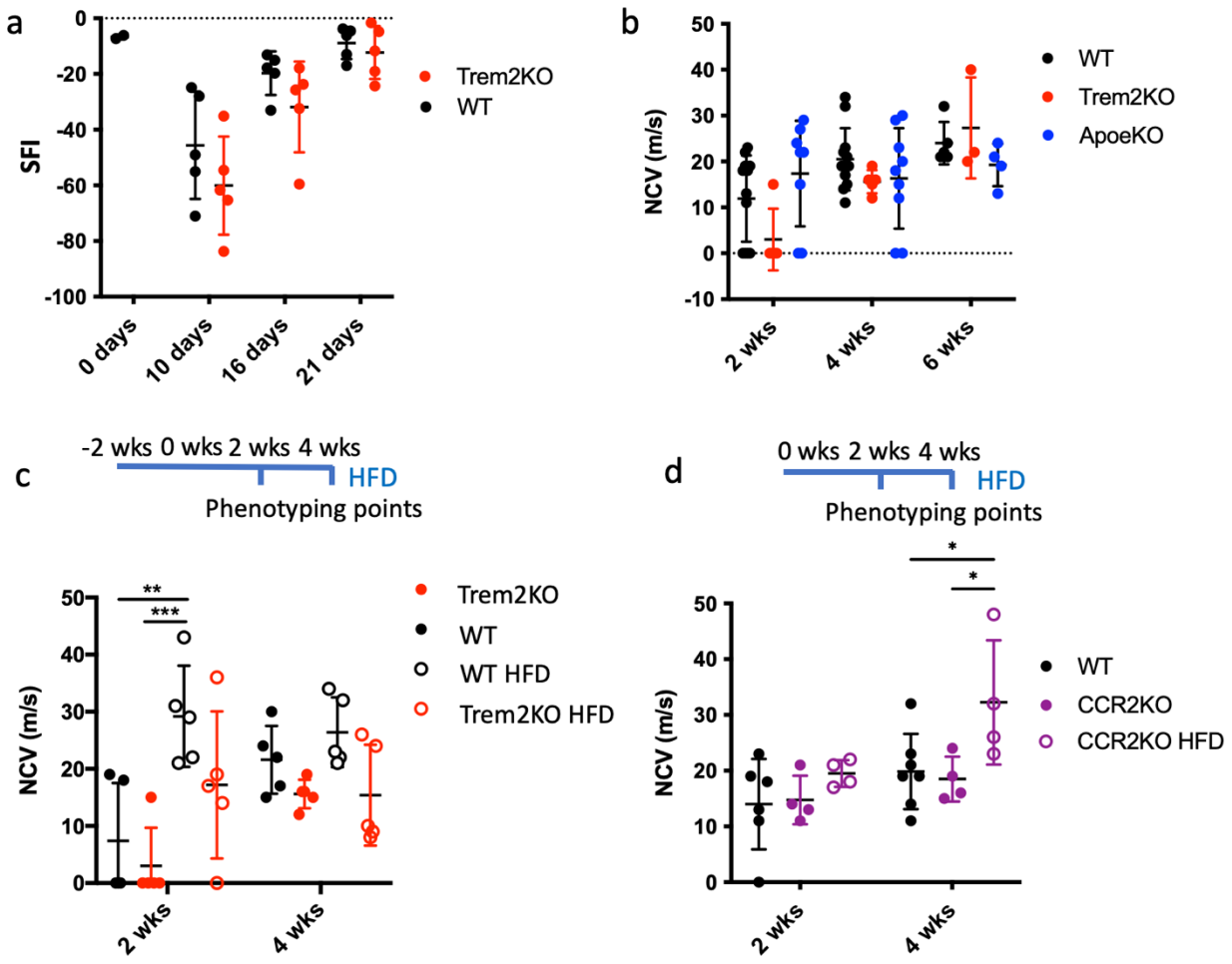

Figure 36. Functional recovery is enhanced after high fat diet feeding. a. Sciatic functional index (SFI) scores in WT and TREM2-KO mice after nerve crush injury. b. Nerve conduction velocity (NCV) in WT, TREM2-KO and APOE-KO mice after sciatic crush injury. c. NCV scores in WT and TREM2-KO mice fed normal chow versus high fat diet (HFD) 2 weeks prior to injury. d. NCV scores in WT and CCR2-KO mice fed normal chow versus high fat diet (HFD) starting on the day of injury.

5. Conclusion and Future Directions:

As unique cells that maintain host defense and tissue homeostasis, macrophages have been a centerpiece in pathology and immunology research. While advances in their study have revealed diverse functions with important implications for regulating disease outcomes, the population of macrophages in the peripheral nervous system (PNS) has been largely overlooked. In this dissertation, I characterized PNS macrophages by revealing their transcriptional identity and ontogeny, as well as their responsiveness to disturbances in the nerve environment. I provide compelling evidence that PNS macrophages are inherently microglia-like yet possess features unique to peripheral nerves. These findings open up new areas of research and provide a broader perspective for examining neural resident macrophages.

I found that PNS macrophages are self-maintaining resident cells that express genes previously thought to be specific to homeostatic microglia [1]. In light of recent studies that demonstrate the inducible expression of microglial genes in naïve cells transplanted into the brain [2,3], it thus appears that shared signals from the central and peripheral nerve environments endow neural resident macrophages with common transcriptional features. Indeed, TGF-β signaling and its promotion of microglial genes, including the transcription factor SALL1, is a prime candidate [4,5]. Future work should examine what other signals are acting on PNS macrophages to elicit expression of microglial genes, and whether boosting or eliminating these signals has an effect on PNS macrophage functions.

PNS macrophages also express unique genes that reflect their specific functions in peripheral nerves [1]. An interesting question for future research will be why PNS macrophages express these genes, and why many of these transcripts are associated with microglial activation. Since microglia activation signatures have been strongly attributed to phagocytosis of neuronal

components, one question is do PNS macrophages constitutively engulf more myelin than CNS microglia? Although it has been shown that myelinating SCs do not actively turn over in mice during adulthood [6], the PNS is more exposed to a multitude of stressors in the real world. Could these physical factors induce myelin "shedding" that requires uptake and recycling by macrophages? Future experiments may examine the range of nerve "damage" needed to induce phagocytic activity in PNS macrophages across various challenges and determine whether consistent challenge affects subsequent regenerative capacity in the same animals.

It will also be important to understand the role of PNS macrophages in normal nerve remodeling throughout adulthood. From our transcriptional profiling experiments, it is apparent that in 6 week-old juvenile mice there is active expression of genes involved in angiogenesis, axon guidance, and extracellular matrix remodeling [1]. Future studies should investigate the degree of PNS macrophage involvement in establishing and maintaining PNS circuitry. For example, do PNS macrophages facilitate motor skill acquisition by helping to strengthen specific circuits? If so, do they act on neuronal synapses by pruning the neuromuscular junction, or on Schwann cells to guide appropriate myelin remodeling, or a combination of both? These studies may have exciting implications for macrophages in neuroplasticity across lifespan.

Another important area for future research is the role of PNS macrophages in nerve infections, including bacterial, fungal, and viral infections. While it remains unclear how PNS macrophages provide host protection, their significant expression of MHC-II and interferon-induced genes suggest that they are highly capable of responding to infections. I showed that macrophage numbers in sciatic nerves are significantly elevated following intravaginal HSV infection. Furthermore, phagocytic macrophages in the sciatic nerve seemed to contain virus particles, suggesting that viral engulfment is a common mechanism in macrophages for

controlling HSV infection [7]. Since HSV travels bidirectionally in nerves [8], it is conceivable that retrograde infection of DRGs from the intravaginal route was followed by anterograde infection of sciatic nerves. This mechanism could also explain how HSV-1 spreads to enteric neurons after intravaginal infection, a process that requires TRPV1+ nociceptors [9]. Future experiments in this model should clarify whether virus needs to be present in the sciatic nerve for macrophages to expand. These studies may reveal new insights about virally-induced neuroinflammation and its potential link to neuropathic pain. Broader studies are also needed to examine whether PNS macrophages affect translocation of neurotropic viruses from peripheral nerves to the CNS.

While the exact origins of PNS macrophages was unknown up to this point, I have shown in mice that they are embryonic- and HSC-derived cells that fully populate the PNS at birth and maintain steady numbers throughout the course of life [1]. Given their origin, which can be traced to embryonic and early hematopoietic sources, PNS macrophages likely play important roles for PNS development and maturation. Future studies should characterize PNS macrophages throughout development and determine what roles they may play in nerve growth and maturation. Do they provide signals for Schwann cells, endoneurial fibroblasts, or endothelial cells to guide nerve development? How do their numbers change across the developmental process and what transcriptional signatures do they express during development? These studies will serve to improve our foundational understanding of PNS macrophages.

Future studies should also examine more closely the role of PNS macrophages in nerve injury. While it has been shown that the majority of PNS macrophages after injury are monocyte-derived [10], it is unclear if resident and recruited macrophages play specific roles. It is interesting to note that after CNS injury, monocytes perform functions that are important for reducing adverse outcomes [11]. For instance, there is evidence that recruited monocytes are more

phagocytic, have unique scar-remodeling capabilities, and have a greater capacity for regulating pro- and anti-inflammatory mediators [12-14]. In the PNS, Boissonnas and colleagues show that injury preferentially induces myelin stripping by recruited macrophages, whereas resident macrophages are more associated with axonal regrowth [15]. Our own observations in nerve injury indicate that *Ccr2*+ macrophages express pro-inflammatory cytokines in the early stages following injury. Future studies in peripheral nerve injury should track inflammation and its resolution over time in peripheral nerve macrophages.

I also found that a subset of *Ccr2*- PNS macrophages expresses lipid handling genes reminiscent of foamy macrophages from atherosclerotic lesions. This raises the question of why macrophages utilize lipids after nerve injury. One explanation could be that fatty acid oxidation fuels PNS macrophages to perform their known repair programs. It has been shown that in heart repair after ischemic injury, macrophages utilize fatty acid derived from engulfment of apoptotic cells as a fuel source for shifting towards an anti-inflammatory tissue repair phenotype [16]. Indeed, inflammation resolution after nerve injury has also been associated with IL-10 production in macrophages [17], and our own data further shows that foamy macrophages after injury specifically express *Arg1*, which has been attributed to immunosuppression. Furthermore, PNS macrophages may use fatty acids in cholesterol efflux, which has also been strongly linked with inflammatory resolution [18,19]. Studies that further characterize lipid metabolism in PNS macrophages after injury may reveal targets for improving inflammatory resolution after injury.

Lastly, I show that high fat diet (HFD) feeding improves regeneration after nerve injury. Although it remains unclear whether these benefits work primarily through macrophages or other cells, the attenuation of diet-enhanced nerve recovery in TREM2-KO mice suggests that the phenotype is at least partially dependent on macrophages. Future studies may determine the

extent of macrophage involvement and investigate whether lipid supplementation reduces inflammation, improves remyelination, or both. Furthermore, research is needed to determine optimal timing, dosage, and lipid specificity. These studies may have implications for personalized treatment of nerve injuries and the prevention of adverse outcomes such as injury-associated chronic pain.

Up to now, the brain and spinal cord of the CNS are the only tissues thought to possess microglia. Our comparison of resident macrophages from both the PNS and CNS challenges this notion and supports the idea that some microglial features and transcriptional programs are shared in macrophages across the nervous system, whereas critical features remain distinct. These findings provide new implications for the health and preservation of the PNS and open the door to unexplored topics in neuroimmune research.

5.1 References

1. Wang, P.L., et al. Peripheral nerve resident macrophages share tissue-specific programming and features of activated microglia. *Nat. Commun.* 11, 2552 (2020).
2. Bennett, F. C., et al. A combination of ontogeny and CNS environment establishes microglial identity. *Neuron* 98, 1170-1183 (2018).
3. Cronk, J. C., et al. Peripherally derived macrophages can engraft the brain independent of irradiation and maintain an identity distinct from microglia. *J. Exp. Med.* 215, 1627-1647 (2018).
4. Butovsky, O., et al. Identification of a unique TGF-beta-dependent molecular and functional signature in microglia. *Nat. Neurosci.* 17, 131-143 (2014).
5. Buttgereit, A., et al. Sall1 is a transcriptional regulator defining microglia identity and function. *Nat. Immunol.* 17, 1397-1406 (2016).

6. Stierli, Salome., et al. The regulation of the homeostasis and regeneration of peripheral nerve is distinct from the CNS and independent of a stem cell population. *Development* 145, (2018).
7. Lang, J., et al. Acid ceramidase of macrophages traps herpes simplex virus in multivesicular bodies and protects from severe disease. *Nat. Comm.* 11, (2020).
8. Koyuncu O.O., et al. Virus infections in the nervous system. *Cell Host Microbe* 13, 279-93 (2013).
9. Khoury-Hanold, W., et al. Viral spread to enteric neurons links genital HSV-1 infection to toxic megacolon and lethality. *Cell Host Microbe* 19, 788-99 (2016).
10. Ydens, E., et al. Profiling peripheral nerve macrophages reveals two macrophage subsets with distinct localization, transcriptome and response to injury. *Nat. Neurosci.* 23**,** 676–689 (2020).
11. Castellani, G., and Schwartz, M. Immunological features of non-neuronal brain cells: implications for Alzheimer's disease immunotherapy. *Trends Immunol*. 41, 794-804 (2020).
12. Ritzel, R.M., et al. Functional differences between microglia and monocytes after ischemic stroke. *J. Neuroinflammation* 12, (2015).
13. Shechter R., et al. The glial scar-monocyte interplay: a pivotal resolution phase in spinal cord repair. *PLoS ONE* 6, (2011).
14. Shechter R., et al. Infiltrating blood-derived macrophages are vital cells playing an anti-inflammatory role in recovery from spinal cord injury in mice. *PLoS Med.* 6 (2009).
15. Boissonnas, A., et al. Imaging resident and recruited macrophage contribution to Wallerian degeneration. *J Exp. Med.* 217, (2020).
16. Zhang, S., et al. Efferocytosis fuels requirements of fatty acid oxidation and the electron transport chain to polarize macrophages for tissue repair. *Cell Metab.* 29, 443-456 (2019).
17. Siqueira Mietto, B. et al. Role of IL-10 in resolution of inflammation and functional recovery after peripheral nerve injury. *J. Neurosci.* 35, 6431-42 (2015).
18. Zimmer, S., et al. Cyclodextrin promotes atherosclerosis regression via macrophage reprogramming. *Sci. Transl. Med*. 8, (2016).
19. Cantuti-Castelvetri, L., et al. Defective cholesterol clearance limits remyelination in the aged central nervous system. *Science* 359, 684-88 (2018).